CHALMERS

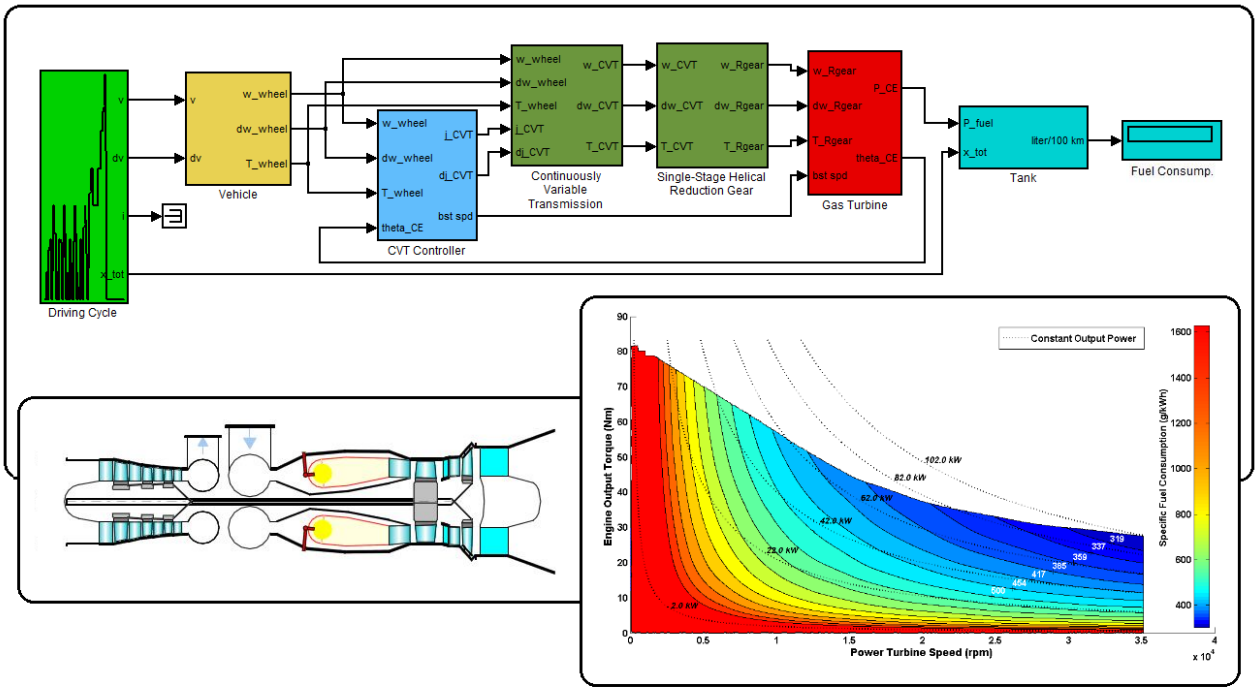

Investigation of the Potential of Gas Turbines for Vehicular Applications

Master's thesis in Fluid Dynamics

HENRIQUE CUNHA

Department of Applied Mechanics
Division of Fluid Dynamics
CHALMERS UNIVERSITY OF TECHNOLOGY
Gothenburg, Sweden 2011

Master's thesis 2011:43

MASTER'S THESIS IN FLUID DYNAMICS

Investigation of the Potential of Gas Turbines for Vehicular Applications

HENRIQUE CUNHA

Department of Applied Mechanics
Division of Fluid Dynamics
CHALMERS UNIVERSITY OF TECHNOLOGY
Gothenburg, Sweden 2011

Investigation of the Potential of Gas Turbines for Vehicular Applications
HENRIQUE CUNHA

Master's thesis 2011:43
ISSN 1652-8557
Department of Applied Mechanics
Division of Fluid Dynamics
Chalmers University of Technology
SE-412 96 Gothenburg
Sweden
Telephone: +46 (0)31-772 1000

Cover:
Simulink Vehicle Model; Gas Turbine Sketch; Gas Turbine Efficiency Map

Chalmers Reproservice
Gothenburg, Sweden 2011

Investigation of the Potential of Gas Turbines for Vehicular Applications
Master's thesis in Fluid Dynamics
HENRIQUE CUNHA
Department of Applied Mechanics
Division of Fluid Dynamics
Chalmers University of Technology

Abstract

The increasing number of passenger cars worldwide and the consequent increasing rate of global oil consumption have raised the pressure on fuel prices and have caused serious problems to the environment. Nowadays, the demand for reducing fuel consumption and pollutant emissions has paved the way for the development of more efficient power generation systems for the transportation sector. In the past decades, environmental advantages of the gas turbine, such as low concentration of hydrocarbon and carbon monoxide emissions, have led some car manufacturers to evaluate the potential of this type of engine as prime mover.

The viability of an engine for road vehicle applications is highly dependent on its performance, mainly in terms of fuel consumption. This assessment is rather complex and involves high costs. Nevertheless, these costs can be mitigated by utilizing simulation tools that predict the performance of the vehicle and its on-board subsystems under a variety of driving conditions.

This work focuses on the development of a methodology and tools for simulating the performance of gas turbines powering road vehicles, in a wide range of simulation conditions. Three different codes were used in order to carry out this study: focusing on simulating the thermodynamic cycle of three different gas turbine models; post-processing the gas turbine performance data generated; and simulating the performance of two different road vehicles at various driving conditions.

Simulations were carried out using a quasistatic approach; the results generated were quite distinct for the different vehicles, driving patterns and engine configurations tested. The simulations indicate that vehicles powered by gas turbines have higher fuel consumption than the ones equipped with reciprocating engines, independently of the driving conditions simulated. Nevertheless, more innovative cycles incorporating advanced technologies could in the future change this picture.

The developed platform permits not only the simulation of innovative and complex gas turbine configurations (with higher efficiency compared to the concepts already assessed) operating as prime movers in road vehicles, but also the modeling of hybrid powertrains, combining electric propulsion with this type of engine. Some car manufacturers argue that the use of a gas turbine operating as range extender in a series hybrid configuration is the most efficiency solution in the coming years. The methodology presented in this work sets the formulation for performing such an assessment and provides a first estimate for the fuel economy of different powertrain topologies.

Keywords: Gas Turbine, Road Vehicle, Fuel Consumption, Computational Simulation

Acknowledgements

First of all, I would like to thank Professor Konstantinos Kyprianidis for providing me the opportunity to work on this topic. His help, support and constant availability guided me through this thesis work. Thank you for your encouragement that kept me going on until the end.

A special thanks for all the Chalmers students and researchers that helped me developing this thesis work, as well as the Division of Fluid Dynamics for providing me with added technology, a workplace and documentation to help me with my research.

I would like to extend a very special thanks to all friends that followed me throughout the past year. Thank you for all the good times and memories. Without them these would have been, surely, hard times.

I would like to thank my family for all the support in time of need, as well as for providing me with the possibility to study abroad and expand my horizons. Without your support things would not have turned out as good as they did.

Finally, thank you to all persons who were not mentioned in the above acknowledgments, but were involved with the work directly or indirectly.

Nomenclature

A	Area $[m^2]$
ADVISOR	Advanced Vehicle Simulator
bwr	Back-work Ratio
c_p	Specific Heat at Constant Pressure $[J\ K^{-1}kg^{-1}]$
c_r	Rolling Resistance Coefficient
c_v	Specific Heat at Constant Volume $[J\ K^{-1}kg^{-1}]$
C_D	Aerodynamic Drag Coefficient
CFD	Computational Fluid Dynamics
CO	Carbon Monoxide
CO_2	Carbon Dioxide
CPU	Central Processing Unit
CVT	Continuously Variable Transmission
DCT	Dual Clutch Transmission
ECE R15	Urban Driving Cycle (European)
EUDC	Extra-urban Driving Cycle (European)
F	Force $[N]$
g	Gravitational Acceleration Constant $[9.81\ m/s^2]$
h	Specific Enthalpy $[J/kg]$
H	Blade Height $[mm]$
H_f	Fuel's Lower Heating Value $[J/kg]$
HC	Hydrocarbon
I	Moment of Inertia $[kg\ m^2]$
IC	Internal Combustion
k	Heat Capacity Ratio
m	Mass $[kg]$
$\dot{m}$	Mass Flow $[kg/s]$
N	High Pressure Spool Speed $[rad/s]$
Nhp	High Pressure Spool Relative Speed
NEDC	New European Driving Cycle
NOx	Nitrogen Oxide
OOL	Optimal Operation Line
p	Pressure $[Pa]$

P	Power $[W]$
Q	Heat $[J]$
QSS	QuasiStatic Simulation
r	Radius
r_p	Pressure Ratio
s	Specific Entropy $[J\ K^{-1}kg^{-1}]$
SFC	Specific Fuel Consumption $[g\ kW^{-1}h^{-1}]$
SUV	Sport Utility Vehicle
t	Time $[s]$
T	Temperature $[K]$ or Torque $[Nm]$
U	Compressor Blade Speed $[m/s]$
v	Specific Volume $[m^3/kg]$ or Velocity $[m/s]$
w	Rotational Speed $[rad/s]$
W	Work $[J]$

Greek Symbols

α	Grade Angle $[rad]$
γ	Gear Ratio
η	Efficiency
ρ	Air Density $[kg/m^3]$

List of Figures

List of Tables

Contents

1 Introduction

Within this chapter, the issues addressed by the present research work are contextualized in a broader setting. The driving forces behind this effort shall be followed by the description of the objectives set for this work. After that, the thesis structure shall be outlined. The last section of this chapter focuses on explaining how this work contributes to knowledge.

1.1 Motivation

The increasing number of passenger cars worldwide, and consequently, the increasing rate of global oil consumption, urgently demands for the development of more efficient power generation systems for the transportation sector. For the first time ever, the number of vehicles in operation worldwide surpassed the 1 billion-unit mark in 2010 [Sou11]. It is proved empirically that the demand for personal transportation increases with the economic growth. In wealthier societies, such as the United States of America, Japan or most European countries, the car density saturates at a ratio of approximately 400 to 800 cars per 1000 inhabitants. The developing countries, such as China with 1.3 billion inhabitants, or India with 1.1 billion inhabitants, are expected to experience a substantially increase in car density within the next 20 years, a fact that will further increase the pressure on fuel prices and cause serious problems to the environment [Guz+07].

The health risks in urban areas associated to the atmospheric pollution, mainly from internal combustion engine vehicles, have mobilized public environmental awareness, leading to stringent national and international exhaust emission control regulations for vehicle manufacturers. Furthermore, the urban areas of some major European capital centers are so heavily congested that the imposition of access limitations is already a reality. These problems combined with the increasing demand for mobility, have led to a situation where the reduction of fuel consumption and pollutant emissions has become a top priority for society and economy.

Many approaches that promise to reduce the fuel consumption and the emissions of passenger cars have been presented so far, and new ideas emerge on a regular basis. In the past decades, a number of experiments by vehicle manufacturers and engine builders have been conducted to evaluate the capabilities of gas turbines as prime movers. Several advantages can be attributed to gas turbine engines over the conventional reciprocating engines, i.e. spark-ignition engines (petrol) and compression-ignition engines (diesel). For instance, gas turbines are relatively free from smoke and emit less concentrations of hydrocarbon (HC) and carbon monoxide (CO), compared to the piston engines. Besides that, the reduced number of moving parts confers to gas turbines a high reliability and a low cost maintenance. The viability of gas turbines in road vehicles is highly dependent on the performance of this type of engine, in terms of fuel consumption. For this reason, a proper assessment of this parameter reveals to be essential in this analysis.

The design of new powertrain systems involves high costs. However, these costs can be mitigated by utilizing, during design, simulation tools that can predict the performance of the vehicle and its on-board subsystems under a variety of driving conditions. Simulations are particularly useful in the automotive industry, but they can also be applied to academic projects.

1.2 Objectives

The main purpose of this thesis concerns the investigation of the potential of gas turbine engines for vehicular applications, in terms of fuel economy.

In order to develop this investigation, a number of objectives were set, as it is enumerated below:

1. Perform thermodynamic investigations of different gas turbine configurations for different types of vehicles;
2. Carry out a literature review looking at past efforts with respect to gas turbine designs for vehicles;
3. Carry out preliminary sizing of the chosen gas turbine concept;

4. Investigate potential requirements and difficulties with respect to integrating the gas turbine concept in the vehicle;
5. Down-select the most promising concept (gas turbine configuration and vehicle);
6. Draw conclusions from the work carried out and make recommendations for future work.

1.3 Thesis Outline

In chapter 2 it is carried out a literature review. This chapter provides an overview of the gas turbine operating system, at the same time that gives a special focus to the past efforts with respect to gas turbine design for road vehicles. Apart from that, it is also introduced the approaches used to predict the fuel economy of road vehicles. The most relevant drivetrain systems are stressed as well.

Chapter 3 includes the description of the modeling procedures adopted for both gas turbine models and vehicle models. It includes the description of the software used, as well as the limitations associated to the approach adopted.

In chapter 4, the simulation results are exposed and discussed. The results analysis is subdivided in two parts, according to the type of driving cycles tested: default or custom.

In chapter 5, the conclusions on the developed models are discussed, as well as some proposals of future work.

1.4 Contribution to Knowledge

1. Development of a platform capable of simulating the performance of gas turbines applied in road vehicles. The author's effort focused on the development of two tools:
   - an executable code capable of creating the efficiency map of any gas turbine model, based on data generated by a commercial software ($GasTurb$) that evaluates the engine thermodynamic cycle for both design and off-design operational conditions.
   - a simulating program representative of a road vehicle powered by a gas turbine engine, capable of analyzing the energy consumption effects associated to its driving.
2. Assessment of the fuel consumption of road vehicles powered by gas turbines, in a wide range of simulation conditions, dependent on the setting of the following parameters:
   - driving conditions;
   - chassis characteristics;
   - gearbox system (manual or automatic gearbox);
   - gearbox controller, in case of automatic gearboxes;
   - gas turbine configuration (simple, intercooled or recuperated cycle);
   - fuel type.

It is important to refer that this assessment is determined based on a quasistatic approach, also called *backwards* formulation. This approach has the advantage of allowing fast calculations, due to its relatively low numerical effort, however it is not suited to analyze the best-effort performance, for instances acceleration tests, since it assumes that the vehicle meets the speed trace pre-defined by a driving cycle.

2 Literature Review

2.1 Gas Turbine Engine

2.1.1 Overview

A gas turbine is a type of internal combustion engine and it can be viewed as an energy conversion device that converts energy stored in the fuel to useful mechanical energy in form of rotational power. This rotary engine has, in its simplest configuration, an upstream compressor coupled to a downstream turbine, and a combustion chamber in between. Since Sir Frank Whittle first ran his jet engine in 1937, the gas turbine has had an immeasurable impact upon society. Serious developments in gas turbines began not long before the Second World War with shaft power in mind, but attention was soon transferred to the turbojet engine for aircraft propulsion. The gas turbine began to compete successfully in other fields only in the mid 1950s. The favorable power-output-to-weight ratio of gas turbines makes them suitable for several applications and today there are few people in the developed world whose daily life is not touched by it. The ready access to global air travel, low cost electricity, natural gas pumped across continents, and the defence of nations both in the air and at the sea are a sample of the things that depend upon gas turbine power. The challenge for the forthcoming decades will be undiminished with ever increasing demands to minimize pollution and energy consumption to preserve the world for the next generations.

2.1.2 Brayton Cycle

The *Brayton cycle* is the basis of the cyclic gas turbine power plants. Gas turbine power plants may operate on either *open* or *closed* basis. The more common cycle is the *open* circuit, with internal combustion (figure 2.1.1a). In this cycle, air and fuel pass across the single control surface into the compressor and combustion chamber, respectively, and the combustion products leave the control surface after expansion through the turbine. Part of the turbine work developed is used to drive the compressor, while the remainder is available to generate electricity, to propel a vehicle, or for other purposes. In the *closed* cycle (figure 2.1.1b), a heat exchanger adds heat to the fluid, which is provided by an external heat source, such as a nuclear reactor. The fluid is cooled down in another heat exchanger after it leaves the turbine and before it enters the compressor.

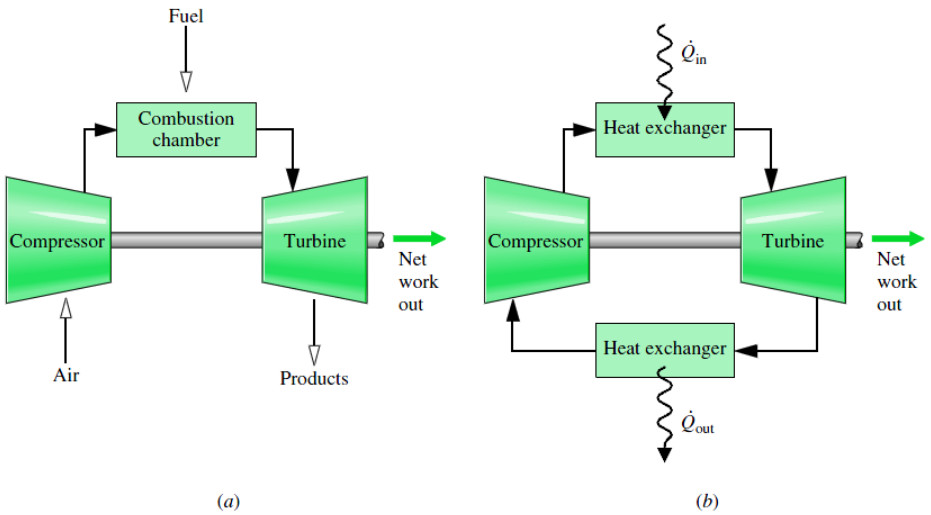

Figure 2.1.1: *Simple gas turbine: a) open to the atmosphere; b) closed [Mor+06]*

Ideal Air-Standard Brayton Cycle

An idealization often used in the study of *open* gas turbine power plants is an air-standard analysis, which implies two assumptions [Mor+06]:

- The working fluid is air, which behaves as an ideal gas;
- The temperature raise that would be achieved in the combustion process is brought about by a heat transfer from an external source.

An air-standard analysis simplifies the study of gas turbine performance considerably, since complexities as well as composition changes, associated to the combustion process, are avoided.

The ideal Brayton cycle consists of four processes:

- Isentropic[1] Compression Process (1 - 2)
- Isobaric[2] Combustion Process (2 - 3)
- Isentropic Expansion Process (3 - 4)
- Isobaric Cooling Process (4 - 1)

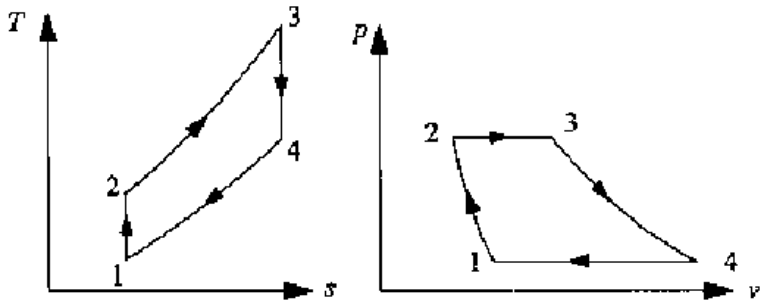

Figure 2.1.2: *Brayton Cycle T-s and p-v diagrams [Wu04]*

Applying the first and second laws of thermodynamics, for an *open* system, to each of the processes of the Brayton cycle yields:

$$Q_{12} = 0 \tag{2.1.1}$$

$$W_{12} = m(h_2 - h_1) \tag{2.1.2}$$

$$W_{23} = 0 \tag{2.1.3}$$

$$Q_{23} = m(h_3 - h_2) \tag{2.1.4}$$

$$Q_{34} = 0 \tag{2.1.5}$$

$$W_{34} = m(h_4 - h_3) \tag{2.1.6}$$

$$W_{41} = 0 \tag{2.1.7}$$

$$Q_{41} = m(h_1 - h_4) \tag{2.1.8}$$

[1]Isentropic process is defined as an adiabatic and reversible process, i.e. a process where both heat transfer and friction effects are excluded.

[2]Isobaric process is a thermodynamic process where the pressure is constant.

Considering the previous formulae and neglecting the effects of kinetic and potential energy, the net work ($Wnet$), which is also equal to the net heat ($Qnet$), is

$$W_{net} = W_{12} + W_{34} = Q_{net} = Q_{23} + Q_{41} \tag{2.1.9}$$

The thermal efficiency of the cycle is

$$\eta = W_{net}/Q_{23} = Q_{net}/Q_{23} = 1 + Q_{41}/Q_{23} = 1 + (h_1 - h_4)/(h_3 - h_2) \tag{2.1.10}$$

The enclosed area on each $T - s$ and $p - v$ diagrams of figure 2.1.2 can be interpreted as the net heat added or, equivalently, the net work output. The overall cycle efficiency can be calculated as a function of the turbine firing temperature (T_3) or the pressure ratio (r_p) assuming certain simplifications such as: the gas is calorically and thermally perfect, which means that the specific heat at constant pressure (c_p) and the specific heat at constant volume (c_v) do not change; the pressure ratio (r_p) in both compressor and turbine are the same; and all components operate at 100% efficiency [Wu04]. With these assumptions, the ideal cycle efficiency meets the following relationships:

$$\eta = 1 - (T_4 - T_1)/(T_3 - T_2) = 1 - (r_p)^{(k-1)/k} \tag{2.1.11}$$

where k is the heat capacity ratio and r_p is the compressor pressure ratio which is defined by the equation:

$$r_p = p_2/p_1 \tag{2.1.12}$$

These formulae show that the thermal efficiency of the gas turbine increases for higher values of pressure ratio or turbine firing temperature, a temperature that is limited by the maximum temperature that turbine blades can withstand.

In the gas turbine cycle, the ratio of the compressor work to the turbine work is called *back-work* ratio (bwr). Typical *back-work* ratios of gas turbines range from 40% to 80% [Mor+06].

$$bwr = |W_{12}/W_{34}| = |(h_2 - h_1)/(h_4 - h_3)| \tag{2.1.13}$$

Accounting for Irreversibilities and Losses

The irreversibilities and losses associated to power plant components have been ignored in the previous cycle analysis, however these considerations have a pronounced effect on overall performance. The overall efficiency of a gas turbine cycle depends primarily upon the pressure ratio of the compressor. The difficulty of obtaining a sufficiently high pressure ratio with an adequate compressor efficiency was not resolved until the science of aerodynamics could be applied to the problem. After decades of development effort, efficiencies of 80 to 90% can now be achieved for turbines and compressors in gas power plants [Mor+06].

Actual Brayton Cycle Efficiency

Considering an actual cycle, the compressor (η_c) and turbine (η_t) efficiencies must be taken into account in the overall cycle efficiency calculation, considering the firing temperature T_f and the ambient temperature T_{amb}. This relationship is given by the following equation [Boy02]:

$$\eta_{cycle} = \left(\frac{\eta_t . T_f - \frac{T_{amb} . r_p^{\left(\frac{k-1}{k}\right)}}{\eta_c}}{T_f - T_{amb} - T_{amb}\left(\frac{r_p^{\left(\frac{k-1}{k}\right)} - 1}{\eta_c}\right)} \right) \left(1 - \frac{1}{r_p^{\left(\frac{k-1}{k}\right)}} \right) \tag{2.1.14}$$

Contrarily to what happens in the ideal cycle, in the actual one there is entropy generation due to the several loss mechanisms that take place as the fluid flows through the compressor and turbine. As a consequence, the compressor outlet temperature is higher for a given pressure ratio, compared to what would be expected from an ideal compression process. On the other hand, the turbine outlet temperature is higher for a given power requirement, compared to what would be expected from an ideal expansion process (see figure 2.1.3). In practise, losses result in an increase of the power absorbed by the compressor and a decrease of the power output by the turbine. It is, therefore, useful to define efficiency parameters for the compressor and turbine.

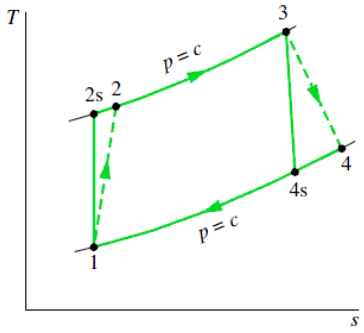

Figure 2.1.3: *Effects of irreversibilities on the air-standard gas turbine [Mor+06]*

Isentropic Efficiency is defined as the ideal specific work input, or total temperature rise, for a given pressure ratio divided by the actual.

$$\eta_{c,is} = \frac{h_{2s} - h_1}{h_2 - h_1} \tag{2.1.15}$$

Although the isentropic efficiency is a useful parameter, it may also be misleading if used for comparing the efficiency of turbomachines with different pressure ratios. In other words, the isentropic efficiency is not a suitable parameter for optimization studies. For such studies a different efficiency parameter should be used instead, the polytropic efficiency [Kyp11].

Polytropic Efficiency is defined as the isentropic efficiency of an infinitesimally small step in the compression (compressor) or expansion (turbine) process, and thus it can be assumed constant throughout the entire process.

The transformations from the ideal Brayton cycle to the actual one is summarized in the following items and illustrated in figure 2.1.3:

- Compression Process: Isentropic (1 - 2s) → Adiabatic (1 - 2)
- Combustion Process: Isobaric (2s - 3) → Isobaric (2 - 3)
- Expansion Process: Isentropic (3 - 4s) → Adiabatic (3 - 4)
- Cooling Process: Isobaric (4s - 1) → Isobaric (4 - 1)

Among the irreversibilities of the actual gas turbine power plants, combustion irreversibility is the most significant by far, however an air-standard analysis does not allow the evaluation of this irreversibility.

Improvements to Brayton Cycle

The thermal efficiency or net work of the Brayton cycle can be improved by several modifications applied in the basic cycle.

Regenerative Brayton Cycle

In a gas turbine cycle the exhaust temperature is quite high, indicating that a large portion of available energy is wasted. One way of transforming this high temperature, from exhaust gases, into available energy consists of using these same gases to preheat the combustion air before it enters in the combustion chamber. This action increases the overall efficiency by decreasing the quantity of fuel burnt. A schematic diagram, as well as the $T - s$ diagram of an *ideal* regenerative gas turbine cycle are illustrated in figure 2.1.4.

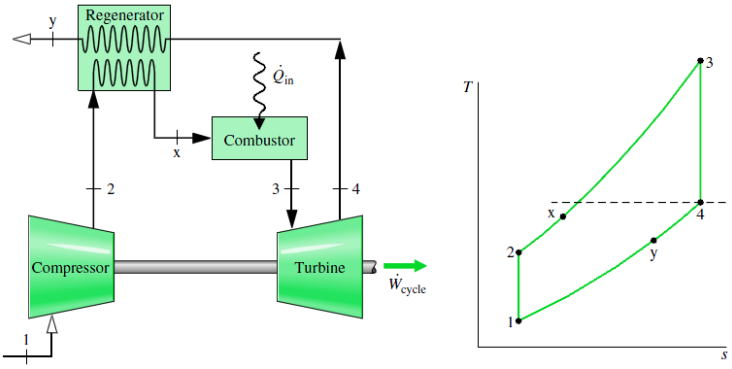

Figure 2.1.4: *Regenerative air-standard gas turbine cycle [Mor+06]*

Reheat and Intercooled Brayton Cycle

The improvement of the cycle net work can be achieved by reducing the compressor work or by increasing the turbine work. Intercooling the working fluid between compressor stages and reheat it between turbine stages provide important advantages. Since the gases exiting the combustor contain sufficient air for combustion, some more fuel can be injected (reheat). The products of combustion entering in the second turbine (T_8) are usually at the same temperature as those entering in the first turbine (T_6). The schematic and $T-s$ diagrams for an reheat and intercooled gas turbine cycle are illustrated in figure 2.1.5. Notice that reheat and intercooling increase the net work of the gas turbine cycle, but not necessarily the efficiency, unless a regenerator is also added.

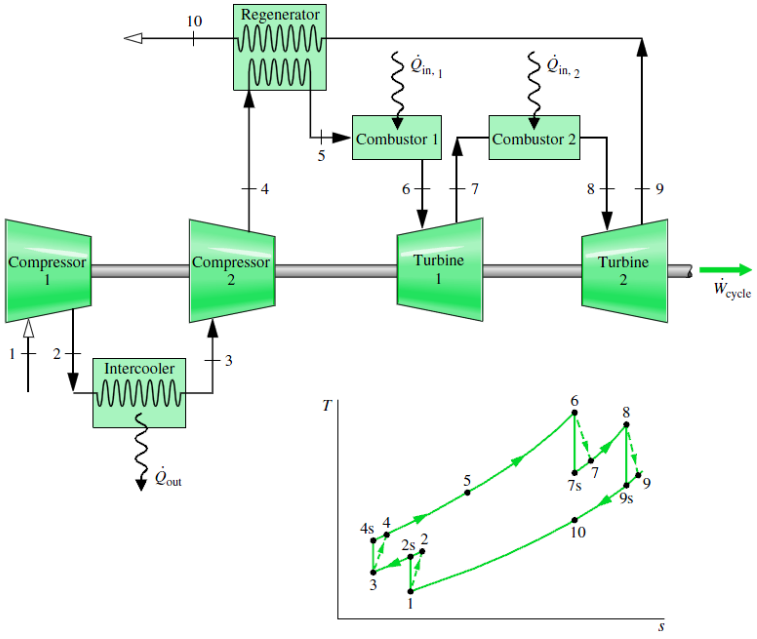

Figure 2.1.5: *Regenerative gas turbine with intercooling and reheat [Mor+06]*

These refinements are used to increase the power output and efficiency of the plant at the expense of added complexity, weight and cost. The way in which these components are linked together not only affects the maximum overall thermal efficiency, but also the variation of the output power and torque with the rotational speed.

The suitability of the different cycle arrangements presented depends on the application requirements: while one arrangement may be suitable for driving an alternator under varying load at constant speed, another may be more suitable for driving a ship's propeller where the power varies as the cube of the speed.

2.1.3 Major Gas Turbine Components

The following section contains an introduction of the major components that make up a gas turbine engine.

Compressor

The purpose of a compressor is to increase the total pressure of a gas stream with the lower shaft power consumption. The types of compressor used in gas turbines fall into two categories: centrifugal and axial compressors. These compressors have different operating performance, specially in terms of efficiency and pressure ratio, which makes them suitable for different applications. Basically, axial flow compressors dominate in applications where low frontal area, low weight and high efficiency are essential, which make them the only choice for large gas turbines. On the other hand, centrifugal compressors dominate in small size units where cost is a priority. The suitability of axial and centrifugal compressors can also be assessed through the mass flow ranges required by the application, as it is shown in table 2.1.1. According to Walsh and Fletcher (2004),

	Aircraft Engines (kg/s)	Industrial , marine and automotive engines (kg/s)
Predominantly Centrifugal	< 1.5	< 5
Centrifugal or axial depending upon requirements	1.5 - 10	5 - 15
Predominantly Axial	> 10	> 15

Table 2.1.1: Mass flow ranges suited to axial and centrifugal compressors [Wal+04]

centrifugal compressors are mostly used in automotive engines, where low unit cost outweighs a low frontal area and weight.

Turbines

A turbine is a component that extracts power from a gas stream to drive either engine compressor, or, in the case of a power turbine, a load such as a propeller or electrical generator. There are two types of turbine used in gas turbines, which consist in the axial-flow and the radial-inflow type. The axial-flow turbine is used in more than 95% of all applications [Boy02]. Like the compressors, the turbines with an axial geometry are preferable in applications in which it is required low frontal area, low weight and high efficiency, contrarily to the radial ones that are more suitable for low cost units with small size.

Heat-Exchangers

In gas turbines, the number of compressors and turbines are not limited to one stage. More compressors and turbines can be added, with intercoolers between the compressors, and reheat combustion chamber between the turbines. A heat-exchanger, which uses some of the energy stored in the exhaust gases to preheat the air entering the combustion chamber, may also be introduced. The heat transferred increases combustor inlet temperature and hence reduces the fuel required to achieve a given turbine inlet temperature, improving the cycle efficiency. The thermal efficiency of small gas turbines, with a power range between 5 - 200 kW, is about 20% or less if no heat-exchanger is used in the system [Sha05]. According to Shah (2005), using a heat-exchanger operating at 87% effectiveness, the efficiency of the gas turbine system increases to about 30%, a substantial performance improvement.

Two types of heat-exchangers can be identified: recuperators and regenerators. Whereas heat transfer occurs through the passage walls of a recuperator, a regenerator physically transports heat between streams. During the 70's, rotating ceramic regenerators were generally used in the gas turbines for automotive applications. Nowadays, metallic recuperators, in spite of their somewhat lower effectiveness and higher volume, are preferable due to their advantage of negligible leakage [OS05].

2.1.4 Category of Gas Turbines

The gas turbine has proved itself to be an extremely versatile prime mover and has been used for a wide variety of functions, ranging from electric power generation, mechanical drive systems and jet propulsion. Of the various means of producing mechanical power, the turbine is in many respects the most satisfactory. The absence of reciprocating and rubbing members means few balancing problems, an exceptionally low lubricating oil consumption and high reliability.

Gas turbines for power generation can be classified into five broad groups [Boy02]:

- *Frame Type Heavy-Duty Gas Turbines*: The frame units are the large power generation units raging from 3MW to 480MW in a simple cycle configuration, with efficiencies raging from 30-46%.
- *Aircraft-Derivative Gas Turbines*: As the name indicates, these are power generation units, which have origin in the aerospace industry as aircraft prime movers. These units have been adapted to the electrical generation industry by removing the bypass[3] fans, and adding a power turbine at their exhaust. These units range in power from 2.5MW to about 50MW. The efficiencies of these units can range from 33-45%.
- *Industrial Type Gas Turbines*: These vary in range from about 2.5MW-15MW. This type of turbine is used extensively in many petrochemical plants for compressor drive trains. The efficiencies of these units is in the low 30s.
- *Small Gas Gas Turbines*: These gas turbines are in the range from about 0.5MW-2.5MW. They often have centrifugal compressors and radial inflow turbines. Efficiencies in simple cycle applications vary from 15-25%.
- *Micro-Turbines*: These turbines are in the range from 20kW-350kW. The growth of these turbines has been dramatic from the late 1990's, as there is an upsurge in the distributed generation market.

2.1.5 Road Vehicle Applications

In the late 1960's, research scientists in California managed to relate the *smog* in the air of certain U.S. cities to a complex photochemical reaction involving nitrogen oxides (NOx) and hydrocarbons (HC). Both of these compounds are found in automotive exhaust gases, which led to strict national legislation affecting the exhaust, crankcase and fuel systems of the automobile. These strict vehicle emissions standards actually enabled the gas turbines to be seriously considered for automobile applications. Since, the compressor of a gas turbine supplies several times the amount of the theoretically required air for complete fuel combustion, the exhaust gases are relatively free from smoke and emit less levels of hydrocarbon (HC) and carbon monoxide (CO), compared to piston engines. The only type of emissions that gas turbines emit in higher levels is the nitrogen oxide (NOx); however, there are some promising modifications which may reduce NOx emissions to the compliance level [Chr79]. According to Boyce (2002), new research in combustors such as catalytic combustion have great promise, and values of as low as 2 ppm are expected to be achieved in the future.

Gas Turbine versus Reciprocating Engine

The gas turbine constitutes the third basic type of internal combustion engine. Unlike, the spark ignition (gasoline) and compression ignition (diesel) engines, gas turbines operate in a continuous combustion mode. It is important to realize that, in a gas turbine, the compression, combustion and expansion processes do not occur in a single component as they do in a reciprocating engine. They occur in components which are separated, in the sense that they can be designed, tested and developed individually, and thereafter linked together to form a gas turbine unit in a variety of ways.

Single and Twin-Shaft Gas Turbines

Gas turbines can be arranged either in *single-shaft* or *twin-shaft* configuration. The *single-shaft* arrangement requires the turbine to provide power to drive both the compressor and the load, which means that the compressor is influenced by the load (figure 2.1.6a). Since the compressor efficiency is a function of the speed,

[3]Bypass engines incorporate large fans of high flow and low pressure rise; part of the flow bypasses the core providing a second exhaust jet of low velocity.

at low shaft speed the compressor will be inefficient and the output torque will be very low. Therefore, the *single-shaft* gas turbine type is appropriate for fixed speed operation, such as propelling an aircraft [Ing95]. Considering automotive applications, where the engine operates at continuously variable loads and speeds, the twin-shaft configuration, due to its operating mode, seems to be the most suitable gas turbine arrangement. At this configuration, the sole function of the first-stage turbine is to drive the compressor at steady speed without being influenced by the load, while the net power of the gas turbine is produced by the "free" turbine, as shown in figure 2.1.6b [Wu04].

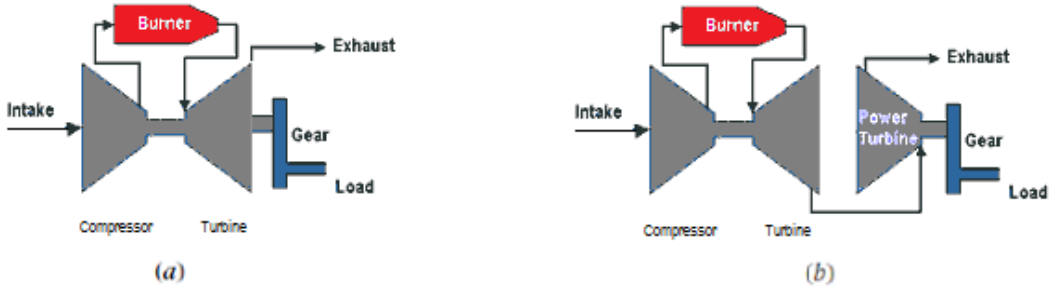

Figure 2.1.6: *Gas Turbine Configurations: a) Single-shaft; b) Twin-shaft*

This feature means that the gas generation can operate at high speed and power output, while the power turbine is at low speed. As shown in figure 2.1.7, a *twin-shaft* gas turbine offers excellent torque at low engine output speeds, which better matches the vehicle requirements, specially for hill climb and acceleration conditions.

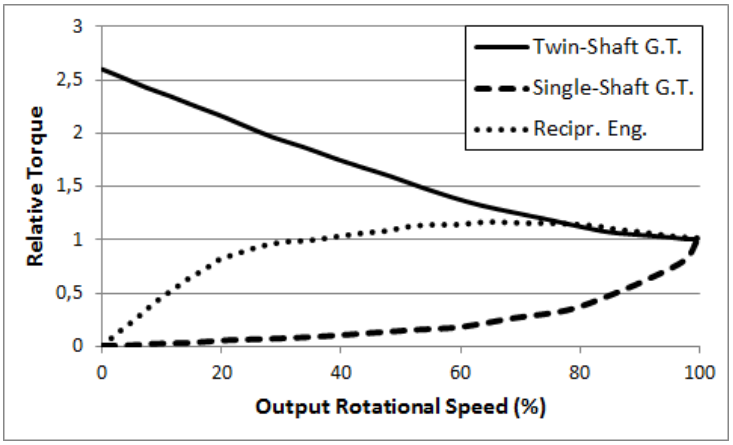

Figure 2.1.7: *Relative Torque vs. Output Rotational Speed (based on data from [Wal+04])*

In other words, the *twin-shaft* gas turbine torque is greatest at breakaway, from a standing position, and decreases as the car speed increases, where it is less necessary. This contrasts with the reciprocating engine torque, which builds to a maximum in the mid-speed range and then declines (see figure 2.1.7).

Gas Turbine Advantages

Beyond its better torque capability (twin-shaft arrangement), as illustrated in figure 2.1.7, the main benefits of the gas turbine as an automotive power plant are its light weight, compactness and reliability. Its high reliability results from the reduced number of moving parts (approximately 80% less than a piston engine), which means a vibration free engine operation with few balancing problems (absence of reciprocating and rubbing), low lubricating oil consumption and lower on-going costs due to the reduced maintenance. Another advantage of a gas turbine engine, over the spark and compression-ignition engines, is its capacity of operating satisfactorily with a variety of fuels, including kerosene, diesel fuel, natural gas, hydrogen and others [Chr79].

Gas Turbine Disadvantages

The major disadvantage of a gas turbine is its extremely low efficiency under no load or partial load, which constitutes a considerable fraction of the actual operation in an automotive application. Even at idle conditions, turbines turn at very high rotational speeds *(around 20000 rpm)* and thus consume considerable amounts of fuel. Another drawback is the relatively long time that gas turbine spools require for accelerating from idle to full load. This slow throttle response, usually called *acceleration lag*, is even more pronounced in a *twin-shaft* configuration, where the acceleration time depends upon the "free" turbine inertia, as well as the inertia and loading characteristics of the driven equipment [Wal+04]. A final problem of employing the gas turbine as an automotive power plant is its high production costs. An estimate from the 70's reveals that a production volume of 400 gas turbines per day would cost two and a half times more than an equivalent piston engine production [Nor74]. Ingersoll (1995) points out a cost of $125 per hp for a mass production of automotive gas turbines, a cost that is still five or six times higher than the cost of a good spark ignition engine.

Previous Projects

Light Road Vehicles

Due to environmental issues, a considerable amount of work was done in gas turbines for cars, specially during the 60's and 70's, in the US with a great support from the government. Chrysler Corporation was the American car manufacturer that conducted the larger number of experiences with gas turbine-powered cars. During that period, Chrysler achieved significant advances in fundamental gas turbine engine technology by running experiments with gas turbines not only on dynamometers but also in test vehicles. As a result, several prototypes were demonstrated, including the *Chrysler Gas Turbine*, as shown in figure 2.1.8a [Chr79]. By its turn, Volkswagen began its turbine program in 1964, when Chrysler had 50 turbine cars running in everyday use by individual users in a giant field test. To shorten the development time, Volkswagen signed a contract with Williams Research Corporation in order to have access to Williams' know-how and patents. With a gas turbine model rated at 75 hp, the *VW* turbine program aimed at powering small cars, such as the *VW Squareback sedan*, illustrated in figure 2.1.8b [Nor74].

Figure 2.1.8: *Light Road Vehicles: a) Chrysler Gas Turbine [Chr79]; b) VW Squareback [Nor74]*

More recently, General Motors created the *Ecojet* in 2006 (figure 2.1.9). This concept car uses a helicopter turbine engine, with 650 hp and 790 Nm, and resulted from the desire of a millionaire customer of having a modern sports car powered by a gas turbine [Jay].

Figure 2.1.9: *GM Ecojet [Jay]*

Heavy Road Vehicles

The gas turbine capability to operate on a wide range of fuels and its exceptional torque characteristics played an important role, not only in the automotive industry but also among truck manufacturers. The 1965 *Chevrolet Turbo Titan III* and the 1972 *GMC Astro Gas Turbine* are some of the many operational prototypes that ran test beds aiming at a possible future production (see figure 2.1.10) [Nor65]. The efforts toward the conception of the full-size truck for the heavy-duty market were compromised by the manufacturing costs, the continuing technology refinement and the strict Government regulations, concerning NOx emissions, that could not be complied. By the end of the 70's, almost all gas turbine truck programs were canceled [Sen03].

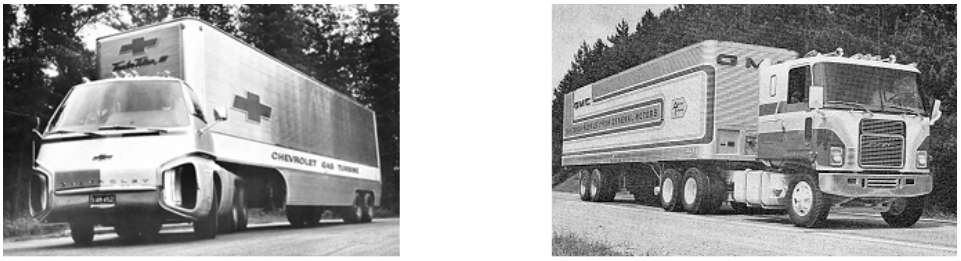

(a) (b)

Figure 2.1.10: *Heavy Road Vehicles: a) Chevrolet Turbo Titan III; b) GMC Astro Gas Turbine [Sen03]*

Racing Vehicles

The gas turbine also left its mark on the racing tracks. The first racing turbine car, the *Rover-BRM*, participated in 1963 at the 24 hours of Le Mans and achieved a top speed of 235 km/h. The 8th position in the overall ranking, with 4133 km recorded, proved the reliability of this technology for racing purposes. The fuel consumption of 45 l/100km was an acceptable value for racing use [Aut]. This type of engine also made its appearance in Formula 1 in 1971, through the Lotus Team (*Lotus 56*). This turbine car had important differences, specially in terms of power: 600 hp compared with the 425 hp from the traditional engines. The turbine was smaller and lighter than a regular piston engine, the drivetrain was simpler and there was no need for cooling system; however, the acceleration lag, associated to gas turbines operation, determined the end of this project two years after its first race [F1j].

(a) (b)

Figure 2.1.11: *Racing Vehicles: a) Rover-BRM [Aut]; b) Lotus 56 [F1j]*

Hybrid Configuration

The attempts in the past to develop gas turbines for road vehicle applications have failed to produce viable competitors to spark ignition and compression ignition engines. However, the interest in gas turbines has been revived in the last decades with regard to the hybrid electric vehicle propulsion system. A hybrid electric vehicle is a vehicle that combines an electric propulsion systems with, at least, another type of energy source, store or converter. This solution poses a compromise between reducing environmental pollution and the limited range capability of today's purely electric vehicles. In this configuration, the gas turbine is only used for maximum power and for charging the vehicle's propulsion batteries, which solves many of the drawbacks previously attributed to this type of energy converter. The use of single-shaft units, operating at constant speed and power, overcomes the problem of the gas turbines part-load fuel consumption, and since this arrangement uses electric power to accelerate the vehicle, the slow throttle response associated to gas turbines operation does not constitute a disadvantage anymore.

A few number of prototype vehicles have been developed in recent years using hybrid drivetrains. In 1993, General Motors introduced the first commercial gas turbine powered hybrid vehicle with a limited production run of the *EV-1 series hybrid*. The powertrain of this model is based on a Williams International 40 kW turbine that drives an alternator to power the battery-electric powertrain [Ev1]. In the same year, Volvo unveiled the *Environmental Concept Car* (ECC), based on the 850 production model (see figure 2.1.13). This vehicle achieves a maximum speed of 180 km/h, requires 13 seconds to accelerate from 0-100 km/h and registers an average fuel consumption of 5.5 l/100km; quite satisfactory results for a vehicle that weights 1500 kg [Ing95]. However, it has not only been the major automobile manufacturers to develop efforts in this area. In 2009, ETV Motors, a developer of advanced energy generation and storage technologies for automotive applications, presented a modified Toyota Prius equipped with a micro-turbine generator as range extender to the propulsion batteries [Etv]. Also the micro-turbines producer Capstone Turbine Corporation developed the *CTM-380*. Entitled as the world's first micro-turbine-powered supercar, this hybrid sports car achieves a top speed of 240 km/h (electronically limited) and an acceleration of 0-100 km/h in 3.9 seconds, always with an extremely high fuel economy and reduced greenhouse gas emissions [Cap]. The most recent study unveiled by the automotive industry is the *Jaguar C-X75* (see figure 2.1.12). This concept car uses a pair of twin-shaft micro-turbines acting as range extenders, a solution that Jaguar claims to be even cleaner than the current hybrids, with just 28g of CO_2 emitted per km. In May 2011, Jaguar confirmed its intention of launching this hybrid supercar in the market by 2013. Jaguar claimed that, in order to bring this project to showroom reality within the timescales of a conventional model programme, the micro-turbines will be replaced by a conventional internal combustion engine in the commercial version. However, Jaguar will continue to develop the use of the micro-turbine technology that was showcased in the original concept. As proof of that, Jaguar has taken a significant stake in Bladon Jets (a micro-turbines producer), and publicly acknowledged that would continue the development of this technology as a medium-term aspiration for its future vehicles [Jag].

Figure 2.1.12: *Jaguar C-X75 [Jag]*

In terms of heavy vehicles, Volvo developed in the early 1990's, both the *Environmental Concept Truck* (ECT) and the *Environmental Concept Bus* (ECB), two prototypes that served as a test platform for ideas to be incorporated in the future series-produced Volvo trucks and buses (see figure 2.1.13). A hybrid propulsion system with a gas turbine (developed within the Volvo organization) was chosen with the purpose of achieving a combination of both zero-emissions in sensitive environments (such as urban areas) and the possibility of driving any distance. Currently, tests are being carried out in secret in laboratories and in selected test vehicles as a test bed for the future [Vol].

Figure 2.1.13: *Volvo Environmental Concept Vehicles: ECT, ECB, ECC [OS05]*

2.1.6 New Technology in Gas Turbines

The gas turbine technology has been suffering a continuous evolution since its inception. In the last decades, research on automotive gas turbines has focused in raising the operating turbine inlet temperature in order to increase the thermodynamic efficiency, i.e. fuel efficiency. For example, Chrysler engineers stated that the increase of 400 ° in the nozzle inlet temperature would mean a 40% increase in the specific output power for a given size power plant, or conversely, a reduction in size for a fixed horsepower. The same 400 ° would, at the same time, improve fuel economy over 20% without needing to take advantage of any further increase in component efficiency [Chr62]. Computer design, specifically Computational Fluid Dynamics (CFD) and finite element analysis, along with material advances allow to reach, not only higher temperatures, but also higher compression ratios, a more efficient combustion and better cooling of the engine parts. It is important to note that the processes involved are still complex and require expensive materials, which means that further engineering development is needed to make gas turbines a viable technology, capable of competing with reciprocating engines in road vehicle applications.

2.2 Vehicle Energy and Fuel Consumption

This section is subdivided in two parts. In the first one, it is analyzed the dynamics of the longitudinal motion of a road vehicle and the main energy consuming effects occurring in the vehicle drive. The second part introduces the most important approaches used to predict the fuel economy of road vehicles.

2.2.1 Vehicle Performance Analysis

To move a vehicle forward, a propulsive force must be delivered by the engine. This force is also known as tractive force F_t, and it must be such to overcome the resisting forces, which can be described as the sum of the following [Wal+04]:

- Aerodynamic Drag Force, F_d
- Rolling Resistance Force, F_r
- Gravitational Force, F_g
- Acceleration Force, F_a

The tractive force is as follows:

$$F_t = F_d + F_r + F_g + F_a \tag{2.2.1}$$

The forces acting on the vehicle are shown in figure 2.2.1:

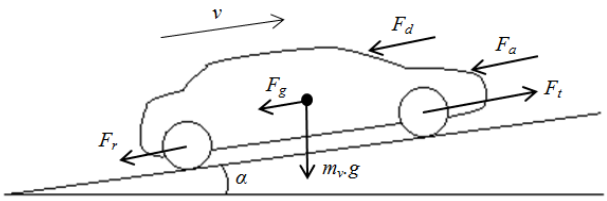

Figure 2.2.1: *Schematic representation of the forces acting on a vehicle in motion*

Aerodynamic Drag Force

The aerodynamic resistance F_d is the result of the viscous friction of the surrounding air on the vehicle surface and the pressure distribution of the air over the body, working against the motion of the vehicle. Aerodynamic resistance is caused mainly by the car body, but other items like the wheel housing, the external mirrors or the engine ventilation also have an important contribution to the aerodynamic drag coefficient C_D. This parameter can be estimated using CFD programs or experiments in wind tunnels. To simplify the calculation of the aerodynamic drag force, the vehicle is considered to be a body with a frontal area A_f. The force is given by

$$F_d = \frac{1}{2}.\rho.A_f.C_D.v^2 \tag{2.2.2}$$

where ρ is the air density.

Rolling Resistance Force

The rolling resistance force is often given by the following

$$F_r = c_r.m_v.g.\cos\alpha \tag{2.2.3}$$

where m_v is the total mass of the vehicle, g is the gravitational acceleration constant, and α is the grade angle with respect to the horizon. The rolling resistance coefficient c_r depends on many variables. The most important influencing quantities are the tire pressure p, the road surface conditions and the vehicle speed.

The primary cause of rolling resistance is the tyre hysteresis[4] that promotes repeated cycles of deformation and recovery of the tyre, resulting in the dissipation of energy in the form of heat. Rolling resistance can be minimized by keeping the tires as much inflated as possible (increase p), which reduces the hysteresis. To evaluate the rolling resistance depending on the surface conditions, table 2.2.1 provides typical coefficients for radial tyres.

Surface	Coefficient of rolling friction
Paving stones	0.015
Smooth concrete	0.015
Rolled gravel	0.02
Tarmacadam	0.025
Dirt road	0.05
Tracked vehicle on arable soil	0.07-0.12

Table 2.2.1: Rolling resistance coefficients for radial tyres on various surfaces [Wal+04]

Vehicle speed has a small influence at lower speeds, but its influence substantially increases when it approaches a critical value. As simplification, the rolling resistance coefficient may be assumed to be constant.

Gravitational Force

The gravitational force is the force caused by the gravity when driving on non-horizontal roads, i.e. it depends on the slope of the roadway. The force is positive when climbing a grade and is negative when descending a downgrade roadway. The gravitational force to be overcome by the vehicle moving forward is

$$F_g = m_v.g.\sin\alpha \tag{2.2.4}$$

where m_v is the total mass of the vehicle, g is the gravitational acceleration constant, and α is the grade angle with respect to the horizon.

Acceleration Force

To change the vehicle speed it is necessary to apply a force beyond the ones already mentioned. This force is based on the Newton's second law which is given by

$$F_a = m_v.a \tag{2.2.5}$$

This equation takes into account the inertia force induced by the vehicle mass (m_v), but not the inertia associated to the rotating mass of both powertrain and drivetrain. Nevertheless, for simpler calculations, it may be convenient to add the inertia of the rotating parts to the vehicle mass. The inertia torque associated to the wheels is given by

$$T_w(t) = I_w.\frac{d}{dt}.w_w(t) \tag{2.2.6}$$

where I_w is the inertia of all rotating parts that are present on the wheel side of the gearbox, and w_w is the correspondent rotating speed. This torque acts in the vehicle as an additional inertia force

$$F_w(t) = \frac{T_w(t)}{r_w} \tag{2.2.7}$$

where r_w is the wheel radius. Usually, the wheel slip is not considered in a first approximation, i.e. $v = r_w.w_w$. In this case

$$F_w(t) = \frac{I_w}{r_w^2}.\frac{d}{dt}.v(t) \tag{2.2.8}$$

Consequently, the equivalent mass of the rotating parts from the drivetrain is given by the following term

$$m_w = \frac{I_w}{r_w^2} \tag{2.2.9}$$

[4]Hysteresis is a characteristic of deformable materials. In the case of the tyres, it is attributed to the viscoelastic characteristics of the rubber.

The same can be applied to the rotational parts of the engine, assuming a constant gear ratio γ.

$$T_e(t) = I_e.\frac{d}{dt}w_e(t) = I_e.\frac{d}{dt}(\gamma.w_w(t)) = I_e.\frac{\gamma}{r_w}.\frac{d}{dt}v(t) \tag{2.2.10}$$

$$F_e(t) = \frac{\gamma}{r_w}.T_e(t) = I_e.\frac{\gamma^2}{r_w^2}.\frac{d}{dt}v(t) \tag{2.2.11}$$

$$m_e = \frac{\gamma^2}{r_w^2}.I_e \tag{2.2.12}$$

Note that in these equations it is considered a gearbox with an efficiency of 100%, i.e. without losses. However, these losses can be considered in the inertia force by the following

$$F_e(t) = I_e.\frac{\gamma^2}{r_w^2.\eta_{gear}}.\frac{d}{dt}v(t) \tag{2.2.13}$$

where η_{gear} is the efficiency of the gearbox system.

The calculation of the tractive force, based on the previous formulae, allows the assessment of the power and energy required to drive a vehicle in a pre-specified driving pattern.

2.2.2 Methods for the Prediction of Fuel Consumption

In order to analyze the efficiency of the propulsion system for a road vehicle, and consequently, the correspondent fuel consumption, there are three possible approaches [Guz+07]:

- Average Operating Point Approach
- Quasistatic Approach
- Dynamic Approach

Average Operating Point Approach

This method is often used as the first assessment of the fuel consumption of a road vehicle. This approach implies the estimation of one single representative average engine operating point, based on a specific test cycle, that requires to be specified *a priori*. With the engine regime assessed, the mean mechanical power at the wheel P_v can be estimated. In order to assess the fuel consumption of the propulsion system it must be considered the efficiencies associated to the following vehicle components:

- powertrain/engine (η_e)
- drivetrain, which implies the gearbox and differential (η_g)
- all auxiliary devices, such as power steering, generation of electric energy, etc (η_a)

With the fuel power consumed by the engine (P_f), the overall power balance

$$P_v = \eta_e.\eta_g.\eta_a.P_f \tag{2.2.14}$$

permits the computation of the mean fuel mass flow

$$\dot{m_f} = P_f/H_f \tag{2.2.15}$$

where H_f is the fuel's lower heating value. The average operating point method is able to yield reasonable estimates of the fuel consumption of simple powertrains (IC engines or battery electric propulsion systems), however it is not well suited to problems in which complex propulsion systems must be optimized.

Quasistatic Approach

A quasistatic approach is very similar to the average operating point method. The only difference is that, in the quasistatic simulation the test cycle is divided into several intervals in which the average operating point method is applied. For each time interval, the input variables are the speed v and the acceleration a of the vehicle, as well as the grade angle α of the road. These parameters are assumed to be constant in each step, which must correspond to a time interval small enough in order to satisfy this assumption. Usually this time interval is constant and has a value equal to one second [Guz+07]. The force required from the vehicle powertrain, at each time step, is calculated directly from the speed trace of the driving cycle that is being simulated (formula 2.2.1). After that, the simulation determines the torque and speed necessary to overcome the inertial forces of the vehicle and reach the desired velocity. The quasistatic simulation may also be designated as *backward-facing* approach [Sam+10], since the calculation proceeds backwards from the tire/road interface through the drivetrain, ending with the energy source (engine and fuel tank). In this approach, the fuel consumption necessary to sustain a pre-defined torque and speed combination is determined by the engine efficiency map, directly mapped into the torque-speed plane, as figure 2.2.2 illustrates. When the driving profile contains coasting or slow-speed phases, the propulsion system operates at idle, with a pre-defined idling fuel consumption. In the case of reciprocating engines, if the deceleration of the car provides enough power to cover, in addition to the aerodynamic and rolling friction losses of the vehicle itself the losses of the complete propulsion system (friction losses of the powertrain, power consumed by the auxiliaries, engine friction and pumping losses, etc.), the fuel may be completely cut off.

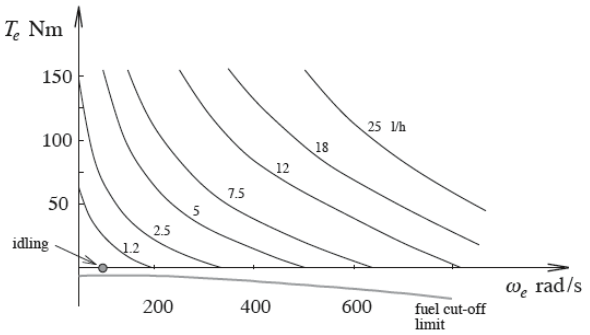

Figure 2.2.2: *Reciprocating engine fuel consumption (l/h) as function of engine torque and speed [Guz+07]*

The quasistatic approach is well suited to the fuel consumption minimization of complex powertrain structures, allowing, for instance, the assessment of the influence of the driving pattern in these calculations. Despite these capabilities, the numerical effort remains relatively low allowing simple and fast calculations. The main drawback of the quasistatic method is its *backwards* formulation. Since it is assumed that the vehicle meets the pre-defined speed trace, this approach is not suited to analyze best-effort performance, for instance acceleration tests. Therefore, this method is not able to study control systems due to the lack of throttle and brake information. A simplified block diagram of a generic quasistatic simulation approach is presented in figure 2.2.3.

Figure 2.2.3: *Generic Diagram of Quasistatic Approach*

Dynamic Approach

In contrast to the quasistatic approach, in the dynamic approach the inputs of the powertrain model are the same as the ones present in the real propulsion systems. In this method there is a module that simulates the behavior of the driver by inputting the throttle position and braking based on the desired speed. These inputs are used to calculate the torque and energy use rate applied to the drivetrain. The computation proceeds forward from the engine, through the transmission and finally to the wheels, resulting in the calculation of a tractive force at the tire/road interface. For this reason, this method may also be called *forward-facing* approach. The versatility of this method, that is illustrated in figure 2.2.4, makes it desirable in detailed control

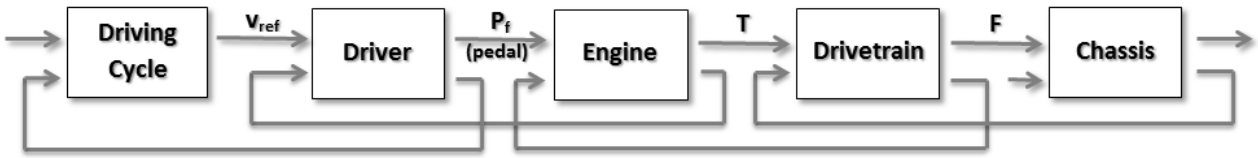

Figure 2.2.4: *Generic Diagram of Dynamic Approach*

simulations and hardware development. The design of feedback control systems is an example of an optimization problem that can only be solved using this method. The drawback of using a dynamic approach is its relatively high computational demand, turning this into a too much time-consuming approach for preliminary design. For this reason the quasistatic method is the most used approach for predicting road vehicles fuel consumption, being the dynamic methods practically used when no other option is available [Guz+07].

2.3 Drivetrain System

Vehicles' drivetrain, also called transmission, refers to the set of devices that provides power output from the engine to the wheels. The whole drivetrain includes, in most cases, the gearbox, clutch, differential and final drive shafts. In almost all vehicle applications, the engine output speed differs from that of the wheels. Such engines need to operate at a relatively high rotational speed, which is inappropriate for starting, stopping, and slow travel. The transmission reduces the higher engine speed to the slower wheel speed, increasing torque in the process. To obtain a good acceleration performance as well as good fuel consumption, the main requirements of a transmission are a sufficient ratio coverage and a smooth operation. For conventional drivetrains, the demand for higher efficiency and better dynamic performance has led to an increase of ratio coverage for transmissions. In the 60's, it was common the use of three or four gear ratios, but today the most usual gearboxes have 5 or 6 gears ratios. In addition, shifting without torque interruption (smooth operation), thereby increasing the dynamic performance, is the latest development in the field of transmissions: *Dual Clutch Transmission* (DCT) and *Continuously Variable Transmission* (CVT) [Hof+01]. The most relevant transmissions that are involved in conventional vehicles are discussed in the following section.

2.3.1 Gearbox Topologies

The automobile transmission systems can be classified into two types, manual and automatic transmissions.

Manual Gearbox

Manual transmissions are characterized by selectable gear ratios operated by the driver. They generally use a driver-operated clutch, typically actuated by a pedal or lever, for regulating the torque transferred from the engine to the transmission. In this process, the driver has more direct control over the vehicle, which may be an advantage in situations of rapid acceleration, such as when overtaking on the highway, since it is possible to put into a lower gear ahead. Because manual transmissions are mechanically simple and have few moving parts, they require low maintenance and are easy to repair. The losses associated to this type of gearbox are related to the friction of its involved components rotating in oil [Hyb].

Automatic Gearbox

In an automatic transmission the gears are changed automatically depending on the vehicle speed. This type of transmission can be accomplished in several ways, but the traditional solution uses a hydraulic torque converter that essentially replaces the function of a clutch. The slippage that takes place in the torque converter increases the losses of this type of gearbox compared to the losses in a manual shift transmission. It yields an average efficiency of 86%, compared to a typically manual transmission with 97% efficiency [Lan00]. Automatic transmissions are easy to use, but their complexity and the high number of components make them an expensive investment with a costly maintenance.

Continuously Variable Transmission

Continuously Variable Transmission (CVT) is another possible type of automatic transmission. CVTs are mechanically designed to provide an infinite number of gear ratios, and thus enable the engine to operate close to the called *Optimal Operation Point*[5], resulting in an increased fuel economy. The most common CVT design is the one constituted by a v-shaped drive belt and two pulley sets, as it is illustrated in figure 2.3.1. On both pulley sets, one sheave is fixed and the other can move in the axis direction. The moveable pulley is hydraulically actuated. By moving the pulley, the running radius of the drive belt and therefore the shaft speed can be varied and the continuously variable ratio is realized [Bog06]. CVTs offer improved efficiency over conventional automatic transmissions, as is described in the table 2.3.1, and their efficiency depends less on the driving habit than manual transmissions. On average, the CVT solution offers an efficiency around 90 %, a value between the traditional automatic gearbox and the manual transmission efficiencies [Hyb].

[5]The *Optimal Operation Points* are the engine torque-speed combinations in the entire engine power range, with the minimum specific fuel consumption.

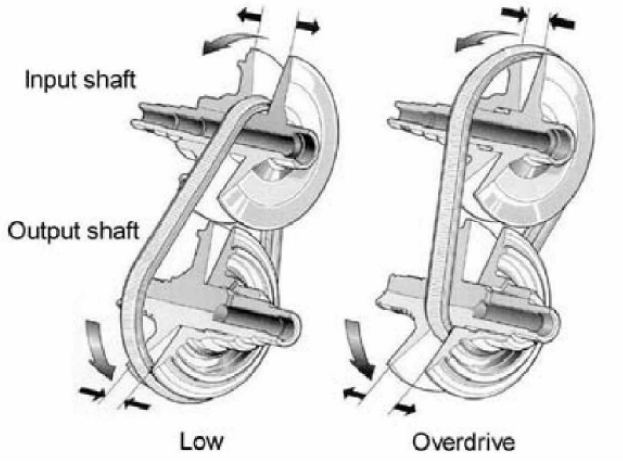

Figure 2.3.1: *Schematic presentation of a Continuously Variable Transmission (belt mechanism)*

CVT Mechanism	Efficiency Range
Rubber Belts	90 - 95 %
Steel Belts	90 - 97 %
Toroidal Traction	70 - 94 %
Nutating Traction	75 - 96 %
Variable Geometry	85 - 93 %

Table 2.3.1: Efficiency of various CVT designs [Lan00]

Although CVTs have all these inherent advantages, the development of this kind of transmission has progressed slowly for a variety of reasons. Perhaps more than anything else, CVTs development has been hampered by cost. Low volume and lack of infrastructures have driven up manufacturing costs, which inevitably yield higher transmission prices. One of the major complaints with previous CVTs has been the slippage in the drive belt or rollers. This is caused by the lack of discrete gear teeth, which form a rigid mechanical connection between the gears. Friction drives are inherently prone to slip, especially at high torque, however new developments in this area have enabled the most recent CVTs to tolerate a maximum torque load up to 386 Nm (285 lb-ft). In addition, CVTs require the implementation of a controller. Manual transmissions have manual controls, i.e. the driver shifts when desired; automatic transmissions have relatively simple shifting algorithms to accommodate between three and five gears. However, CVTs require far more complex algorithms to accommodate an infinite division of speeds and gear ratios. Much of the delay in the CVTs development could also be attributed to this fact, nevertheless CVT control has recently come to the forefront of research and more refined CVTs have been developed. Due to the benefits associated to this type of transmission, several auto-makers are currently studying the implementation of CVTs in their vehicles, a scenario that will foster the development of this technology [Lan00].

2.3.2 Selection of Gear Ratios

Considering vehicular applications, the ideal power plant should have a performance characteristic with a constant output power (P) over the entire vehicle speed range. This constant power characteristic provides the vehicle with a high tractive effort at low speeds, i.e. in situations where demands for acceleration or grade climbing capability are high. In this ideal profile, the torque (T) varies hyperbolically with speed (w), according to formula 2.3.1.

$$T = P/w \tag{2.3.1}$$

However, at low vehicle speeds the maximum torque is limited by the tyres traction on the road, as shown in figure 2.3.2.

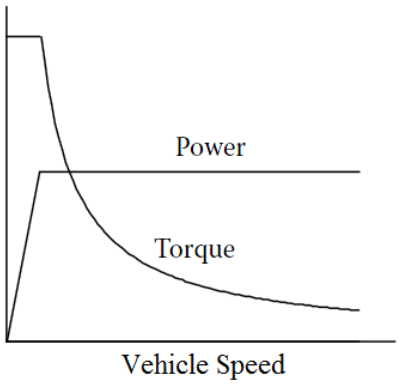

Figure 2.3.2: *Ideal performance characteristics for a vehicle traction power plant [Ehs+10]*

Reciprocating Engine

In the case of reciprocating engines, the torque-speed profile is almost flat compared to an ideal power plant, as described in figure 2.3.3.

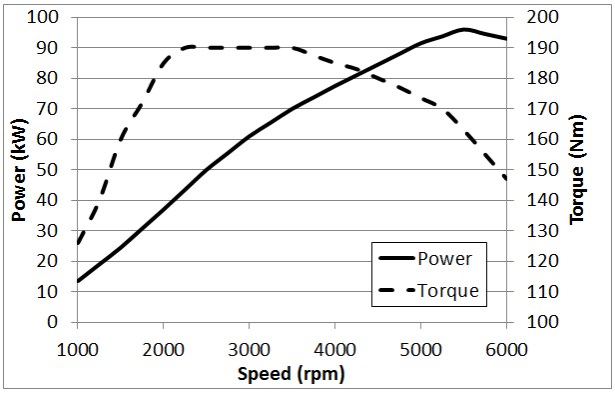

Figure 2.3.3: *Engine performance of a 96kW reciprocating (petrol) engine (based on data from [Ren])*

Consequently, a multi-gear transmission is usually employed in order to convert the piston engine torque characteristic closer to the ideal one, as illustrated in figure 2.3.4. The performance of a vehicle is usually described by its maximum cruising speed, gradeability[6], and acceleration. The achievement of the required performance is made by the choice of the adequate gear ratios. The maximum gear ratio (the lowest gear in a manual gearbox) is determined by the requirement of the maximum tractive effort or gradeability. On the other hand, the smallest gear ratio (the highest gear in a manual gearbox) can be chosen either to reach the top-speed limit or to maximize the fuel economy. These two approaches can be combined by choosing the second-smallest gear to satisfy the maximum speed requirements and the smallest gear to maximize the fuel economy ("overdrive" configuration) [Hyb].

[6]Gradeability is usually defined as the grade (or grade angle) that the vehicle can overcome at a certain constant speed.

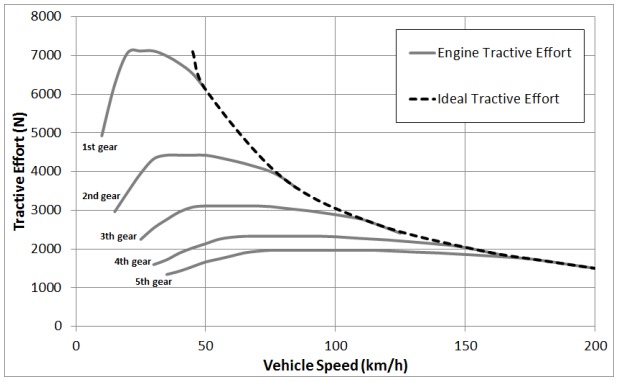

Figure 2.3.4: *Tractive effort characteristics of a 96kW reciprocating engine powered vehicle*

Gas Turbine Engine

As described in section 2.1.5 and shown in figure 2.3.5, a gas turbine engine in a twin-shaft configuration offers excellent torque and power at low engine output speeds for hill climb and vehicle acceleration. This is achieved by operating the gas generator at high speeds and output power while the power turbine is at low speeds.

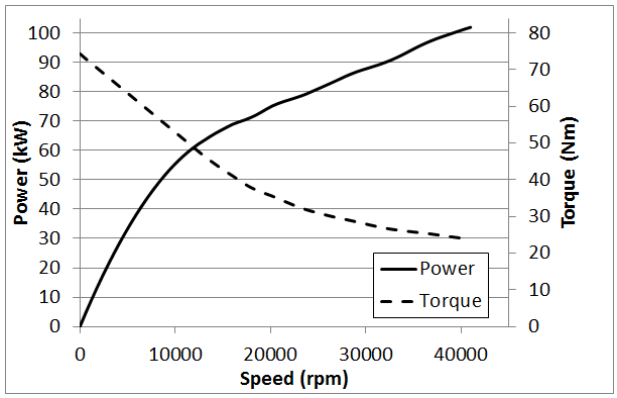

Figure 2.3.5: *Engine performance of a 102kW twin-shaft gas turbine*

Since the speed-torque profile is much closer to the ideal one, the twin-shaft gas turbines only require a small number of gears, as demonstrated in figure 2.3.6.

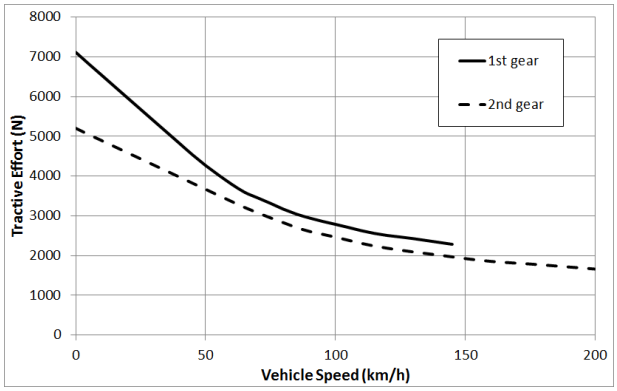

Figure 2.3.6: *Tractive effort characteristics of a 102kW twin-shaft gas turbine powered vehicle*

3 Methodology

3.1 Gas Turbine Modeling

The design process of an engine starts from a specification, resulting from either market research or a customer requirement. The specification is rarely a simple statement of required power and efficiency, but a junction of several factors such as weight, cost, volume, life or noise, whose importance is strongly influenced by the engine application. An automobile gas turbine must be quieter and have a lower exhaust temperature than an aircraft gas turbine. The automobile engine must be also compact so it can fit in the engine compartment, and its manufacturing cost must be low so that it is within the reach of the average automobile buyer.

In gas turbines, the first major design step consists in carrying out thermodynamic design point studies. The *design point performance* stands for a reference point of the engine cycle in which the mass flows, total pressures and total temperatures at the inlets and exits of all components are calculated. These are detailed calculations in which the engine configuration, cycle parameters, components performance levels and sizes are selected to meet a given specification.

With the engine geometry fixed by the *design point calculations*, the performance of the gas turbine over the complete operating range of speed and power output can be evaluated. This operation condition is referred as *off-design performance*. All off-design calculations depend on satisfying the essential conditions of compatibility of mass flow, work and rotational speed between the various components.

3.1.1 Component Performance Characteristic

The variation of mass flow, pressure ratio and efficiency with rotational speed of the compressor and turbine is obtained from the compressor and turbine characteristics, respectively.

Compressor

It is convenient to represent the compressor characteristic as shown in figure 3.1.1, with the variation of isentropic efficiency along each constant corrected speed line plotted against both corrected mass flow and pressure ratio.

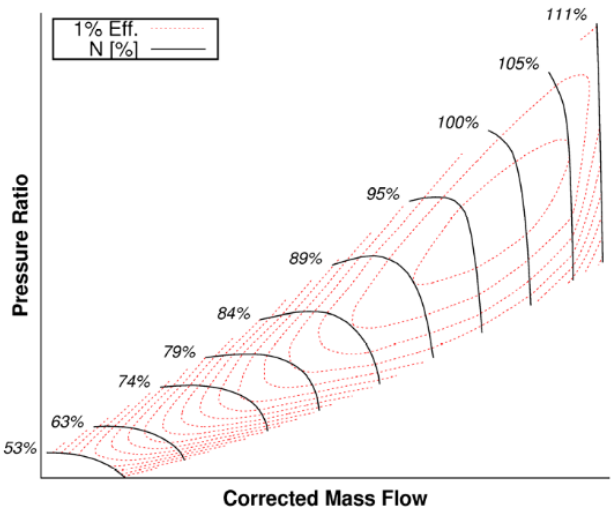

Figure 3.1.1: *Compressor Characteristic [Kyp11]*

Turbine

The turbine characteristic can be represented in the form given in figure 3.1.2.

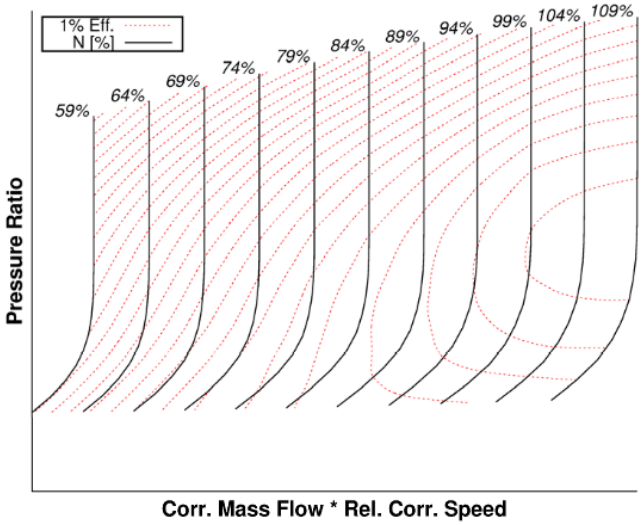

Figure 3.1.2: *Turbine Characteristic [Kyp11]*

For accurate calculations it is necessary to consider secondary effects such as the variation of pressure losses in the inlet ducting, the combustion chamber and the exhaust ducting. These considerations increase the accuracy but also the complexity of calculation routines, in such a way that they are ideally suited to digital computer programs, such as the commercially available software *GasTurb*.

3.1.2 Software Description

GasTurb started to be developed in the 90's by Joachim Kurzke, a gas turbine performance specialist who has worked for more than 30 years in the field of gas turbines simulation and development. *GasTurb* is a user-friendly software that evaluates the thermodynamic cycle of most common gas turbine architectures, both for engine design and off-design. In addition to the performance calculations, *GasTurb* also covers the preliminary geometrical design of engines, including disk stress calculations. The wide applicability, given by range and detail level of calculations, and the simplicity of use, connected with fine graphical output, make *GasTurb* a very professional software used not only for engine design, research and development, but also for tutoring of future turbine engine engineers [Kur11].

3.1.3 Proposed Models

In this study an attempt is made to assess the applicability of gas turbines in road vehicles. For this purpose, it is required the modeling of a suitable engine. However, the suitability of a given engine design to a certain application is complex and difficult to assess, since it depends up to a large number of key parameters.

Model 1: *Chrysler G.T. Model*

As a starting point, an engine was modeled based on a complete spec sheet of a gas turbine developed by Chrysler Corporation for automotive applications during the 60's [Chr79]. Chrysler Corporation engineers developed a practical automotive gas turbine, with a *regenerator* that recovers much of the heat from the exhaust gases, enabling the achievement of acceptable exhaust temperatures and fuel consumption, at least for that period. The gas turbine specifications provided by the engine manufacturer are detailed in table 3.1.1, while an operating diagram is illustrated in figure 3.1.3. Some parameters such as the efficiency of the compressor and both turbines (high and low pressure) are not contemplated in the Chrysler's spec sheet. Therefore, polytropic efficiencies of 82 and 83.5% were considered for the compressor and turbines, respectively [Kes+03].

Specifications of Chrysler Corporation's Gas Turbine Engine	
General	
Type:	Regenerative Gas Turbine
Rated Output	
Power:	130 bhp / 97 kW at 35154 rpm low pressure turbine speed
Torque:	576 Nm at zero rpm output shaft speed
Maximum Gas Generator Speed:	44600 rpm
Compressor Air Flow:	1 kg/s at design point operating conditions
Idle Fuel Flow:	2 kg/h
Fuels:	Unleaded gasoline, Diesel, Kerosene, JP-4
Weight:	186 kg
Components	
Compressor Section	
Single Stage	
Centrifugal	
Pressure Ratio 4:1	
Turbine Section	
High Pressure	
Single Axial Stage	
Fixed Nozzle Vanes	
Low Pressure	
Single Axial Stage	
Variable Nozzle Vanes	
Regenerator	
Type:	two rotating disks
Effectiveness:	90%
Burner	
Type:	single can, reverse flow
Effectiveness:	99%

Table 3.1.1: Specifications of Chrysler Corporation's Gas Turbine Engine [Chr79]

Apart from that, in order to use realistic pressure loss values in the inlet ducting, burner and heat-exchanger, it was consulted a spec sheet from a gas turbine developed by Volvo for heavy truck application [OS05].

The thermodynamic design point of this engine was assessed in *GasTurb* taking into account the specifications previously mentioned. The file generated by *GasTurb* with the performance of this model at design conditions are shown in figure A.0.1 (appendix).

In order to describe the steady state performance variation of the engine in different operation conditions, it was also conducted an off-design analysis using this same software. This analysis was simulated through parametric studies in which the rotational speeds of the gas generator and power turbine were gradually changed. Due to the compressor and turbines characteristic maps available in *GasTurb*, it was not possible to assess the engine behavior in a complete operating range of output speed and power. Figure 3.1.4 shows the limitation associated to the low pressure turbine characteristic map, which is not able to generate results for power turbine speeds lower than a certain value, depending on the gas generator speed. In order to get the complete engine performance spectrum, it was formulated some assumptions that are detailed in the *Post-Processing Data* section.

Model 2: *Chrysler G.T. Model without Heat-Exchanger*

According to Chrysler statements, a gas turbine without a regenerator would require several times the amount of fuel normally used in a regenerator-equipped engine [Chr79]. To assess the influence of heat-exchangers in the thermodynamic cycle of a gas turbine applied as an automotive power plant, a similar gas turbine was also

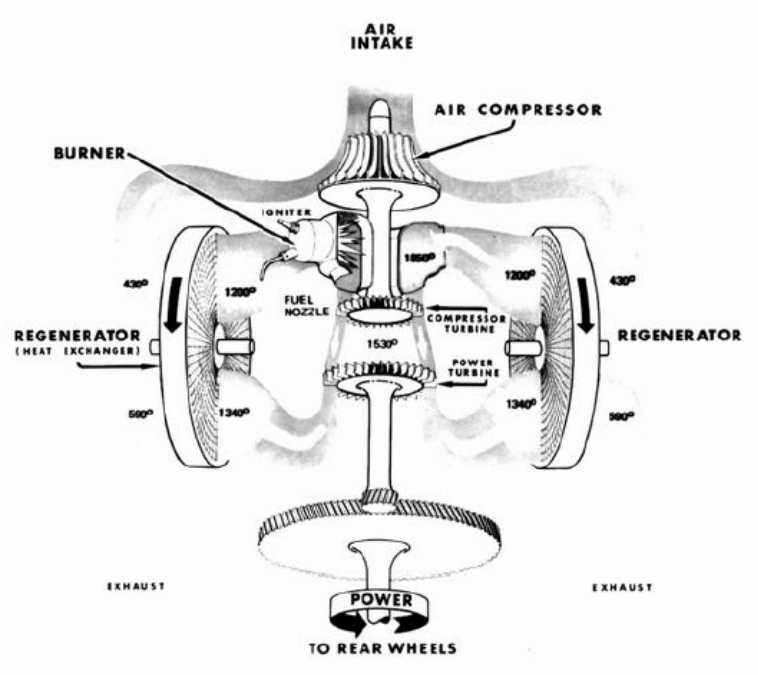

Figure 3.1.3: *Diagram of Chrysler Gas Turbine Operation [Chr79]*

modeled, but without a regenerator. The design performance analysis of this gas turbine model is presented in figure A.0.2 (appendix).

Model 3: *Modern Gas Turbine Model*

The main purpose of this study attempts to assess the viability of gas turbines as road vehicle power plants in terms of fuel consumption. As previously mentioned, the *Chrysler* gas turbine was developed and produced aiming an automobile application. Although relevant for this study, the *Chrysler* gas turbine is an "antique" model with component efficiencies substantially lower to what can be achieved with the latest technology. Aims to establish a fair comparison with modern reciprocating engines, a third engine was modeled representing the *modern* gas turbine.

The design process of this model had as its starting point the *Chrysler* gas turbine. Parameters such as the efficiency and pressure losses in the heat-exchanger and burner were kept from model 1. The major changes were carried out in terms of turbine inlet temperature and efficiencies of both compressor and turbines. As it is stated by McDonald (2003), the turbine inlet temperature is the parameter with the most pronounced effect on the overall gas turbine performance. The increase of this parameter is constrained by the maximum temperature that both turbine blades and heat-exchanger material can withstand. The eventual utilization of ceramic materials in the rotors and heat-exchanger would allow a considerable increase in the turbine inlet temperature, and consequently the improvement of the engine performance. Nevertheless, this solution requires a level of technology that is extremely expensive and that is not still commercially available. Therefore, it was assumed the use of a reasonable cost material, the *super 347 stainless steel* for the *hot-end* gas turbine components. This material withstands a turbine inlet temperature of about 1350 K [McD03]. This same temperature was used in a gas turbine conceived by Volvo for heavy vehicle applications, during the 90's [OS05].

The change of the turbine inlet temperature, at nominal conditions, implies the selection of overall pressure ratio and recalculation of compressor/turbines efficiency, aims to achieve the most efficient operation conditions. A parametric study was performed, in which the variation of the gas turbine specific fuel consumption[1] was evaluated in a range of compressor pressure ratio between 3.5 and 6. The assessment of the most suitable

[1] *Specific fuel consumption* is an engine performance parameter that corresponds to the mass of fuel burnt per unit of time per unit of output power. SFC is also used as a measure of the cycle efficiency.

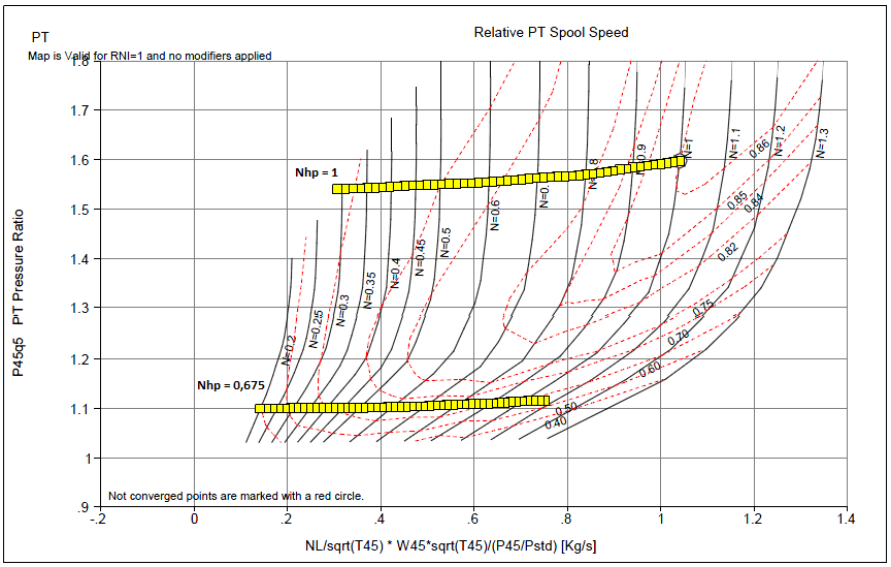

Figure 3.1.4: *Low pressure turbine characteristic map, with parametric study results for high pressure spool relative speeds (Nhp) equal to 0.675 and 1 - Source: GasTurb11*

pressure ratio, for a fixed compressor efficiency, is influenced by the number of compressor stages. The assessment of this number was guided by the compressor *loading*. *Loading* is a sizing parameter that measures how much work is demanded of the compressor or stage. The *stage loading* is defined by the amount of enthalpy increased per unit of air mass flow, divided by the blade speed squared, as it is represented by formula 3.1.1.

$$loading = c_p \frac{(T_3 - T_2)}{U^2} \tag{3.1.1}$$

where T_2 and T_3 are, respectively, the inlet and exit temperatures of the compressor stage, c_p is the specific heat capacity at constant pressure, and U is the mean blade speed. In order to determine U, it was assumed a compressor rotational speed (N), i.e. a high pressure spool speed, based on the blade tip speed (U_{tip}) of the first compressor stage, as it is shown in formulae 3.1.2 and 3.1.3.

$$N = \frac{U_{tip}}{r_{outlet}} \tag{3.1.2}$$

$$U = N.r_{mean} \tag{3.1.3}$$

where r_{outlet} and r_{mean} are, respectively, the outlet and mean radius of the first stage compressor blade. Typically, U_{tip} assumes values in a range between 350 and 450 m/s [Sar+01]. Considering both formula 3.1.1 and chart represented in figure 3.1.5, it is possible to assess that increasing the blade speed results in a lower loading, and consequently in a higher efficiency. For this reason, it was chosen a blade tip speed equal to the maximum value of this range (450 m/s).

An axial geometry (the only one possible to be analyzed in *GasTurb*) was assumed for the compressor. The axial compressor polytropic efficiency versus stage loading is shown in figure 3.1.5. Walsh and Fletcher (2004) states that the loading along the pitch line should be between 0.25 and 0.5 for all compressor stages. Based on that, it was set a number of stages, for each pressure ratio analyzed, so that a reasonable loading value of about 0.45 could be achieved. The table 3.1.2 demonstrates that when the pressure ratio increases, a higher number of stages for the compressor has to be considered, in order to keep the loading, and consequently the polytropic efficiency constant.

The compressor polytropic efficiency corresponding to a certain stage loading, depends on the technology level associated. According to figure 3.1.5, a compressor with a stage loading of 0.45 may have a polytropic efficiency

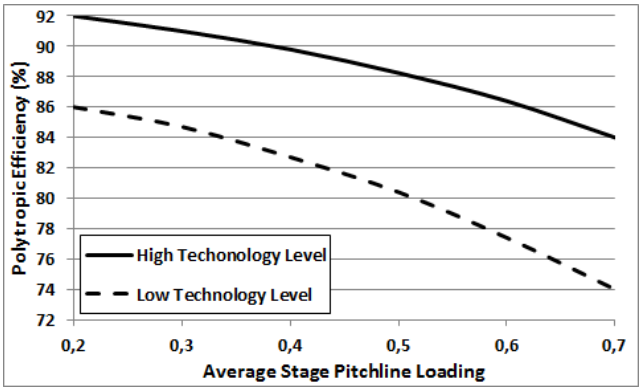

Figure 3.1.5: *Axial compressor polytropic efficiency versus stage loading (based on data from [Wal+04])*

Pressure Ratio	Number of Stages
3,5	3
4	3
4,5	4
5	4
5,5	5
6	5

Table 3.1.2: Different pressure ratios analyzed with the correspondent number of compressor stages

between 81.5% (low technology level) and 89% (high technology level). A corrected polytropic efficiency was calculated taking into consideration formula 3.1.4 [Kyp11].

$$\eta_{pol,corr} = 1200\left(1 - \left(\frac{1}{\left(\frac{H}{13}\right)^{0.6}}\right)\right) - \eta_{pol,uncorr} \tag{3.1.4}$$

$\eta_{pol,uncorr}$ stands for the polytropic efficiency for a high level of technology (figure 3.1.5), $\eta_{pol,corr}$ is the corrected polytropic efficiency and H corresponds to the height of the last stage blade, in millimeters. For each pressure ratio tested, it was assessed the influence of changing 1% of the polytropic efficiency in the specific fuel consumption of the gas turbine. This parameter was used, together with the corrected polytropic efficiency, in order to calculate a *corrected* specific fuel consumption value. Figure 3.1.6 shows the SFC values calculated for the different pressures ratios, taking into consideration the uncertainty associated to the height of the blade. This uncertainty was estimated based on the influence of changing the polytropic efficiency from 84 to 85% and from 87 to 88%. According to figure 3.1.6, 4 seems to be the most suitable pressure ratio for this gas turbine model, since it corresponds to the lowest corrected specific fuel consumption value. In this same

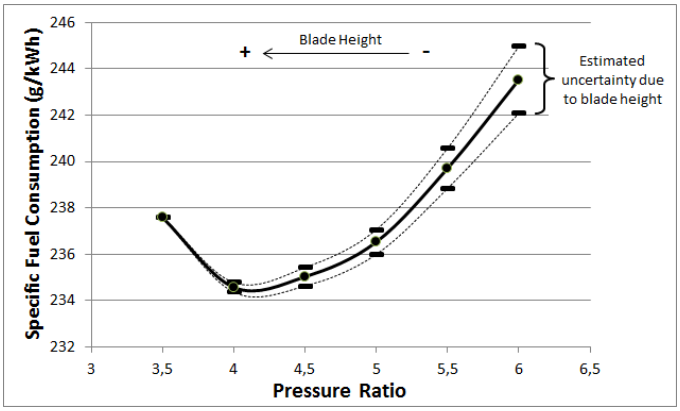

Figure 3.1.6: *Corrected specific fuel consumption for different pressures ratios*

figure, it is also shown that for a certain *stage loading*, higher pressure ratios mean smaller blade heights at the last compressor stage, which increases the uncertainty concerning the corrected SFC. This uncertainty results from the existence of some physical effects whose influence is more relevant on small length scales. Effects associated with the gaps between rotating and stationary components, viscous drag, heat transfer and Reynolds number have a considerable impact on the efficiency of components designed for small scale operation. In fact, figures A.0.5 and A.0.6 (appendix) show computational results of the total pressure loss factor as function of Reynolds number for a given 2D compressor and turbine geometry from a microturbine [Lan09]. In these graphs it is possible to verify that a small Reynolds number (based on the rotor blade chord and rotor inlet flow properties) can significantly reduce the polytropic efficiency of a compressor or turbine.

The pressure ratio assessment required the performance of an iterative process, in which the procedure described above, was repeated till the convergence of the compressor efficiency. After determining the pressure ratio, the compressor efficiency and its rotational speed, the focus of the study was moved to the analysis of the *high* and *low pressure* turbines. For the same reason mentioned above during the compressor design process, an axial geometry was also considered in the turbines design. The turbine efficiency can be determined based on the chart represented in figure 3.1.7, which correlates the axial turbine isentropic efficiency with the loading and axial velocity ratio. The loading was calculated using formula 3.1.1 adapted to turbines, while axial velocity ratio was determined based on a dashed line, illustrated in figure 3.1.7, which is located in the typical design area.

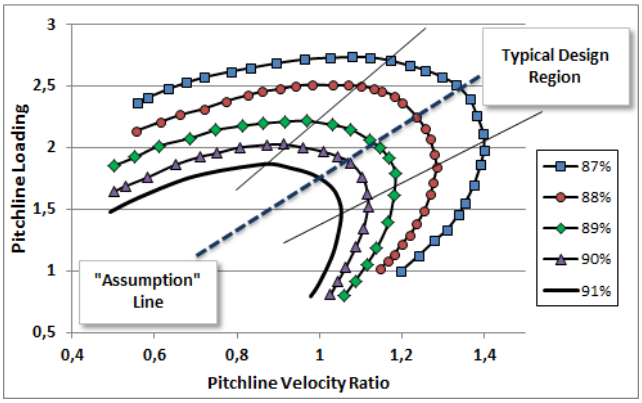

Figure 3.1.7: *Axial turbine isentropic efficiency versus loading and axial velocity ratio [Wal+04]*

In *GasTurb*, the stress in both high and low pressure turbine discs was assessed, and based on that, an adequate power turbine rotational speed was chosen in order to avoid mechanical overloads. The efficiency values chosen for this gas turbine model are summarized in table 3.1.3.

Polytropic Efficiencies (%)	
Compressor	88,0
High Pr. Turbine	91,9
Low Pr. Turbine	87,6

Table 3.1.3: Compressor and Turbines Polytropic Efficiencies of Gas Turbine Model 3

The calculation process described above is a rough estimate supported by several assumptions that may have a negative effect in the results accuracy. Nevertheless, the efficiencies achieved for both compressor and turbines can be considered quite reasonable values, when compared with the ones detailed in the spec sheet of a gas turbine developed for heavy truck applications [OS05]. In order to achieve a maximum output power equal to the remaining gas turbine models simulated (model 1 and 2), the inlet mass flow was iteratively adjusted. Specifications as well as design point performance of the *modern* gas turbine model are detailed in figure A.0.3 (appendix).

Beyond the performance evaluation, the conception of this third model had also the purpose of assessing the outline dimensions of an axial geometry gas turbine with the specifications presented above. When considering automotive applications, a special focus has to be given to the components dimensions, since the space available is limited, constituting one of the main project constrains. A scaled sketch of this gas turbine model is shown in figure 3.1.8. Nevertheless, it is important to refer that gas turbines equipped with centrifugal compressors and radial turbines can achieve more compact dimensions.

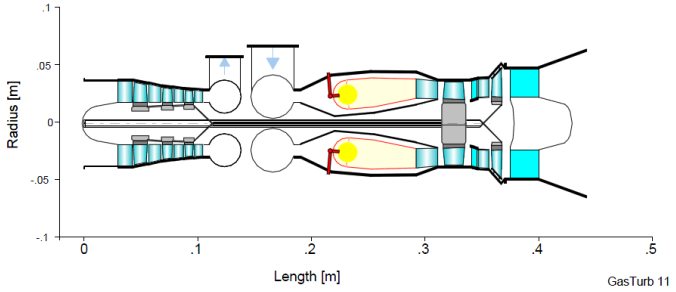

Figure 3.1.8: *Scaled Sketch of Gas Turbine Model 3 - Source: GasTurb11*

3.1.4 Limitations

The results generated by *GasTurb*, specially concerning gas turbine model 1, can be considered quite reliable when compared with the spec sheet provided by the manufacturer (Chrysler Corporation). However, it is important to mention that the gas turbines modeling process was constrained by some software limitations.

As previously mentioned, *GasTurb* only allows the modeling of gas turbines with axial geometries for both compressor and turbine stages. Therefore, an axial geometry compressor was considered in the gas turbine simulation, instead of a centrifugal one, as it is detailed in the specifications of the original *Chrysler* gas turbine. Nevertheless, the effects associated to this constraint are expected to have a low impact in the final results, specially when compared with the influence of components efficiency.

Due to the compressor and turbines characteristic maps available in *GasTurb*, it was not possible to assess engine performance in the full range of output speed (from stall to nominal operating conditions). As it is exemplified in figure 3.1.9, the gas turbine performance could not be obtained for output shaft speeds lower than a certain value, depending on the gas generator speed. In *GasTurb* it was performed parametric studies, in which the output shaft speed was varied for fixed values of gas generator relative speed, in a range between 0.675 and 1 with a step size equal to 0.025.

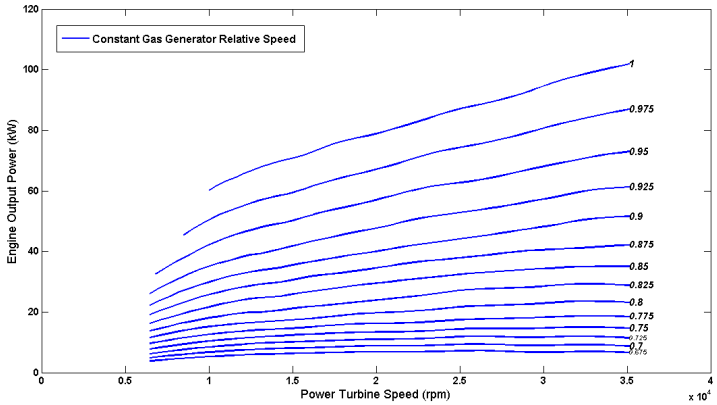

Figure 3.1.9: *Output Power as a function of the Power Turbine Speed for several values of Gas Generator Speed (g.t. model 1)*

3.1.5 Post-Processing Data

Results generated by *GasTurb* revealed to be both limited and sparse, considering the gas turbine operating range. To allow the implementation of *GasTurb* database in a suitable software for vehicle fuel consumption analysis, it was required a post-processing of these same results. To do so, it was developed an algorithm in *Matlab*[2], which is a numerical programming language [Mat].

Algorithm

As it is described in section 2.2.2, the estimation of the fuel consumption of a road vehicle can be done by two main simulation approaches (*quasistatic* or *dynamic* formulation). In this assessment, it is necessary to determine the thermodynamic efficiency of the vehicle's powertrain, which is defined by

$$\eta_e = \frac{w_e.T_e}{P_c} \tag{3.1.5}$$

where w_e is the engine angular speed, T_e the engine torque, and P_c the enthalpy flow associated with the fuel mass flow

$$\dot{m_f} = P_c/H_f \tag{3.1.6}$$

where H_f is the fuel's lower heating value.

The engine input and output variables depend on the simulation approach considered, as it is displayed in figure 3.1.10.

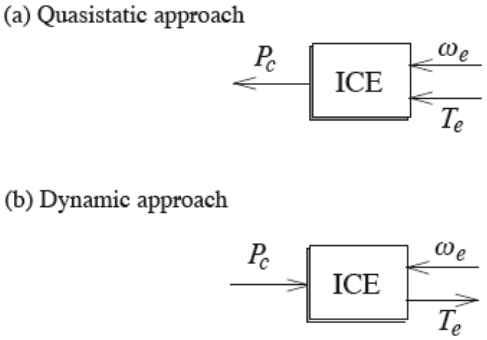

Figure 3.1.10: *Engine input and output variables in the: a) quasistatic approach; b) dynamic approach [Guz+07]*

In both approaches, it is evident that the engine thermodynamic efficiency η_e mainly depends on the engine speed w_e and torque T_e. Therefore, the engine map requires its disposal in a torque-speed plane.

The algorithm developed in *Matlab* has the purpose of conceiving engine maps for any gas turbine modeled in *GasTurb*, in order to assess its fuel consumption as a road vehicle powertrain. The first part of this algorithm consists in reading the data contained in the *ASCII* files generated by *GasTurb* (see example in figure A.0.4), which describe the performance of the gas turbine models analyzed. As previously mentioned, the data available is limited in both torque and speed ranges. In order to have a *complete* engine map, this same data was extrapolated, based on assumptions that are detailed in the following section. Figure 3.1.11 illustrates the procedure described above. The second part of the algorithm consists in fulfilling the sparse data matrixes, through the use of linear interpolations, in order to enable the assessment of the fuel consumption necessary to sustain any torque/speed combination. This procedure is illustrated in figure 3.1.12, where fuel mass flow, in g/s, is represented as function of output shaft toque and rotational speed.

[2] *Matlab* is a registered trademark of the MathWorks, Inc., Natick, MA.

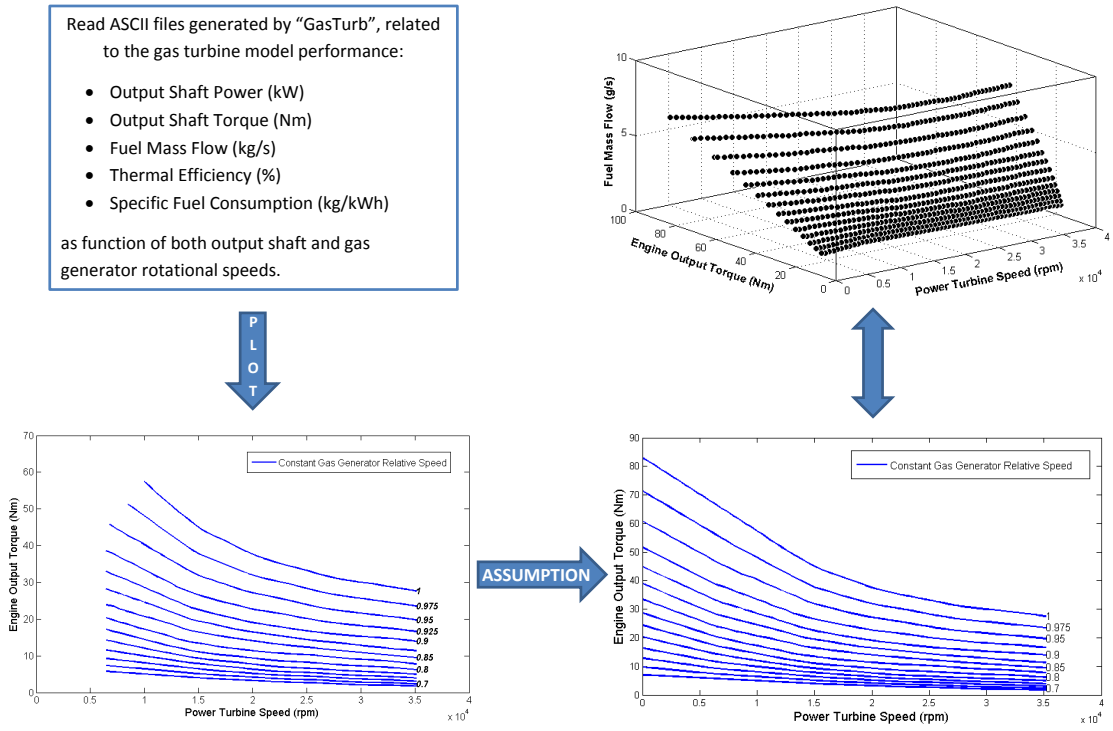

Figure 3.1.11: *Algorithm Diagram - part 1*

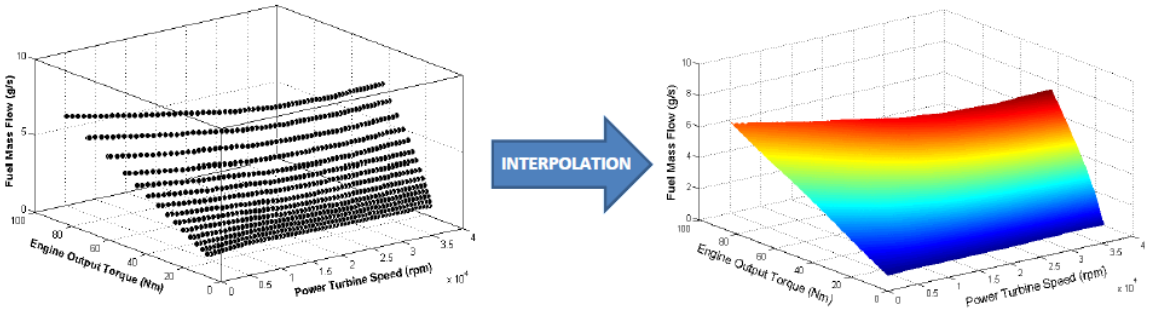

Figure 3.1.12: *Algorithm Diagram - part 2*

Gas Turbine Efficiency Map

In figure 3.1.12, the engine map is represented in terms of fuel mass flow, i.e. fuel consumption per unit of time. The *fuel consumption map*, as it is called, is useful for assessing the engine fuel economy in any operating conditions. Nevertheless it is inappropriate for comparing fuel efficiency between different engines. Therefore, instead of using *fuel consumption maps*, it is common to represent the engine performance through *efficiency maps*, in which the fuel mass flow is replaced by the specific fuel consumption parameter. Specific fuel consumption corresponds to the mass of fuel burnt per unit of time and per unit of output power (g/kWh). Due to its definition, this parameter is often used as a measure of the cycle efficiency. In figure 3.1.13, the efficiency map corresponding to the first gas turbine modeled in *GasTurb* (the *Chrysler* gas turbine with heat-exchanger) is represented. In this same figure it is possible to realize that the gas turbine achieves its highest efficiency at maximum output speed and power. At lower rotational speeds, the pressure of the compressed air decreases, resulting in a dramatic drop in both thermal and fuel efficiency.

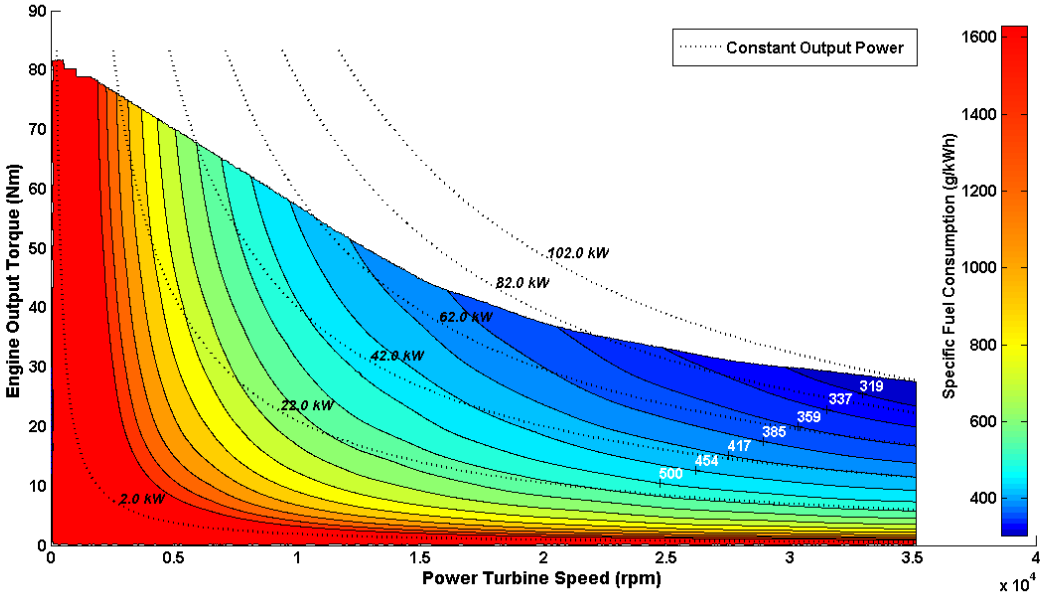

Figure 3.1.13: *Efficiency map - G.T. Model 1*

On the other hand, reciprocating engines are more efficient at maximum load (torque) as figure 3.1.14 shows.

Assumptions

One of the major adversities felt during the gas turbine modeling process, was concerned with the limited data generated by *GasTurb*. In order to generate the "missing" data, it was assumed a linear evolution of the engine output shaft torque, in the range between the lowest power turbine speed analyzed and zero, for each gas generator speed simulated. As it is demonstrated in figure 3.1.11, the torque slope is different for every gas generator speed, assuming a gradual increase as the speed becomes higher.

Although this assumption was not supported by any reference, the results achieved seem to be quite reliable, when compared with the efficiency map of a twin-shaft gas turbine developed and tested by Volvo, for heavy truck applications (see figure A.0.7 in appendix) [OS05]. The referred gas turbine assumes two different operating modes, which can be designated as *Max* and *Eco*. While *Max* operating mode corresponds to the maximization of the gas turbine performance, the *Eco* mode privileges the fuel economy. For each mode, the gas turbine efficiency map has different torque-speed profiles, resulting in different maximum torque values at stall conditions. In the reducing gear, installed "downstream" of the gas turbine, it was measured a maximum torque of 3380 Nm and 2600 Nm in the *Max* and *Eco* mode, respectively. These values correspond to a torque increase of about 199% and 173%, relatively to the output torque at nominal speed (1700 Nm at *Max* mode, and 1500 Nm at *Eco* mode). On the other hand, the *Chrysler* gas turbine model, generated in *GasTurb*,

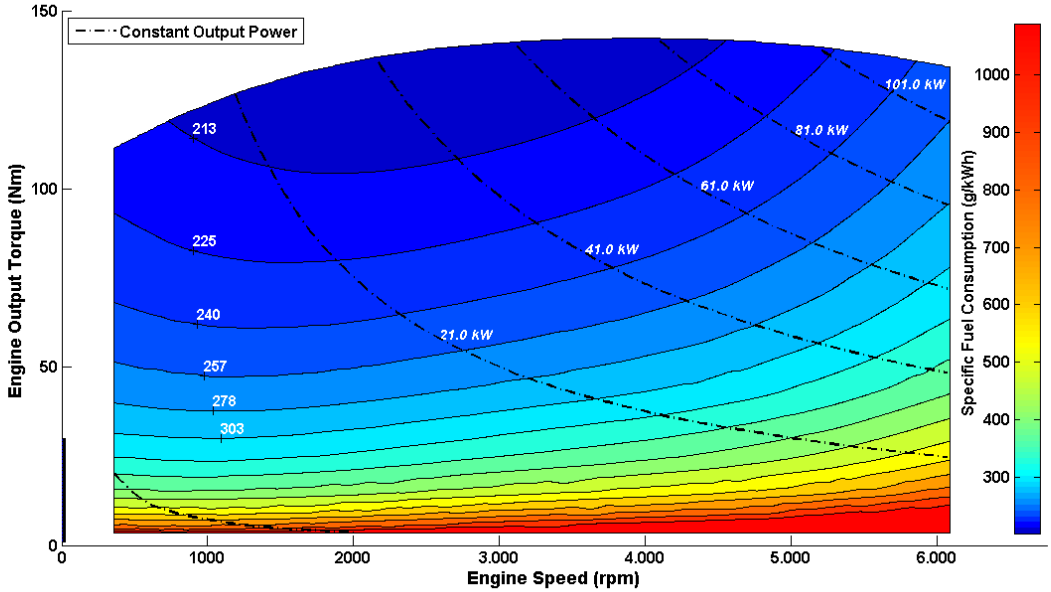

Figure 3.1.14: *Efficiency map of a typical spark ignition engine*

performs a torque increase equal to 182%, a number that can be considered reasonable, since it stands between the values corresponding to the *Volvo* gas turbine. Besides that, the results obtained are also supported by Walsh and Fletcher (2004) that states that stall torque (at zero output speed) is estimated to be around 2 times higher that the torque value measured at full power and 100% speed.

Considering the gas turbine fuel consumption in the "unknown" operation domain, it was assumed that the fuel mass flow is equivalent to the engine efficiency evolving quadratically, from the minimum known output shaft speed till stall operating conditions. Regarding the domain between the lowest known torque and zero, it was assumed that the fuel consumption would decrease linearly. An example of a fuel consumption map is shown in figure 3.1.12. The results achieved in *GasTurb*, at idle conditions (output shaft stopped), are slightly higher comparing with the *official* specifications (*Chrysler* model): 0.997 g/s against 0.556 g/s. Nevertheless, this difference may be justified by the variable nozzle mechanism that was installed in the real model, but that was not simulated in *GasTurb*. According to Chrysler Corporation, the introduction of a nozzle mechanism results in a multiple engine brake capacity, improved acceleration and improved idle fuel consumption [Chr79].

3.2 Vehicle Modeling

This study attempts to evaluate and compare the performance, in terms of fuel consumption, of several road vehicles powered with different internal combustion engines, with a special focus on gas turbines. For this purpose, it was built a simulation model that describes all aspects of the vehicle that are significant for the efficiency and fuel consumption estimation.

3.2.1 Software Description

This simulation model was designed using the Matlab/Simulink platform. Simulink is, basically, a graphical extension to Matlab, for modeling and simulating systems. The capability of drawing systems on screen as block diagrams, confers to Simulink the ability of easily reconfiguring these same systems, according to the simulation goals. In this simulation, the vehicle models were designed in Simulink, and thereafter fed with input parameters and executable codes, via Matlab, which facilitates the adjustment of the examined variables. Another important advantage, that makes Simulink a widely spread simulation program both in industry and in academia, is its user-friendly graphical interface which allows an easy overview of the systems modeled.

Considering that the vehicle fuel economy and performance is mainly determined by energy flows, it was used a quasistatic approach. In this method, the parameters do not change during the simulation time window, as it was further described in chapter 2.2. There are several Matlab/Simulink based *quasistatic simulation tools* available, such as ADVISOR (acronym for Advanced Vehicle Simulator), a program developed by the National Renewable Energy Laboratory (USA). However, in this study it was used a simulation tool designated *QSS* (acronym for QuasiStatic Simulation).

3.2.2 *QSS* Toolbox

QSS is a Matlab/Simulink toolbox developed by ETH in Zurich (Swiss Federal Institute of Technology Zurich). This toolbox is a collection of Simulink blocks and m-files that is freely available for academic purposes. The *QSS* toolbox permits the design of powertrain systems in a flexible manner and allows a fast and simple estimation of the fuel consumption of such systems. Due to the extremely short CPU time required, *QSS* is an ideal computational platform for modeling and simulate powertrains under various control strategies, for instance optimization routines [GA05]. The key idea behind the *QSS* toolbox is to reverse the usual cause-and-effect relationships of dynamic systems. Rather than calculating speeds from given forces, based upon given speeds (at discrete times), this toolbox calculates accelerations and determines the necessary forces. There are several parameters that can be set in the simulation blocks, concerning the driving pattern, chassis of the vehicle, its type of engine, the gear system in use or even the type of fuel. This section attempts to describe the implementation of some of the *QSS* sub-models shown in figure 3.2.1, at the same time that introduces most of the parameters associated to them.

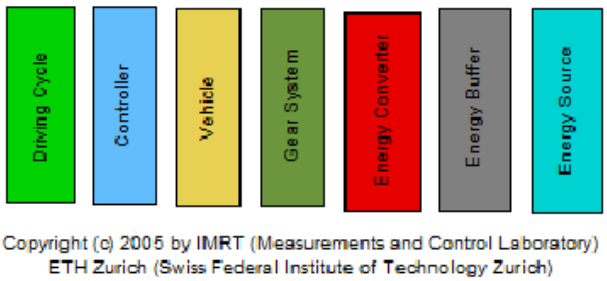

Figure 3.2.1: *The top level of the QSS toolbox library [GA05]*

Driving Cycle Block

It is of interest to simulate the vehicle under different driving conditions. Parameters such as vehicle speed and acceleration or operating gear are defined in the block designated *Driving Cycle*. This block contains

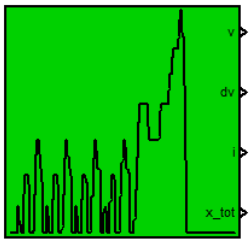

Figure 3.2.2: *Driving Cycle block [GA05]*

several driving cycles to choose from. Some of the cycles are internationally accepted standard cycles developed in different continents, while the others were customized to represent some desirable driving conditions. Since different driving cycles imply different demands, and consequently different results, it was of interest to simulate distinct driving cycles. The chosen ones are described in section 3.2.3.

Vehicle Block

The *Vehicle* block includes the chassis specifications, such as the overall vehicle weight, wheel diameter or frontal area, in order to calculate the tractive force required by the vehicle to reach the performances pre-defined in the driving cycle. As previously detailed in chapter 2.2, the propulsive force can be described as the sum of four forces: Aerodynamic Drag Force, Acceleration Force, Rolling Resistance Force and Gravitational Force (formula 2.2.1). The *Vehicle* block only considers the first three of these forces. It is also important to note that this calculation only considers linear movement, which means that aspects of stability and road handling are not included.

The variables input in this block are the vehicle speed and acceleration provided by the *Driving Cycle* block, while the output variables are the rotational speed, acceleration and torque measured in the wheels. The *Vehicle* block with the correspondent variables can be visualized in figure 3.2.3.

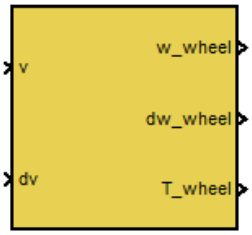

Figure 3.2.3: *Vehicle block [GA05]*

Gear System Block

The *Gear System* block simulates the torque converter, transmission, differential and drive shafts. It provides the transmission of mechanical work between the *Vehicle* and *Energy Converter* blocks, through three possible blocks (see figure 3.2.4):

- *simple transmission* (i.e., fixed relationships between torque levels or rotational speed levels)
- *manual gearbox* (i.e., a finite number of relationships between torque levels or rotational speed levels)
- *CVT* (i.e., continuously variable relationships between torque or rotational speed levels)

While the manual gearbox is controlled by the *Driving Cycle* block, i.e. the gear ratio selection is defined *a priori*, the operating gear ratio of the CVT is determined by an online controller.

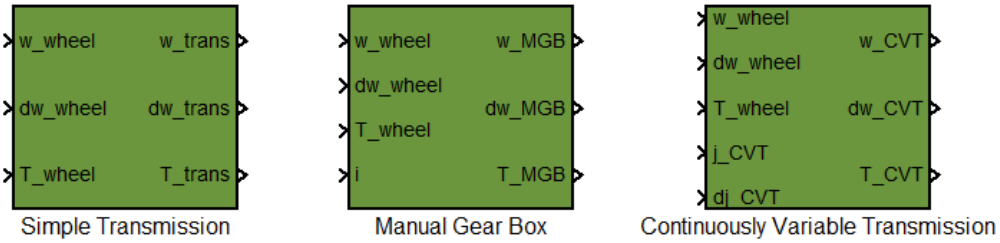

Figure 3.2.4: *Gear System blocks: simple transmission, manual gear box, CVT [GA05]*

In the three different gearbox systems, the losses are described by the following relationship

$$P_{out} = \eta_{gear}.P_{in} - P_0 \tag{3.2.1}$$

where P_{out} and P_{in} represent the power leaving and entering the system, respectively. In QSS, efficiency (η_{gear}) and power losses (P_0) associated to the gearbox system were modeled as being invariable, in particular, as being independent of the gear ratio. However, efficiency depends on a number of factors, especially gearbox loading.

Energy Converter Block

There are three different types of energy converters included in the QSS toolbox library:

- *Combustion Engine*
- *Electric Motor and Generator*
- *Fuel Cell*

In terms of combustion engines, the QSS toolbox has blocks capable of simulating both petrol and diesel engines, following two different approaches:

- Computing the fuel consumption from a consumption map
- Approximating the efficiency by means of the Willans approximation

Considering the purpose of this study, it will be only analyzed the *Combustion Engine*, based on the *consumption map* approach, for the *Energy Converter* block. According to the *consumption map* approach, the internal combustion engine determines the fuel consumption based on a two dimensional matrix that contains the fuel mass flow data, in kg/s, correspondent to different torque and rotational speed combinations.

Besides that, the *Combustion Engine* block also accounts for some special engine operating cases:

- idle
- fuel cutoff
- overload and overspeed

These special cases are described below:

Consumption at idle - Idle speed is detected as soon as both demanded engine rotational speed and torque values drop below a certain limit. In this case, the fuel consumption is equal to a pre-define value.

Fuel Cutoff - As soon as the demanded torque, at idle speed, falls below a pre-defined limit, this function is activated. The engine cutoff function is standard in modern fuel injection systems, and it can be enabled or disabled in the *Combustion Engine* block.

Overload and Overspeed - Every combustion engine has limits in terms of output torque/rotational speed combinations. In the *Combustion Engine* block these limitations are taken in consideration. As soon as the values for rotational speed and torque exceed their maximum values (torque depends on rotational speed) the simulation is stopped.

-

The *QSS* model for this type of combustion engine, based on a *consumption map*, is shown in figure 3.2.5.

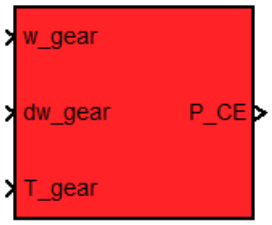

Figure 3.2.5: *Combustion Engine block (consumption map approach) [GA05]*

In figure 3.2.6 it is possible to verify that the engine inertia is also accounted for by adding an auxiliary torque that is proportional to the engine inertia and the engine acceleration. The auxiliaries such as air conditioning and lights cause increased fuel consumption due to their power demands, whereby this fact was also taken into account in the *Combustion Engine* block.

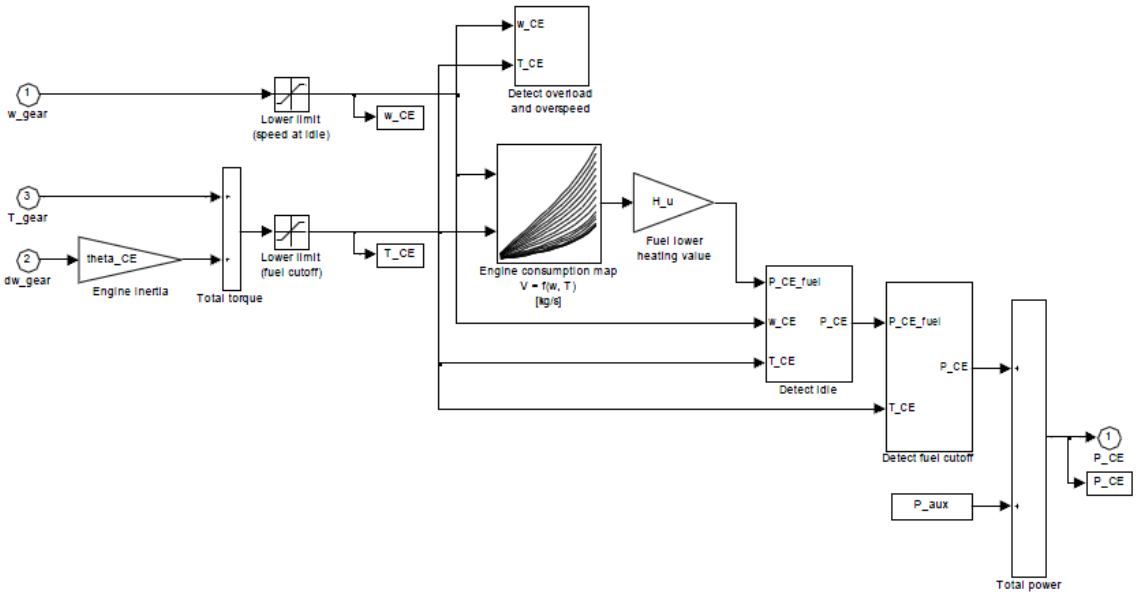

Figure 3.2.6: *Top view of the Combustion Engine model based on the consumption map approach [GA05]*

Energy Source Block

The power produced by the *Combustion Engine* block is divided by the lower heating value of the fuel in use, to compute the corresponding actual fuel mass flow (formula 3.1.6). Then, the fuel mass flow is integrated in order to obtain the consumed fuel mass along the driving cycle. The total fuel mass is finally divided by the total distance covered and transformed in liters/100 km. The *Energy Source* block enables the account of typical losses associated to the cold start of the engine (see figure A.0.12 in appendix).

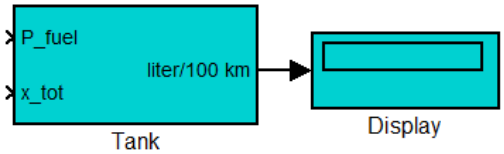

Figure 3.2.7: *Energy Source block [GA05]*

3.2.3 Gas Turbine Powered Vehicle Model

The sub-models described in the previous section were used to model a vehicle powered by a gas turbine and thus determine the performance and fuel consumption in various driving conditions. This section describes the vehicle model developed (see figure 3.2.8), at the same time that explains the options taken during this modeling process.

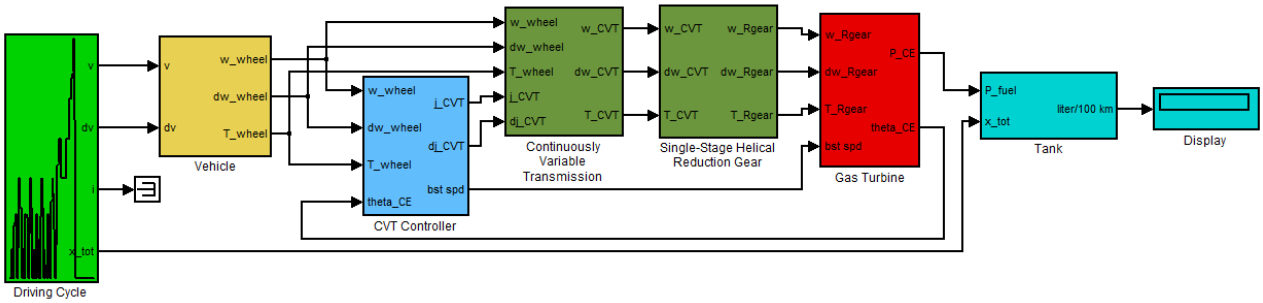

Figure 3.2.8: *Simulink model of a vehicle powered by a gas turbine*

Driving Cycles

In the simulations performed, it was not used all the cycles available in the *Driving Cycle* block. Nevertheless, this study attempts to take conclusions about the fuel consumption of a vehicle operating under different driving conditions. Therefore, three default driving cycles were chosen: an *urban*, *extra-urban* and *combined* driving. Furthermore, custom driving cycles were created in order to analyze the vehicle model in acceleration. The user interface of this block is shown in figure A.0.8 (appendix).

Default Driving Cycles

Regarding the default driving cycles, it was selected three European regulated ones:

- ECE R15
- EUDC
- NEDC

These driving cycles are modal cycles, which means that, in some sections of these cycles, the speed is constant.

The ECE R15 is an urban driving cycle that was devised to represent city driving conditions, and that is characterized by low vehicle speed (max. 50 km/h) and low engine load. The vehicle speed versus time chart corresponding to this cycle is represented in figure 3.2.9.

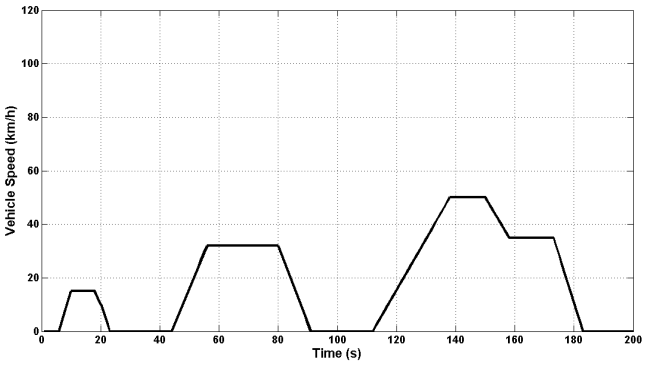

Figure 3.2.9: *Urban driving cycle (ECE R15)*

By contrast, the EUDC describes a suburban route, where both speed and acceleration are higher than the ECE R15. In figure 3.2.10, it is possible to see that at the end of this cycle the vehicle accelerates to highway-speed, reaching a maximum speed of 120 km/h.

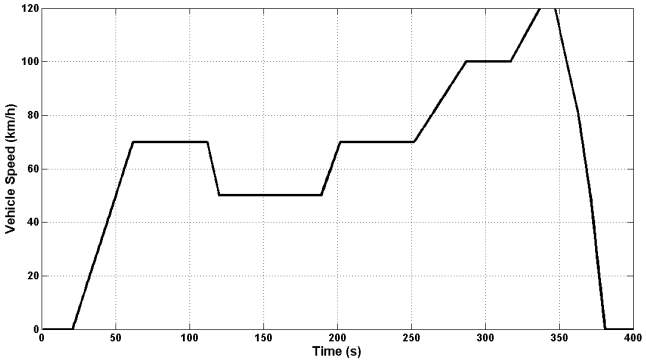

Figure 3.2.10: *Extra-urban driving cycle (EUDC)*

The following table includes a summary of the parameters of both ECE R15 and EUDC.

Characteristics	Unit	ECE R15	EUDC
Distance	km	4 x 1,013 = 4,052	6,955
Duration	s	4 x 195 = 780	400
Average Speed	km/h	18,7 (with idling)	62,6
Maximum Speed	km/h	50	120

Table 3.2.1: Summary of the parameters of both ECE R15 and EUDC [Die]

The NEDC (acronym for New European Driving Cycle) is a *combined* cycle consisting of four ECE R15 (urban driving) followed by an EUDC (extra-urban driving), as it is illustrated in figure 3.2.11.

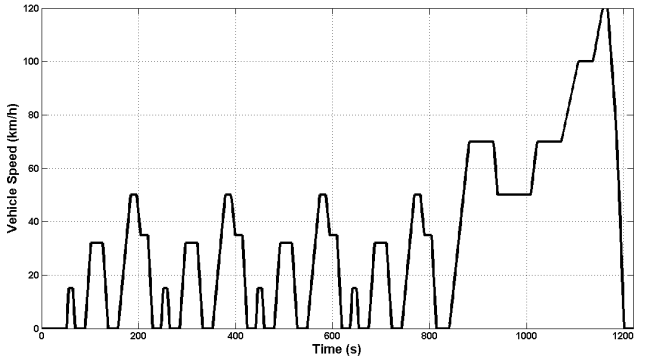

Figure 3.2.11: *Combined driving cycle (NEDC)*

There is a special interest in considering this cycle, since it is the regulated European cycle chosen for defining the specific fuel consumption (in liters per 100 km/h) and emissions of passenger cars. Moreover, a cycle analysis on the basis of the NEDC allows a direct comparison with the fuel consumption of current cars as given by the car manufacturers.

Custom Driving Cycles

In this simulation it was used a quasistatic approach. As previously mentioned, this method is not suitable for analyzing the best-effort performance, for instance acceleration tests. Instead, it assumes that the vehicle meets the speed trace defined by the driving cycle, i.e. the acceleration is treated "predictively", which leads to less realistic values. Even though it was made an attempt to simulate the vehicle acceleration, in order to evaluate how close the engine operates to its maximum load conditions. To do so, custom driving cycles were designed according to the features of each vehicle tested. In all driving cycles, it was simulated the vehicle acceleration, from a static position to 100 km/h. Since dynamic tests are highly influenced by the characteristics of the vehicle, it was assumed realistic acceleration times for each vehicle, in order not to overload the engine. The speed trace of these driving cycles (shown in figure 4.2.1) were designed taking into account the typical acceleration profile of a vehicle, as it is exposed by Hussain (2003) [Hus03].

Vehicle Parameters

In order to make a meaningful and relevant study, three different vehicle categories were chosen: a small, a medium and a large sized car, with the respective designations of city car, family car and SUV (acronym for Sport Utility Vehicle). Most of the parameter inputs (see figure A.0.9), which are detailed in table 3.2.2, were taken from spec sheets of vehicles that are currently in production.

Vehicle Category	Total Mass of the Vehicle (kg)	Vehicle Cross Section (m^2)	Wheel Diameter (m)	Drag Coefficient	Rotating Mass (%)	Rolling Friction Coefficient
City car	1000	1,95	0,6	0,34	5	0,025
Family car	1500	2,2	0,64	0,28		
SUV	2500	2,7	0,74	0,35		

Table 3.2.2: Vehicles parameters

It was made an assumption concerning the vehicle frontal area, which was considered to be 80% of the area resulting from the height times the width of the vehicle. A rolling friction coefficient equal to 0.025 was chosen, as a results of the assumption that the vehicle simulations were performed in a tarmacadam road, as it is shown in table 2.2.1. On the other hand, since the rotating parts have a considerable lower mass comparing with the overall vehicle, they were considered to be 5% of the vehicle's weight, an assumption supported by Ehsani et al. (2010).

Gas Turbine

One of the main limitations of the *QSS* toolbox is the lack of an *Energy Converter* block for simulating a gas turbine engine. Significant changes were performed in the *Combustion Engine* block to simulate the gas turbine operation, and thus assess its performance and fuel consumption. The *fuel consumption map* corresponding to piston engines was replaced by an executable code that generates the fuel consumption of the gas turbine depending on the torque/rotational speed combination demanded by the gear system. The developed code is generic, which means that it is capable of simulating the fuel consumption of any gas turbine modeled in *GasTurb*.

It is important to note that there are some differences between reciprocating engines and twin-shaft gas turbines, concerning the operating mode. For instance, at idle conditions, while the piston engine runs at a minimum rotational speed, the output shaft of the gas turbine stops when the vehicle is immobilized. Nevertheless, this does not mean that the gas turbine is not working and consequently consuming no fuel. In fact, the gas generator is rotating at a minimum speed, which results in a corresponding idle fuel consumption. The input code that calculates the gas turbine fuel consumption is also capable of generating this value, however, as previously mentioned in the *Gas Turbine Modeling* section, it does not correspond to the idle fuel consumption provided by the manufacturer (see table 3.1.1). Since idle operation takes an important part of the driving cycles used in the simulations performed (figures 3.2.9 - 3.2.11), the need of considering the idle fuel consumption provided by Chrysler Corporation was felt, in order to approximate the simulation results to the real ones. Therefore, an idle fuel consumption value equal to 0.556 g/s (2 kg/h) was input in an adapted *Detect Idle* block (see figure 3.2.12) that is activated when an output shaft torque equal to zero is detected.

Another difference between piston engines and gas turbines deals with the fuel cutoff. This function can be activated in the reciprocating engines when the deceleration of the vehicle provides enough power to cover, in addition to the aerodynamic and rolling friction losses of the vehicle itself the losses of the complete propulsion system. At this point, the engine fuel consumption is zero. On the other hand, since it was not considered any mechanical connection between the gas generator and the gear system, and consequently the vehicle wheels, there is no way of using the vehicle movement in order to provide the necessary power to run the gas turbine in decelerating situations. For this reason, the *fuel cutoff* block, present in the *QSS* model (figure 3.2.6), was suppressed, as it is shown in figure 3.2.12.

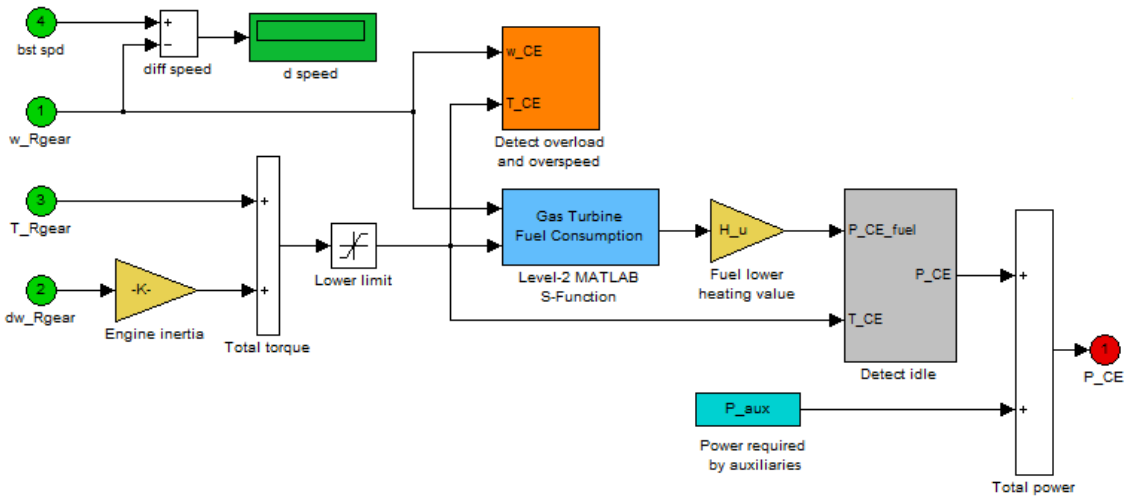

Figure 3.2.12: *Top view of the Gas Turbine block*

In order to simulate a realistic operating mode, it is also essential to have an overload/overspeed detector in the gas turbine engine block, as it is described in figure 3.2.13.

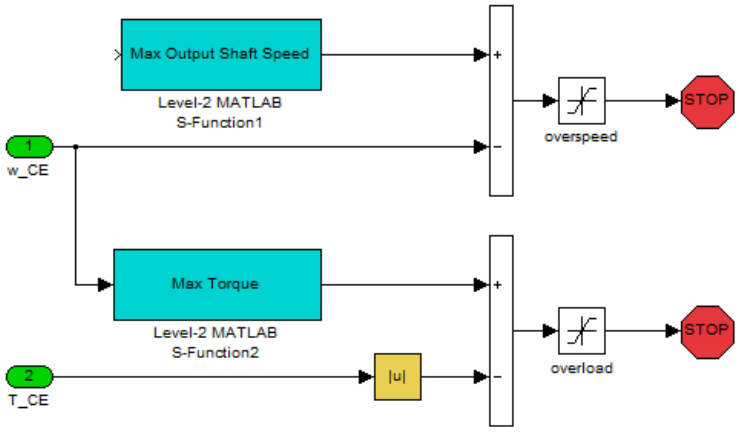

Figure 3.2.13: *Top view of the Detect Overload/Overspeed block*

Instead of the two-dimensional map block used in the default model, it was implemented a code that determines the maximum torque performed by the gas turbine, depending on the output shaft speed. This code is used as a comparative term that detects when the engine is overloaded. For the overspeed detection it is used a block that reads from *GasTurb* files, the maximum output shaft speed reachable by the gas turbine in analysis.

The *engine inertia* is an essential parameter in the determination of the acceleration force imposed to the vehicle, as it is described in the *Vehicle Performance Analysis* section. This parameter has a great influence on

the load provided by the engine to the wheels, affecting considerably the vehicle performance. High inertia values mean high inertia forces, which may result in the overload of the engine in demanding situations, such as fast accelerations. The inertia force assessment in a twin-shaft gas turbine is hampered by the fact that there are two different sets of rotating parts, the high and the low pressure spool, whose speed can be considered independent from each other. In this simulation model it is not possible to assess the high pressure spool speed, and thus the corresponding acceleration. Instead, the changes of speed in the high pressure spool are detected by the variation of the output torque, which is as higher as the gas generator gets closer to its nominal speed. Therefore, the engine inertia forces are calculated taking into consideration only the speed variation of the low pressure spool. The research performed did not allow the assessment of a reliable inertia value for this type of gas turbine. Instead it was assumed a value equal to 0.038 kg/m^2, which corresponds to the inertia of the third gas turbine modeled in *GasTurb* (the *modern* gas turbine model). Although, the inertia forces are only calculated based on the low pressure spool acceleration, a somehow higher inertia was used as an input in an attempt to account for the inertial forces generated when varying the gas generator speed.

In the *engine* block it is also possible to define the fuel used by the engine, which was considered to be diesel, the same fuel type used in *GasTurb* simulations.

In figure 3.2.12, there is a block designated P_{aux} which corresponds to the power demanded by the auxiliaries, such as air conditioning and lights. It was assumed a power equal to 300 W, a value taken from the default *QSS* model (see figure A.0.11). This value was validated by other references, which use auxiliary power values with the same order of magnitude [Boy02].

Gear System

The drivetrain is an essential system in the whole vehicle model, since it is responsible for the transmission of the mechanical work between the gas turbine and the wheels. The great influence of this system in the engine operation, and thus in the vehicle fuel economy, requires special attention to its modeling.

As it is explained in the *Drivetrain System* section, the engine torque-speed profile is a key feature in the gear ratio selection, and thus in the vehicle overall performance. The differences pointed out between reciprocating engines and twin-shaft gas turbines, do not allow the use of the default gear systems, available in the *QSS* toolbox library, in this simulation model. For instance, the use of a manual gearbox, the most common gear system among European cars, requires not only the input of the gear ratios, but also the definition of the operating gear in every time step of the driving cycle. The lack of references regarding manual gearboxes suited for gas turbine applications hampers this assessment. In fact, this is a quite complex and time-consuming process with no guarantee of success. For these reasons, it was chosen another gear system for the gas turbine vehicle model, a *Continuously Variable Transmission* (CVT). Although, CVTs typically offer lower efficiencies than manual gearboxes, their operation depends less on the driving style, i.e. driver behavior. Besides that, a CVT system is mechanically designed to provide an infinite number of gear ratios, which enables the engine to operate close to the called *Optimal Operation Point*, resulting in an increased fuel economy. The CVT operation requires the use of a controller containing an algorithm that determines the ideal gear ratio, depending on the power demanded. This *CVT Controller* is described in the following section.

One of the main disadvantages attributed to CVT systems is their low tolerance to high torque demands, due to the slippage registered in the drive belt or rollers, as a result of the lack of rigid mechanical connection between the gears (no discrete gear teeth). As mentioned in the *Drivetrain System* section, the maximum torque supported by the currently available CVTs is about 386 Nm. This torque capacity is characteristic of a toroidal traction mechanism, which uses a high viscosity fluid to transmit power between the disks and rollers, rather than metal-to-metal contact, as it happens in the conventional belt-driven CVTs (see figure 3.2.14). Since the twin-shaft gas turbine can reach quite high output torque values, it was decided to simulate a toroidal CVT, in order to allow a proper transmission of the engine load to the wheels. According to Lang (2000), toroidal CVTs can reach efficiencies from 70% to 94% (see table 2.3.1). Based on this, it was assumed the maximum value of this range for the CVT efficiency (94%).

Besides the transmission efficiency, also friction losses associated to idling operation must be input. It was assumed 400 W of power losses, a value "imported" from the default *QSS* model (see figure A.0.15).

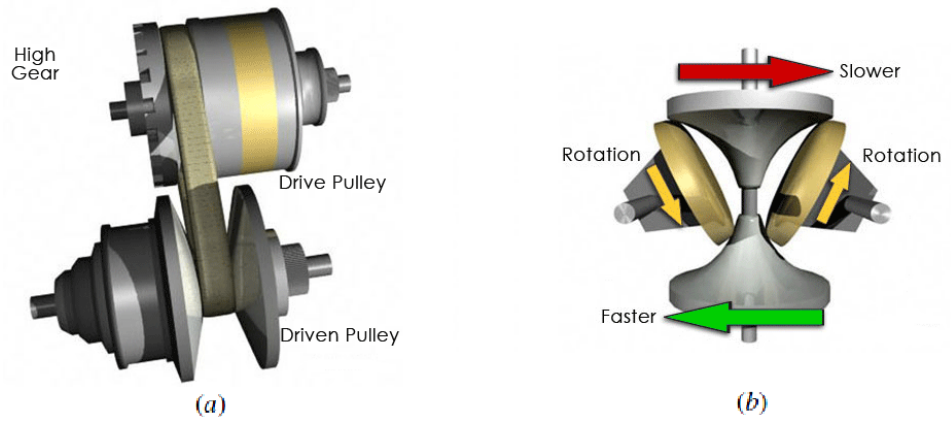

Figure 3.2.14: *CVT Designs: a) Belt Mechanism; b) Toroidal Traction*

Reduction Gear

The extremely high rotational speeds of the power turbine require the use of an extra-gear in the transmission. The main function of this gear is to reduce the output shaft speed, in such a way that it is called *reduction gear*. The reduction gear modeled was based on the one used by Chrysler in its gas turbine concept cars. So, a single-stage helical reduction gear was implemented with a gear ratio of 9.765:1 [Chr79]. It was assumed an efficiency of 99%, a value suited to this type of gear (see figure A.0.14) [Gea].

CVT Controller

As described earlier, the *Continuously Variable Transmission* makes part of a group of gear systems characterized by an automatic operating mode. This mode requires the use of a controller that replaces the driver in the selection of the most adequate gear ratio considering the driving cycle demands.

The purpose of control systems, in general, consists in the processing of the system data, external inputs or cycle data, in order to generate input data for the various system modules. In a real CVT control system, the inputs would include data, such as the rotational speed of the wheels and engine, and the driver's torque demand, expressed by the gas pedal position. The output would include the change of the gear ratio. Contrary to a real system, the model developed makes use of a quasistatic simulation approach. This approach requires a *backwards* formulation of the CVTs physics, which is, somewhat, more complicated: a straightforward model structure has to be developed with a "predictive" online control of the CVT operation. This conception may be achieved through the transmission of the desired speed, generated by the *Driving Cycle* block, directly to the control unit, but with one step delay in its transmission to the *Vehicle* block, as it is shown in figure 3.2.15. In fact, this would be easy to implement in practice, with a drive-by-wire engine, where the step size (the artificial delay) would be on the order of one tenth of a second [GA05].

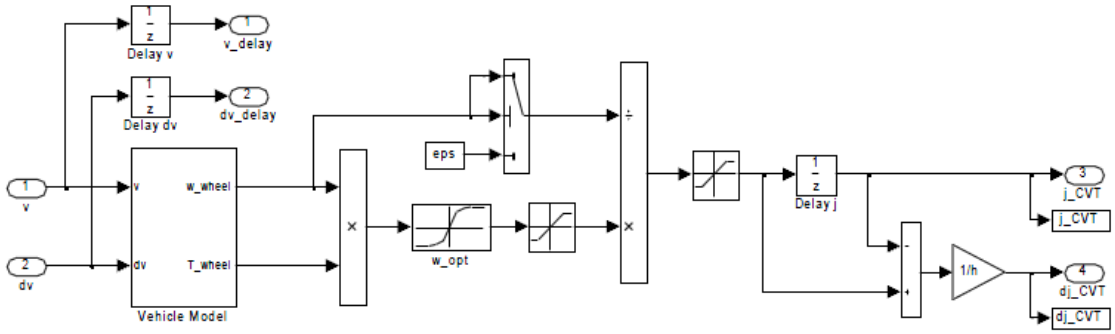

Figure 3.2.15: *Default CVT Controller block - QSS toolbox [GA05]*

The CVT controller shown in figure 3.2.15 corresponds to the one available in the *QSS* toolbox library, however, during the modeling process, it was realized that there was room for improvements in this module. In fact, it was developed a completely new controller, with the purpose of allowing its "interface" with the gas turbine data generated by *GasTurb*, but also to ensure a more accurate calculation of the power required to drive the vehicle.

The main function of the controller consists in determining the optimal CVT gear ratio for any point in time. This procedure starts with the assessment of the power required by the vehicle in order to meet the performances pre-defined in the driving cycle. In the *QSS* controller, the power assessment is exclusively based on the forces calculated in the *Vehicle* block, which means that losses associated to the drivetrain system, as well as inertia forces generated by the engine acceleration are not considered. Although this method is not very accurate, it may be acceptable in vehicles powered by piston engines, but not when it is being considered gas turbines. Gas turbines are characterized by the extremely high operational speeds of their shafts, which may mean fast speed changes (accelerations), and consequently high inertia forces (see formula 2.2.13) that cannot be neglected. For this reason, new diagram blocks were introduced in the controller, that simulate both CVT and reduction gear, as well as the inertia associated to the engine (see figure A.0.17 in appendix).

In this control system, the losses in the vehicle are estimated in the following procedure. Given the requested drive power, the optimal engine speed and required CVT ratio are determined, as a first estimate, without considering any other losses besides the ones calculated in the *Vehicle* block. Using these values, the losses associated to the CVT and reduction gear, as well as the engine inertia forces, can now be accounted for. After that, a new CVT ratio can be set based on a more accurate required power, which was calculated using a "predictive" strategy. In this case, the control system must be enabled to act preemptively, which means that the external data from the driving cycle must be detected and processed before it influences the vehicle. The control system developed for the CVT can be visualized in figure A.0.17 (appendix). It is also important to note that this control system is provided with a "memory", with the purpose of enabling the assessment of shaft acceleration/deceleration (speed evolution), and thus determine inertia forces. The control system developed and shown in figure A.0.17 could have been also made with implicit loops, i.e. when input changes immediately affect the output with no storage device in-between. Generally, the built-in Simulink solver is able to deal with these loops, however it does not always happen. Therefore, Guzzella et al. (2005) states that such loops should be avoided.

Once calculated the power required to drive the vehicle, it is essential to determine at which speed the engine should be operating. This assessment is performed by an executable code that was implemented in the new CVT controller. This code determines the rotational speed at which the required power is best generated by the engine, taking into account the minimum fuel consumption. These engine torque-speed combinations, generated by the new controller, are called *Optimal Operation Points*, whose connection results in a quite erratic curve, designated *Optimal Operation Line* (OOL). In figure 3.2.16, it is evident that the OOL is not a smooth line, a fact that results from the very small fluctuation of fuel consumption levels over a large operating region. Although it was not implemented, Oudijk (2005) recommends the use of a smooth line, in order to ensure a monotonous increase of the engine speed at increasing power request [Oud05]. In fact, Hoffman et al. (2001) makes use of a 6th-order polynomial function fitted through the OOL, in the modeling of a vehicle equipped with a CVT system. The chart illustrated in figure 3.2.16, instead of being generated directly from the *GasTurb* database, it was created based on the "extrapolated" torque vs. speed chart, similar to the one presented in figure 3.1.13. This procedure was used with the purpose of accounting for the same assumptions described in the *Post-Processing Data* section, in terms of the gas turbine performance at low torque and low speed operating conditions. It is important to state that the default CVT controller available in the *QSS* toolbox performs this operation in a less accurate way, since the assessment of the *best* engine speed is based on a block diagram containing a pre-defined relation between the engine speed and power.

Apart from the changes already mentioned, it was also decided to implement a new function in the CVT controller with the purpose of simulating the gas turbine operation more realistically. The transient performance of a gas turbine is characterized by a slow throttle response, usually called *acceleration lag*, a feature that is even more pronounced in a twin-shaft configuration. In this engine configuration, this lag results from the absence of any physical connection between the gas generator and the "free" power turbine. In fact, the "free"

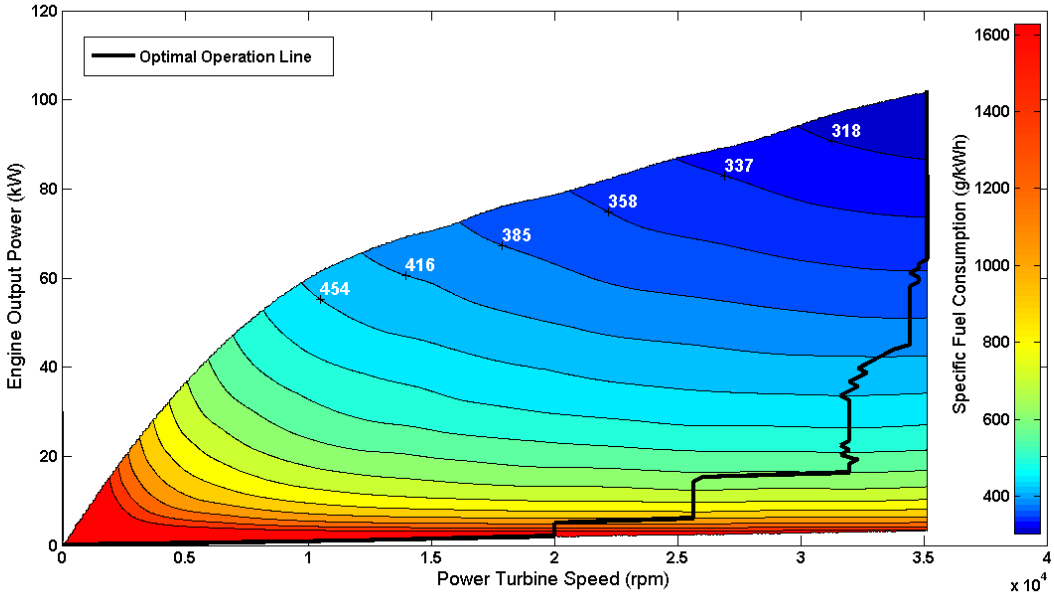

Figure 3.2.16: *Efficiency Map of the G.T. Model 1 with the correspondent Optimal Operation Line (OOL)*

power turbine acceleration is provided by the exhaust gas power, which increases at a similar rate to the gas generator spool speed. For this reason, the acceleration time of a twin-shaft gas turbine is significantly longer than a single spool one, and depends upon its inertia, as well as the inertia and loading characteristics of the driven equipment [Wal+04]. The reduction of this acceleration lag may be achieved through the reduction of the engine inertia. As a matter of fact, Volkswagen developed a profound research in this area as it is demonstrated in a gas turbine prototype presented in 1971 [Nor74]. For instance, *VW* used a compressor-wheel with a shorter diameter than the one used in the *Chrysler* gas turbine model, in order to reduce the engine inertia, and thus decrease acceleration time.

Chrysler Corporation claims that in its gas turbine model, the compressor section takes less than 2 seconds to reach the nominal speed, after the accelerator pedal is depressed [Chr79]. However, this acceleration lag is correspondent to the gas generator speed, and thus it cannot be input in this simulation model, since it only considers the "free" power turbine speed. The determination of this value required the use of assumptions, which were formulated taking into account the acceleration times expected for the different vehicle models in analysis (city car, family car and SUV). According to their characteristics, it was chosen a different acceleration time for each vehicle model, which means that three different acceleration driving cycles had to be designed. The velocity/speed profile of these custom driving cycles are presented in figure 4.2.1. For the family car it was considered an acceleration time of 15 seconds from zero to 100 km/h, a typical value for this type of vehicle, according to Walsh and Fletcher (2004). Considering that the vehicle performance is constrained by the maximum load capacity provided by the engine to the wheels, it was chosen an acceleration lag that would result in an engine operation close to its maximum capacity, but without reaching an overload situation. An acceleration lag equal to 4.5 seconds was input in the family car model. The same procedure was applied in the acceleration tests for the city car and SUV, which resulted in lags of 4 and 6 seconds, corresponding to acceleration times equal to 10 and 25 seconds, respectively. The procedure here described may not be the most accurate one, and the assumptions considered may have high errors associated, however this was the solution found to simulate the acceleration lag inherent to gas turbines operation. Nevertheless, it is important to note that the values input have a physical reason behind them, in the sense that heavier vehicles have higher acceleration lags, due to their greater inertia.

It still remains to discuss four other inputs of the *CVT Controller* block: the minimum and maximum gear ratios, as well as the minimum and maximum CVT speeds. For the minimum and maximum gear ratios (2 and 14, respectively) it was considered a range of values that were taken from a spec sheet of a commercialized

vehicle equipped with a CVT system [Hof+01]. The values input do not correspond to the real gear ratios. Instead, they result from the multiplication between the gear ratio values and the final drive ratio, which represents the real speed ratio between the engine output shaft and vehicle wheels. By its turn, it was input zero and 628 rad/s for the minimum and maximum CVT rotational speeds, respectively. Since the power turbine is independent from the gas generator in a twin-shaft gas turbine, the transmission does not require any clutch device, which means that the power turbine can be connected through its reduction gear directly to the input shaft of the transmission. Therefore, this CVT can have a minimum rotational speed equal to zero, contrary to what happens in reciprocating engines which always have a minimum operational speed, even at idling conditions. Since it was assumed the use of a CVT model "imported" from a conventional vehicle, i.e. powered by a reciprocating engine, it was kept a value for the maximum CVT speed equal to 6000 rpm (628 rad/s), which corresponds to the typical maximum speed of this type of engine (see figure A.0.16).

Model Limitations

In this model, it is used a quasistatic simulating approach. This approach implies a *backward* formulation, which means that physical causality is not respected, since the driving profile has to be known *a priori*. Therefore, this method is not able to handle feedback control problems or to correctly deal with state events [Guz+07]. The engine is assumed to be operating quasistatically, i.e. the cyclic fluctuation of the engine torque is neglected. Instead, it is applied a mean torque value, and torque transients are considered to occur instantly, even though, in reality, the vehicle and all drivetrain parts are in a transient condition during accelerations or decelerations [Hof+01].

This model cannot assess the pollutant emissions generated by the powertrain system, since the relevant mechanisms of the pollutant formation are described on much shorter time scales than those of the fuel consumption. Beyond the emissions, also the temperature effects on fuel consumption are left out of consideration.

As already referred, the gas turbine model developed does not allow the measurement of the gas generator speed. The importance of this parameter in the inertia forces assessment, and thus in the overall engine performance, turns this into a relevant limitation of this simulation model.

3.2.4 Reciprocating Engine Powered Vehicle Model

The investigation of the potential of gas turbines for vehicular applications requires the developed of a comparative model, in order to take conclusive results. A model simulating *convencional* vehicles powered by reciprocating engines was implemented (see figure 3.2.17), and thereafter the results were compared with the gas turbine ones, in terms of fuel consumption, for various driving conditions.

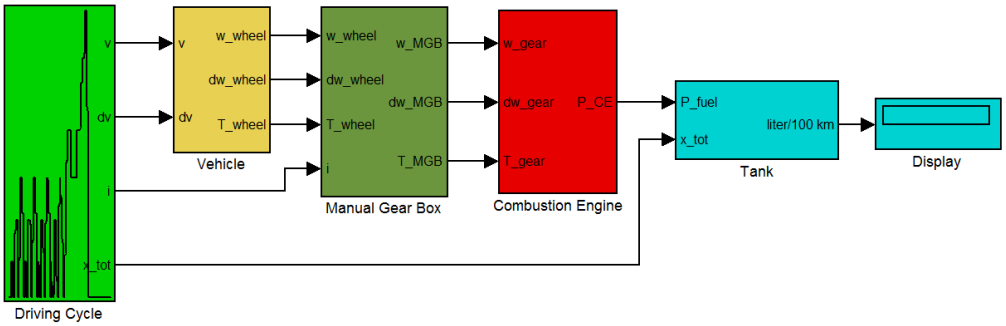

Figure 3.2.17: *Simulink model of a vehicle powered by a reciprocating engine*

The *QSS* sub-models used in this modeling process did not suffer significant modifications, as mentioned below.

Driving Cycles

To establish a fair comparison between the different vehicle models (reciprocating engine and gas turbine), it was used the same driving cycles. Therefore, the *Driving Cycle* block implemented in this model, was directly brought in from the turbine-vehicle one.

Vehicle Parameters

The same can be said about the vehicle characteristics. In this model it was simulated the same three different vehicle categories: city car, family car and SUV.

Reciprocating Engine

Regarding the engine block, it was chosen a *Combustion Engine* block, from the *QSS* toolbox library, that computes the fuel consumption based on the *consumption map* approach. Engine parameters, like the engine displacement and consequently its maximum power were based on commercialized models corresponding to the same vehicle categories in analysis. The idle fuel consumption value was calculated based on the engine displacement and an *idle fuel flow* factor which was assessed by Taylor (2003) [Tay03]. The remaining parameters input in this block were kept from the original *QSS* sub-model (see figure A.0.10).

Gear System

In terms of gear system, it was used in this model a manual gearbox, instead of the CVT system applied in the gas turbine model. This option was mainly taken due to its easier implementation, since it is not required the use of a custom controller, as it happens with automatic transmissions. Although the use of a manual gearbox requires the determination of the gear shift points in the driving cycle, the *QSS* toolbox package has this *gear vector* already defined for the most frequently used driving cycles, such as the European ones. The only new data input in this block was the gear ratios, which were taken from a spec sheet of a commercialized medium sized car (see figure A.0.13). It was chosen this particular manual gearbox model, due to its application in several car models, equipped with engines with a range of power similar to the ones simulated in this study [Jet].

4 Results & Discussion

In this chapter, the results generated by the simulation models are described and discussed. This discussion is focused on the energy consumption of the different engine models tested (both reciprocating engine and gas turbine), and it is made an attempt to achieve conclusive assessments, concerning the potential of gas turbines in road vehicle applications.

4.1 Default Driving Cycles

The first simulations were performed using the default driving cycles mentioned in section 3.2.3: NEDC, EUDC and ECE. The results are illustrated in figure 4.1.1. In this figure, it is evident the differences registered,

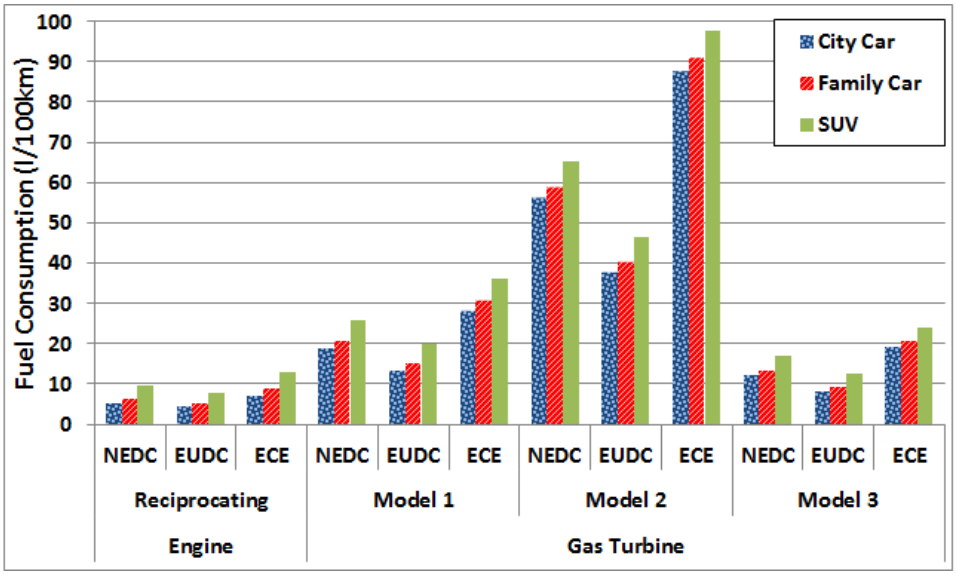

Figure 4.1.1: *Fuel consumption results for all engine types, default driving cycles and vehicle categories simulated*

in terms of fuel consumption, between not only the different engine models, but also regarding the different driving cycles tested. These results are also displayed in table 4.1.1.

Vehicle Category	Fuel Consumption (l/100km)											
	Reciprocating Engine			Gas Turbine								
				Model 1			*Model 2*			*Model 3*		
	NEDC	EUDC	ECE	NEDC	EUDC	ECE	NEDC	EUDC	ECE	NEDC	EUDC	ECE
City car	5,8	4,9	7,4	19,3	13,8	28,6	56,5	38,3	88,0	12,7	8,6	19,6
Family car	6,9	5,5	9,4	21,2	15,5	31,1	59,1	40,5	91,1	13,9	9,8	21,1
SUV	9,7	7,7	13,0	25,8	19,8	36,0	65,1	46,3	97,5	16,9	12,7	24,1

Table 4.1.1: Fuel consumption results for all engine types, default driving cycles and vehicle categories simulated

It is important to note that the predictions for the vehicles powered by piston engines are quite similar to the fuel consumption values provided by some car manufacturers. This fact makes them a credible term of comparison.

According to the results presented, the fuel consumption is always higher in the urban driving (ECE). In this driving cycle, the stop-start traffic conditions, found in the congested urban networks, are simulated through the immobilization of the vehicle in several occasions over time. These idling situations have a severe effect on

the average fuel consumption, since the engine is working, and thus consuming fuel, for a distance covered equal to zero. On the other hand, the *extra-urban* driving cycle (EUDC) presents less liters of fuel consumed per 100km, mainly due to the absence of these idling periods. Finally, the NEDC shows fuel consumption values between the ones presented by the *urban* and *extra-urban* cycles, since this is a *combined* cycle consisting of four ECEs followed by an EUDC. Comparing the results of the different engine models, it is evident the better fuel economy registered in the vehicles powered by a reciprocating engine. A further analysis, between the piston engine and gas turbine results, is developed next.

It is important to note that, in order to do a fair comparison between reciprocating engines and gas turbines, it was disabled the *fuel cutoff* function. As previously mentioned, this is a standard function of piston engines equipped with modern fuel injection systems, which enables the fuel cutoff when the torque value, at idle speeds, falls below a certain limit. Although this function improves considerably the fuel economy, it is not suitable to gas turbines.

The results for the two *Chrysler* gas turbine versions (model 1 and 2) allow as also to assess the importance of heat-exchangers in the overall efficiency of gas turbines. For a *combined* driving cycle (NEDC), model 1 (with heat-exchanger) registered an average fuel consumption lower in, approximately, 64% than the same gas turbine model without any regenerator (model 2), as it is shown in table 4.1.2.

Vehicle Category	Fuel Consumption (l/100km)	Fuel Economy Improvements (%)	
	Model 2	***Model 1***	***Model 3***
	Chrysler g. t. **without** heat-exch.	*Chrysler* g.t. **with** heat-exch.	*Modern* gas turbine
City car	56,5	65,9	77,6
Family car	59,1	64,1	76,4
SUV	65,1	60,5	74,0

Table 4.1.2: Comparison between the fuel consumption of gas turbine models (NEDC)

An even higher fuel economy can be achieved with the third gas turbine tested (about 76% of improvement), a model that not only has components (compressor and turbines) with higher efficiencies, but that also operates at an inlet turbine temperature about 150 ° higher than the one used in the *Chrysler* models. Since model 3 is the gas turbine with the best performance in terms of fuel economy, a detailed comparison was carried out between this model and the results corresponding to the vehicles powered by a piston engine, as figure 4.1.2 and table 4.1.3 show.

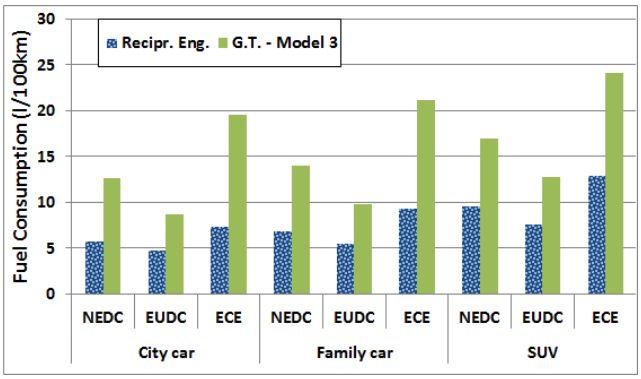

Figure 4.1.2: *Fuel consumption results correspondent to piston engine models and gas turbine model 3*

Although model 3 has the best fuel economy among all gas turbines simulated, it still has a fairly poor performance compared to the reciprocating engines. This observation is verified in all vehicle categories. For the city car, while model 3 demonstrates fuel consumptions about 118% higher than the piston engine model, for the SUV this difference is reduced to 75%. As a matter of fact, it can be observed that the difference between the gas turbine and piston engine reduces as the vehicle weight increases. This trend can be explained by the

Powertrain	Fuel Consumption (l/100km)								
	City car			Family car			SUV		
	NEDC	EUDC	ECE	NEDC	EUDC	ECE	NEDC	EUDC	ECE
Reciprocating Eng.	5,8	4,9	7,4	6,9	5,5	9,4	9,7	7,7	13,0
G.T. - Model 3	12,7	8,6	19,6	13,9	9,8	21,1	16,9	12,7	24,1
Difference (%)	**118,7**	**77,6**	**165,3**	**100,7**	**76,9**	**124,6**	**75,2**	**65,3**	**85,5**

Table 4.1.3: Fuel consumption results correspondent to piston engine models and gas turbine model 3

fact that, in heavier vehicles, it is required more power from the engine. In other words, for heavy vehicles, like an SUV, the gas turbine operates closer to its nominal conditions, i.e. the operating conditions for which it was designed. Basically, it is appropriate to conclude that the gas turbine has a better relative fuel consumption in the SUV, due to the higher operational efficiencies achieved in the simulations (lower overall specific fuel consumption). This statement can be confirmed by figures 4.1.3 and 4.1.4, which show the operation points of model 3 powering, respectively, the city car and the SUV in a *combined* driving cycle (NEDC).

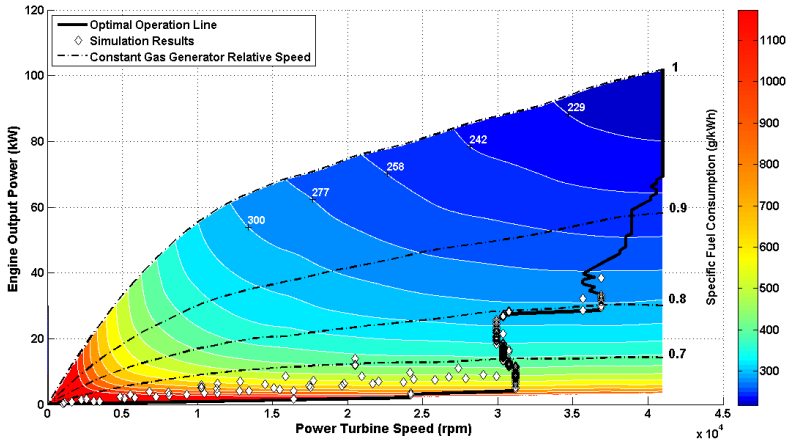

Figure 4.1.3: *Operation points of gas turbine model 3 powering the city car in the NEDC*

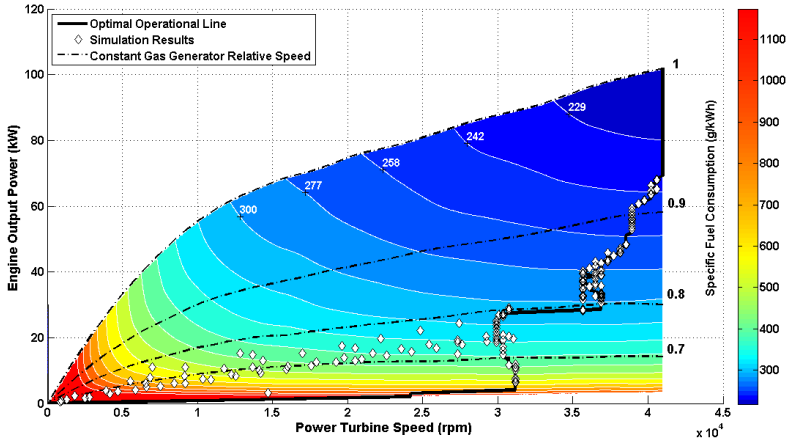

Figure 4.1.4: *Operation points of gas turbine model 3 powering the SUV in the NEDC*

From these two figures, it is also possible to verify the increased proximity of the engine operation points to the *Optimal Operation Line* in the city car than in the SUV. This is a consequence of the higher acceleration lag input to the heavier vehicle, in order to simulate its greater inertia. In situations where the "free" power turbine cannot operate at its *ideal* speed for a given power requirement, represented by the *Optimal Operation Line*, the gas generator increases its speed, in order to increase the output power delivered, and thus achieve the requirements imposed by the driving cycle.

The *acceleration lag* effect can also be observed in figure 4.1.5 that shows the operation of the gas turbine powering the SUV, along the NEDC. This slow throttle response, inherent to gas turbines operation, is represented in the second chart of this figure, which shows a mismatch between the *optimal operation speed* and the *output shaft speed* during the vehicle acceleration periods.

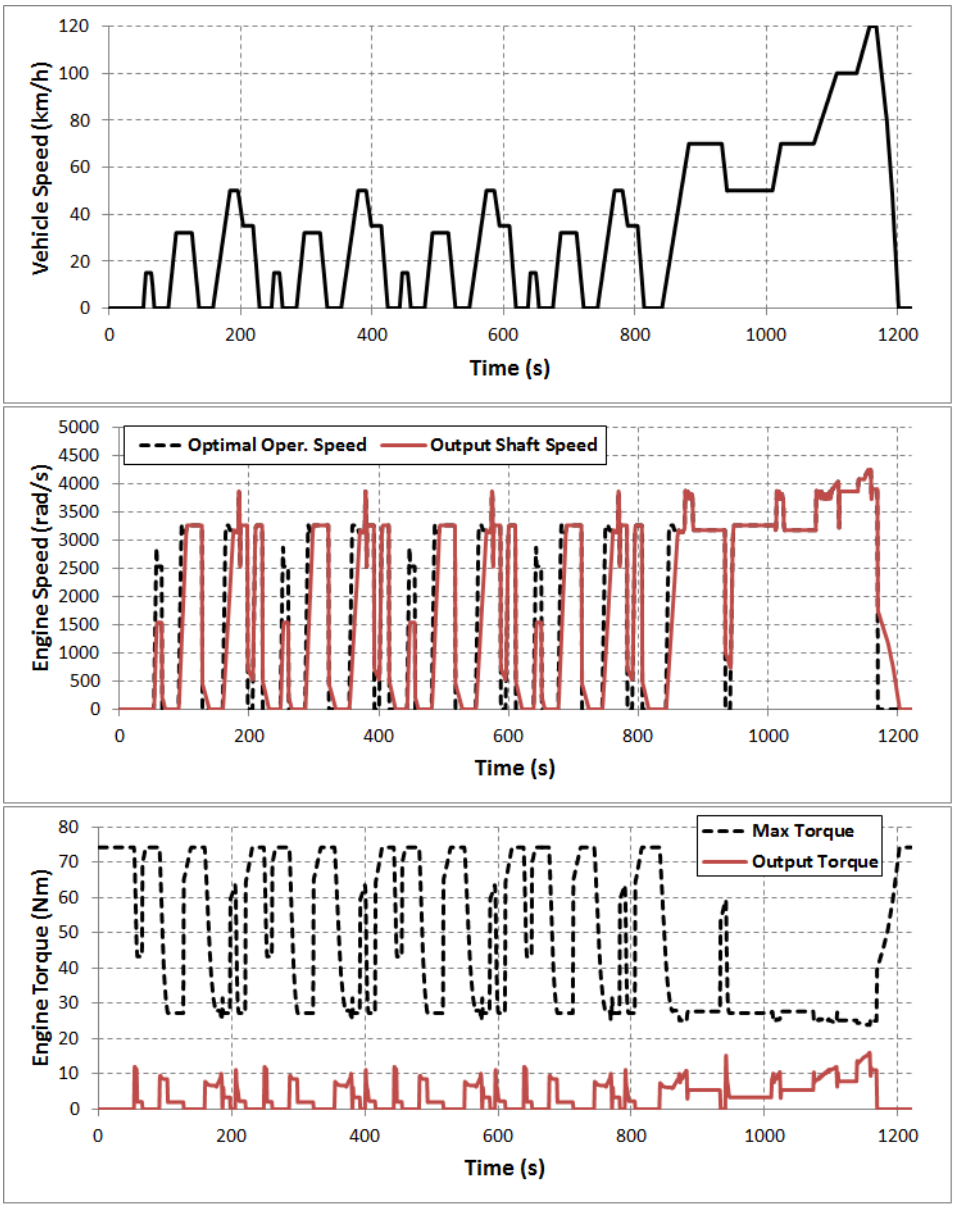

Figure 4.1.5: *Simulation results of the SUV powered by gas turbine model 3 along the NEDC*

In the third chart of figure 4.1.5 it is represented not only the torque delivered by the "free" power turbine, but also the maximum torque capable of being provided by the engine along the driving cycle. This parameter, as it is observed, is highly dependent on the gas turbine output shaft speed, varying between its minimum and

maximum values, according to the vehicle speed. When the *output torque* line overpasses the *maximum torque* line, it means that the engine is overloaded. The relation between these two lines tells how close is the engine to its maximum operating capacity. According to this same chart, the most demanding situation to the gas turbine happens around the 1150^{th} second of the NEDC, at the same moment the SUV reaches the maximum speed in the whole driving. If on one hand, high vehicle speed means high drag forces (more effort required to the engine), on the other hand it also means a decrease in the maximum torque limit; a situation that gets the engine closer to its maximum capacity.

To get a more detailed comparison between the reciprocating engine and model 3, the evolution of the fuel consumption of both engines powering the SUV, along the *combined* cycle (NEDC), is plotted in figure 4.1.6.

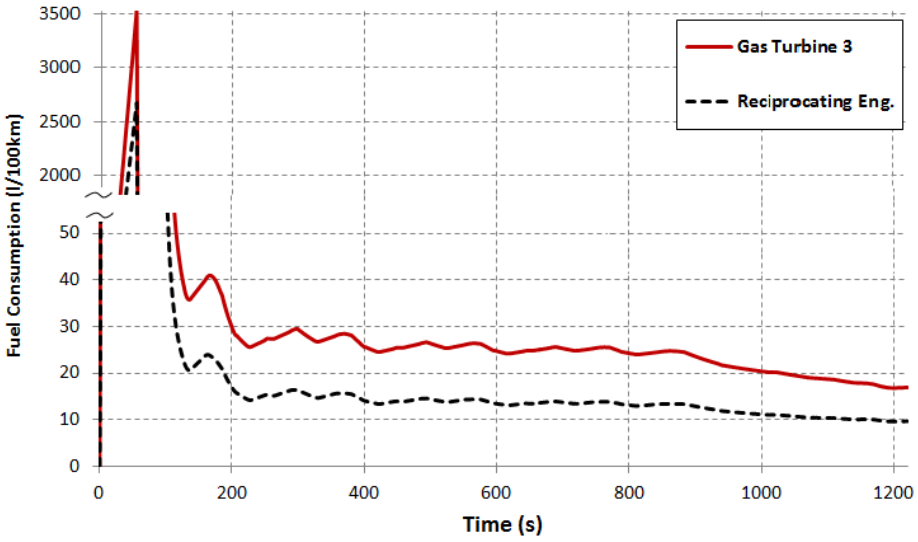

Figure 4.1.6: *Evolution of fuel consumption (l/100km) of both SUV models powered by gas turbine model 3 and reciprocating engine, along the NEDC*

The extremely high fuel consumption found for both engines, at the early stages of the driving cycle, are attributed to idle operating conditions, which represent those situations when the engine is running but the vehicle is immobilized. From this figure, it is also possible to observe that the gas turbine has a higher idle fuel consumption than the reciprocating engine. This means that there is little benefit in using gas turbines in urban driving conditions, as it was previously verified (figure 4.1.1 and table 4.1.1).

In order to understand some of the uncertainties in these results, it is important to assess the percentage of operation points that were calculated based on either the extrapolation or linear interpolation of the data generated in *GasTurb*. This assessment is relevant since it can address two different sources of error in the gas turbine data. On one hand, one has the data generated by the linear interpolation of the original data, which have a higher level of certainty. On the other hand, one also has data obtained by extrapolation (assumptions) and whose accuracy is rather difficult to assess. Depending on the type of vehicle in analysis, the percentage of operation points found inside the "original data" area (the most reliable data) varies. Since heavier vehicles require more power from the engine, the SUV has a higher percentage of operation points inside this area than the city or family car, as it is shown in table 4.1.4. In this same table, the percentage of fuel consumed in the NEDC, that is associated with this area, is also given. The percentages achieved reflect the better level of uncertainty associated with the simulation of those vehicle and driving cycle combinations that force the engine to operate closer to its design point, i.e. in demanding situations.

In order to provide a better understanding of these two different groups of results, it is illustrated in figure 4.1.7 the operation points associated to gas turbine model 3 powering the SUV in the NEDC. In this figure, the operation points located inside the "original data" area are represented by dark dots, while the remaining points (outside this area) have a white coloration.

Inside "original data" Area	Operation Points	Fuel Consumed
City Car	20,5%	31,0%
Family Car	30,4%	42,5%
SUV	53,5%	68,0%

Table 4.1.4: Percentage of operation points (NEDC) located inside “original data” area

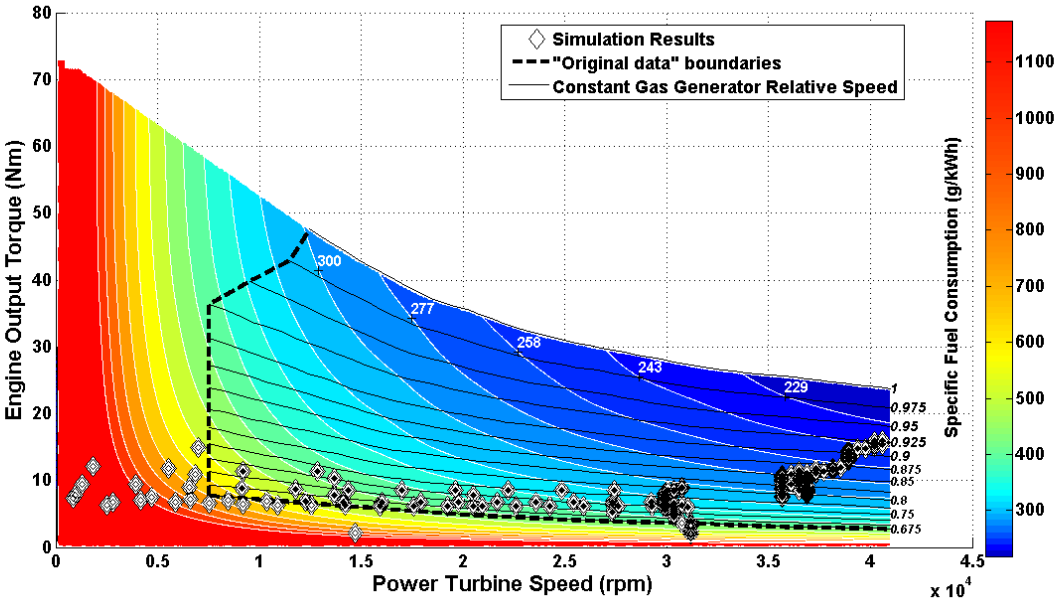

Figure 4.1.7: *Operation points of gas turbine model 3 powering the SUV in the NEDC*

4.2 Custom Driving Cycles

More than comparing the fuel consumption between gas turbines and reciprocating engines, this study also attempts to roughly assess the dynamic performance of different vehicles powered by a 100kW gas turbine. Although the quasistatic approach used in this simulation is not suitable for analyzing best-effort performance, it was made an attempt to simulate the engine operating at demanding conditions. Therefore, it was designed an acceleration driving cycle for each vehicle in analysis. Based on a "trial and error" method, it was achieved a driving pattern capable of making the gas turbine operate close to its maximum capacity, without reaching an overload situation. The three different custom driving cycles, one for each vehicle category, are presented in figure 4.2.1.

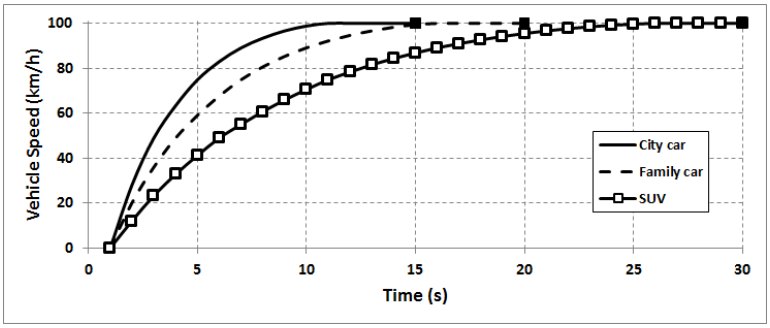

Figure 4.2.1: *Acceleration driving cycles*

As previously mentioned in the *Vehicle Modeling* section, the design of these custom driving cycles was also influenced by another factor: the slow throttle response associated to gas turbines operation. This parameter varies according to the vehicle inertia, i.e. its weight, in such a way that it was assumed different acceleration lags for each vehicle. While in the city car the gas turbine takes 4 seconds to reach the nominal output shaft speed after depressing the acceleration pedal, the family car and the SUV take 4.5 and 6 seconds, respectively. The effect of the acceleration lag can be identified in the following figures (4.2.2, 4.2.3, 4.2.4) where it is shown the operation points associated to the acceleration test of each vehicle powered by the gas turbine model 3.

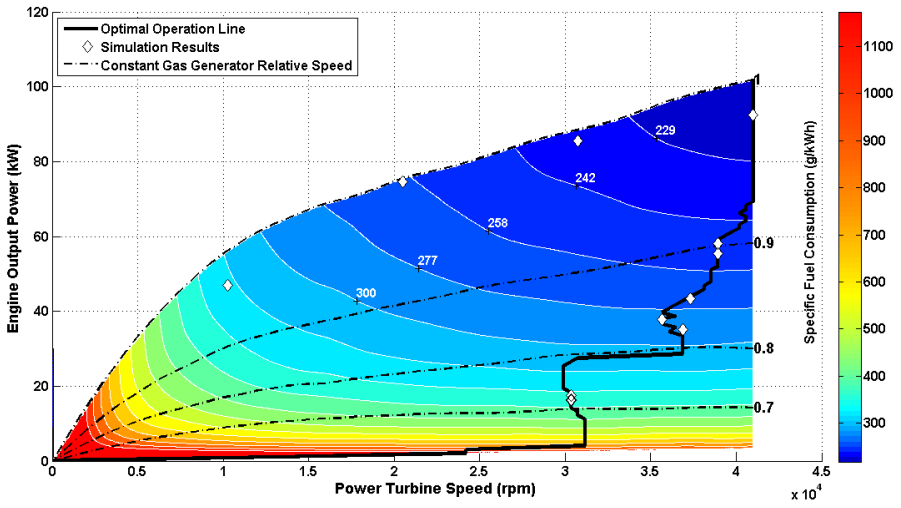

Figure 4.2.2: *Operation points of gas turbine model 3 powering the city car in the acceleration driving cycle*

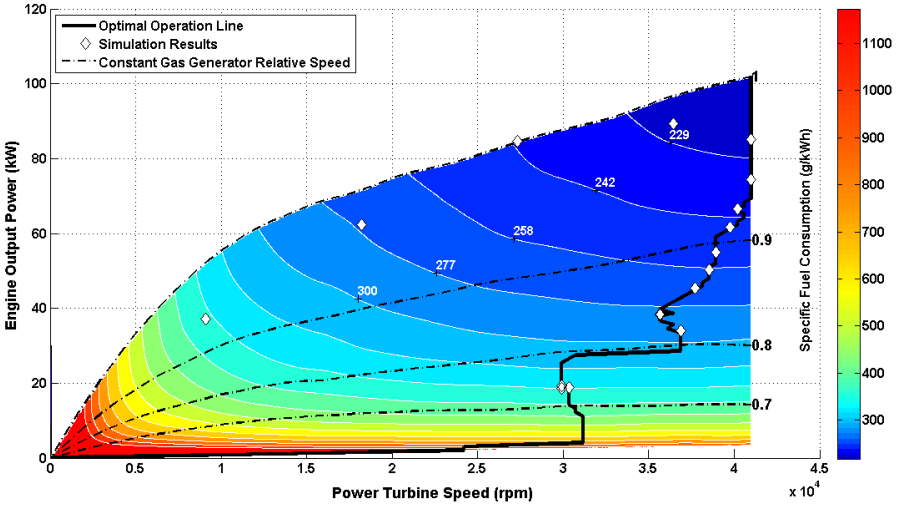

Figure 4.2.3: *Operation points of gas turbine model 3 powering the family car in the acceleration driving cycle*

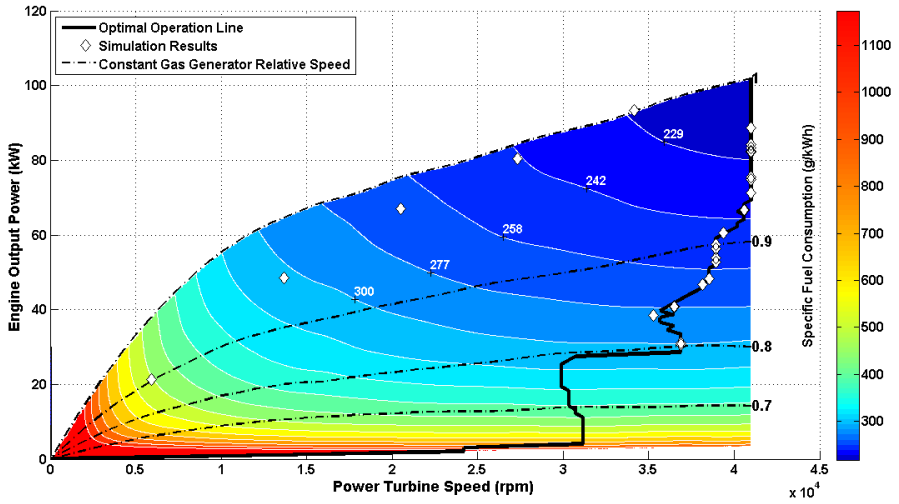

Figure 4.2.4: *Operation points of gas turbine model 3 powering the SUV in the acceleration driving cycle*

Comparing, for instance, the figures corresponding to the city car and the SUV, it is verified that in the heavier vehicle, the "free" power turbine requires more time to reach its nominal speed. This fact is illustrated by the number of white points (operation points) located between the minimum and the maximum output shaft speed, in the upper zone of the graph, which corresponds to the number of seconds addressed to the acceleration lag.

It is also important to refer that in these *dynamic* tests it was not taken into account the friction limit associated to the contact between the tyres and the road. Nevertheless, the acceleration times considered in these simulations were such, that problems concerning the vehicle traction in the asphalt should not arise.

It would be of interest to compare the fuel consumption between the gas turbine and the reciprocating engine in maximum acceleration conditions. However, in order to do an accurate analysis, a dynamic approach needs to be implemented in the simulation model.

Constant Speed - 100km/h

The quasistatic approach allows the assessment of the fuel consumption of a vehicle running at constant speed. For that reason it was carried out a simulation at constant speed (100km/h) for the SUV when powered by either the reciprocating engine or the gas turbine model 3, i.e. the two models with the most similar simulation results at the default driving cycles. In table 4.2.1 it is possible to verify that, even at this driving condition, the gas turbine cannot attain a better fuel economy than the piston engine, requiring 3.6 liters more of fuel per 100km.

	Fuel Consumption (l/100km)	
Constant Speed 100 km/h	Gas Turbine 3	Reciprocating Engine
SUV	11,9	8,3

Table 4.2.1: Fuel Consumption correspondent to the SUV running at a constant speed of 100km/h

Beyond that, it is important to refer that the gear ratios used in the manual gearbox, that is coupled to the reciprocating engine, are not optimized, contrary to what happens in the gas turbine model that uses a CVT system. This means that it may exist room for improving the fuel economy of the piston engine, a situation that would increase even more the difference relative to the gas turbine model.

Another relevant aspect associated to gas turbine vehicles is the maximum torque registered in their drivetrain system during the different simulations performed. The use of a CVT system in these models, whose main drawback is related to its maximum load capacity, imposes this analysis. As previously mentioned in the *Drivetrain System* section, the maximum torque tolerated by a modern CVT is about 385 Nm. This value is much lower than the maximum torque registered downstream the reduction gear (9.765:1) coupled to the gas turbines in study (up to 800 Nm at stall speed). Anyway, it is correct to say that the driving conditions simulated are quite realistic, since it was never registered, in any situation except one, a torque value higher than the one supported by the gearbox system in use, i.e. above 385 Nm. The only exception occurred in the acceleration test of the city car, since it was submitted to a faster acceleration comparing with the other vehicles. In table 4.2.2, it is possible to see the maximum torque values registered in the drivetrain system, under the most demanding driving conditions simulated, i.e. acceleration tests.

Acceleration Test	City car	Family car	SUV
Max. Torque (Nm)	425	380	333

Table 4.2.2: Maximum torque demanded to the engine during acceleration tests

5 Conclusion & Future Work

5.1 Conclusion

The investigation of the applicability of gas turbines as powertrains for road vehicles requires a long and detailed study in several disciplines. The engine performance, the manufacturing costs or even its acceptance in the market are some of the parameters that need to be taken into consideration, in order to achieve reliable conclusions. The work developed in this thesis was mainly focused in the assessment of the gas turbine performance, in terms of fuel consumption. The simulations performed generated quite distinct results for the different vehicle categories, driving patterns and engine models simulated. From these results, it is possible to identify different trends, and hence draw some interesting conclusions:

1. The use of a heat-exchanger in a gas turbine powering road vehicles allows the improvement of fuel economy at around 64%, on average. The application of components with higher efficiencies and the use of a higher inlet turbine temperature (*modern* gas turbine model), produced fuel savings up to 76%.

2. The vehicles equipped with a gas turbine have higher fuel consumption than the ones with reciprocating engines, independently of the driving conditions simulated: urban, extra-urban or combined driving;

3. Gas turbines used as the prime mover in heavier vehicles, such as an SUV, have a better relative fuel consumption compared to lighter vehicles, since the engine operates closer to its design point, resulting in a higher overall efficiency. However, even when considering an SUV powered with the *modern* gas turbine (model 3), it demonstrates on average, 75% higher fuel consumption than the reciprocating engine.

4. At idle conditions, gas turbines have a substantially higher fuel consumption compared to reciprocating engines. This fact indicates a limited benefit from the use of gas turbines in urban driving conditions where the vehicle immobilization occurs frequently. Exception to this could be a hybrid configuration.

5. Operating at a constant regime, i.e. when the vehicle is moving at a constant speed of 100km/h, gas turbines also have a worse fuel economy. Considering the SUV, which is the vehicle where the two different types of engine register closer fuel consumption values, it is still verified that the gas turbine requires 3.6 liters more of fuel than the piston engine, in order to cover 100km.

6. Although the acceleration tests performed with the custom driving cycles are not accurate, due to the quasistatic simulation approach, they give an idea of how much the vehicle's characteristics, mainly the weight, influence its dynamic performance. The greater propulsive force required in heavier vehicles implies the use of longer acceleration times, in order to avoid overloading the engine. The uncertainty concerning the acceleration lag is another parameter with great influence on the accuracy of the dynamic simulations.

7. The choice of the most suitable vehicle category for the application of a 100kW gas turbine is not a trivial question. The answer depends on a trade-off between two parameters: fuel economy and dynamic performance.

It would be of added value to compare the fuel consumption between gas turbines and reciprocating engines, in demanding driving conditions, such as acceleration tests. However, in order to proceed with an accurate analysis, a dynamic approach would need to be implemented in the simulation model, compared to the quasistatic approach utilized within this study.

5.2 Future Work

An interesting proposal for future work is connected with the use of the methodology and tools developed in this study, to simulate and test other gas turbine configurations with higher efficiency. For instance, gas turbines with variable guide vanes or an intercooled and recuperated cycle could be easily modeled in *GasTurb*, and thereafter implemented in Simulink as a road vehicle powertrain. It could also be interesting to study a combined cycle configuration, i.e. a gas turbine with a heat-exchanger on the hot side, recovering part of the waste heat of the exhaust gas to a steam cycle. Generally, combined cycles have higher overall efficiencies, comparing with the remaining gas turbine configurations. As Walsh and Fletcher (2004) presents, a combined gas turbine cycle may achieve a thermal efficiency of about 46.7%, for an inlet turbine temperature equal to 1300K and a pressure ratio around 5. In fact, the idea of implementing a steam cycle in a car is not completely new. In 2005, BMW presented the "Turbosteamer", an innovative assistance drive that, combined with a 1.8 liter petrol engine, achieves a reduction in the fuel consumption by up to 15% and generates 10kW more power. These impressive achievements were reached with a reciprocating engine, whose exhaust gas temperature is considerably lower than the one provided by a gas turbine, in such a way that even greater improvements are expected to be obtained with this type of engine. This BMW project is also relevant because it could prove the feasibility of combining heat and power in a car, with components that are capable of being installed in existing model series [Bmw].

The tools developed in this study also allow the simulation of a hybrid configuration vehicle, with a gas turbine as prime mover. The components required in the modeling of a hybrid vehicle, such as the electric motor, generators or even the battery, can be simulated using the modules available in the *QSS* toolbox. The hybrid configuration has led the automotive industry in the search for the most promising "range extender" technology to be associated with electric propulsion. Some car manufacturers defend that the use of a single-shaft gas turbine, operating at constant speed and power, as prime mover in a series hybrid configuration, constitutes the most efficient solution in the near future. The methodology developed in this thesis could contribute to this assessment by constituting a first estimation for the fuel economy of different powertrain topologies.

A more detailed approach reveals that there is still room for some improvements in the simulation model developed. For instance, the gas turbine module, implemented in Simulink, does not allow the measurement of the gas generator speed. Considering the importance of this parameter in the assessment of inertia forces, and thus in the overall engine performance, some effort should be put into this model. In other words, this model should be "upgraded" in such a way that inertia forces corresponding to each spool (high and low pressure) could be addressed, in order to achieve more reliable results.

It would be also of interest the validation of the models developed in this study with experimental or empirical data. This comparison would allow the assessment of the accuracy level of the results achieved, at the same time that would allow to evaluate how reliable is this tool and how useful it can be for future research works.

References

[Aut] *Genius at work: turbine cars...* Autodrome Paris, Jan. 2011. URL: http://www.autodrome.fr/turbinecar2.htm.

[Bmw] *More efficiency instead of power loss: BMW Group Research and Engineering is using combined heat and power in a car for the first time.* Media Information. BMW AG, Dec. 2005. URL: www.press.bmwgroup.com.

[Bog06] S. Bogemann. *Replacing the secondary cyclinder of a Jatco CK2 to improve efficiency.* Bachelor final project. Jan. 2006.

[Boy02] M. Boyce. *Gas Turbine Engineering Handbook.* Butterworth-Heinemann, 2002. ISBN: 0-88415-732-6.

[Cap] *CMT-380 Microturbine Supercar.* Capstone Turbine Corporation, 2009. URL: www.capstoneturbine.com/_docs/CMT380_lowres.pdf.

[Chr62] Chrysler. *Gas Turbine Vehicles - A review of gas turbine-powered vehicles shown publicly by Chrysler Corporation.* Prepared by technical information engineering office. July 1962.

[Chr79] Chrysler. *History of Chrysler Corporation's Gas Turbine Vehicles.* Prepared by technical information engineering office. Jan. 1979.

[Die] *Emission Test Cycles: ECE 15 + EUDC / NEDC.* Diesel Net, Apr. 2011. URL: http://www.dieselnet.com/standards/cycles/ece_eudc.html.

[Ehs+10] M. Ehsani, Y. Gao, and A. Emadi. *Modern Electric, Hybrid Electric and Fuel Cell Vehicles.* CRC Press, 2010. ISBN: 978-1-4200-5398-2.

[Etv] ETV Motors - Electric Technology for Vehicles, 2011. URL: http://etvmotors.com/.

[Ev1] *EV1 Electric: Series Hybrid.* National Automobile Bankers Associates / Vehicle Information Services, 2001. URL: http://www.autoworld.com/news/GMC/Series_Hybrid.htm.

[F1j] *Gas Turbines in F1 2013.* Formula 1 Journal, Apr. 2010. URL: http://www.formula1journal.com/2010/04/gas-turbines-in-f1-2013-by-sportsman.html.

[GA05] L. Guzzella and A. Amstutz. *The QSS Toolbox Manual.* Swiss Federal Institute of Technology Zurich, Measurement and Control Laboratory, June 2005. URL: http://www.idsc.ethz.ch/Downloads/qss.

[Gea] *Technical Library.* Stock Drive Products/Stering Instruments, Apr. 2011. URL: http://www.sdp-si.com/Sdptech_lib.htm.

[Guz+07] L. Guzzella and A. Sciarretta. *Vehicle Propulsion Systems.* Springer-Verlag Berlin Heidelberg, 2007. ISBN: 978-3-540-74691-1.

[Hof+01] T. Hoffman et al. *A fundamental case study on the Prius and IMA drivetrain concepts.* Technische Universiteit Eindhoven. 2001.

[Hor03] J. Horlock. *Advanced Gas Turbine Cycles.* Elsevier Science Ltd., 2003. ISBN: 0-08-044273-0.

[Hus03] I. Husain. *Electric and Hybrid Vehicles - Design Fundamentals.* CRC Press, 2003. ISBN: 0-8493-1466-6.

[Hyb] *Hybrid Drive Systems for Vehicles - System Design and Traction Concepts.* Lund University. 2006.

[Ing95] J. G. Ingersoll. *Natural Gas Vehicles.* The Fairmont Press, 1995. ISBN: 0-88173-218-4.

[Jag] *Jaguar to Build C-X75 Hybrid Supercar.* Press Release. Jaguar Cars, 2010. URL: http://www.media.c-x75.com/.

[Jay] *Jay Leno Builds a Turbine-Powered Biodiesel Supercar.* Jay Leno's Garage, Feb. 2010. URL: http://www.jaylenosgarage.com/extras/articles/jay-leno-builds-a-turbine-powered-biodiesel-supercar/.

[Jet] *2009 U.S. Jetta, Technical Specifications.* Media Information. Volkswagen of America, Inc., Jan. 2008.

[Kes+03] J. Kesseli et al. «Micro, industrial and advanced gas turbines employing recuperators». In: *ASME Paper No. GT2003-38938* (2003). ASME, New York, NY.

[Kur11] J. Kurzke. 2011. URL: http://www.gasturb.de/index.html.

[Kyp11] K. G. Kyprianidis. *Lecture Notes on Gas Turbine Performance.* Gothenburg: Chalmers University of Technology, Feb. 2011.

[Lan00] K. R. Lang. An Overview of CVT Research Past, Present and Future. 2000.

[Lan09] J. H. Lang. *Multi Wafer Rotating MEMS Machines - Turbines, Generators, and Engines.* Springer, 2009. ISBN: 978-0-387-77746-7.

[Mat] *MATLAB manual. Ordinary Differential Equations*. Version 7.8. Mathworks, 2008. URL: http://www.mathworks.com/access/helpdesk/help/techdoc/ref/ode45.html.

[McD03] C. McDonald. ≪Recuperator considerations for future higher efficiency microturbines≫. In: *Applied Thermal Engineering* 23 (2003), pp. 1463–1487.

[Mor+06] M. Moran and H. Shapiro. *Fundamentals of Engineering Thermodynamics*. John Wiley & Sons, Inc., 2006. ISBN: 978-0-470-03037-0.

[Nor65] J. Norbye. *Turbine Drives Chevy Truck*. Popular Science, Oct. 1965.

[Nor74] J. Norbye. *Volkswagen develops a gas-turbine car*. Popular Science, May 1974.

[OS05] A. Olsson and L. Sundin. ≪The Volvo Heavy Truck Gas Turbine VT300≫. In: *Commercial Vehicle Engineering Congress and Exhibition*. Chicago, Illinois, Nov. 2005.

[Oud05] M. Oudijk. ≪Optimization of CVT control - For Hybrid and Conventional drive lines≫. MA thesis. Eindhoven University of Technology, Nov. 2005.

[Ren] Renault Group, Feb. 2011. URL: http://www.renault.com.

[Sam+10] A. Same et al. ≪A study on optimization of hybrid drive train using Advanced Vehicle Simulator (ADVISOR)≫. In: *Journal of Power Sources* 195 (2010), pp. 6954–6963.

[Sar+01] H. Saravanamuttoo, G. Rogers, and H. Cohen. *Gas Turbine Theory*. Pearson Education Limited, 2001. ISBN: 0130-15847-X.

[Sen03] B. Senefsky. *Chevrolet Turbo-Titan III Concept Vehicle - Space Truckin'*. Sport Truck, 2003. URL: http://www.sporttruck.com/featuredvehicles/chevy/0309st_chevrolet_turbo_titan_3_concept_vehicle/index.html.

[Sha05] R. Shah. ≪Compact Heat Exchangers for Microturbines≫. In: *Micro Gas Turbines* (2005). Educational Notes RTO-EN-AVT-131, Paper 2. Neuilly-sur-Seine, France: RTO, pp. 2.1–2.18.

[Sou11] J. Sousanis. *World Vehicle Population Tops 1 Billion Units*. WardsAuto.com, Aug. 2011. URL: http://wardsauto.com/ar/world_vehicle_population_110815/index.html.

[Tay03] G. W. Taylor. *Review of the Incidence, Energy Use and Costs of Passenger Vehicle Idling*. Office of Energy Efficiency, Natural Resources Canada, 2003. URL: http://oee.nrcan.gc.ca/transportation/idling/calculations.cfm?attr=8#footnotes.

[Vol] *ECT and FL6 Hybrid*. Volvo Trucks. URL: http://www.volvotrucks.com/trucks/global/en-gb/company/history/1990s/Pages/ECT_and_FL6_Hybrid.aspx.

[Wal+04] P. Walsh and P. Fletcher. *Gas Turbine Performance*. Blackwell Publishing, 2004. ISBN: 0-632-06434-X.

[Wu04] C. Wu. *Thermodynamic Cycles, Computer-Aided Design and Optimization*. Marcel Dekker, Inc., 2004. ISBN: 0-8247-4298-2.

A Appendix

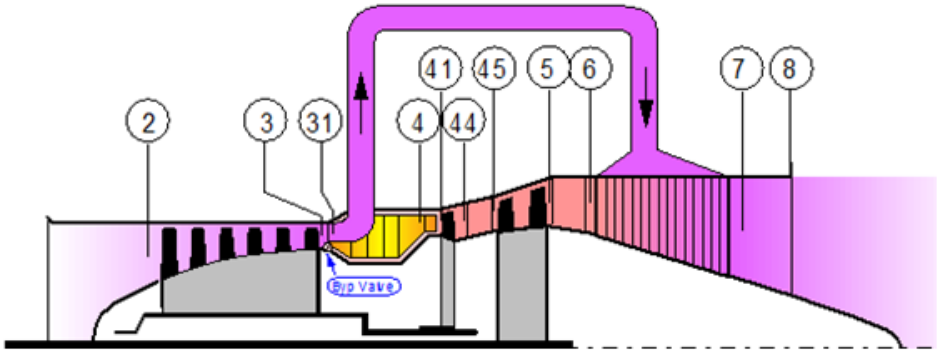

Alt= 0m ISA 60% Relative Humidity , Rel Speed=1.000

Station	W kg/s	T K	P kPa	WRstd kg/s
amb		288.15	101.325	
1	0.965	288.15	101.325	
2	0.965	288.15	97.981	1.000
3	0.955	465.14	391.925	0.314
31	0.902	465.14	391.925	0.297
35	0.902	870.80	384.087	
4	0.911	1200.00	369.107	0.511
41	0.911	1200.00	369.107	0.511
43	0.911	1039.33	181.713	
44	0.959	1012.44	181.713	
45	0.959	1012.44	177.170	1.030
49	0.959	918.44	110.932	
5	0.969	913.59	110.932	1.579
6	0.969	913.59	108.713	
7	0.969	544.95	104.365	
8	0.969	544.95	104.365	1.296
Bleed	0.005	465.14	391.925	

Efficiencies:	isentr	polytr	RNI	P/P
Compressor	0.7831	0.8200	0.967	4.000
Burner	0.9900			0.961
HP Turbine	0.8466	0.8350	0.684	2.031
LP Turbine	0.8429	0.8350	0.399	1.597
Heat Exch	0.9000			
Generator	1.0000			

HP Spool mech Eff 0.9980 Speed 44600 rpm
PT Spool mech Eff 0.9780 Speed 35154 rpm

Ps0-P2= 3.344 Ps8-Ps0= 0.000

hum [%]	war0	FHV	Fuel
60.0	0.00659	42.744	Diesel

PWSD	= 102.0	kW
PSFC	= 0.3030	kg/(kW*h)
Heat Rate	= 12951.5	kJ/(kW*h)
V0	= 0.00	m/s
FN res	= 0.09	kN
P35/P3	= 0.98000	
WF	= 0.00858	kg/s
s NOx	= 0.61727	
Therm Eff	= 0.27796	
P45/P44	= 0.97500	
Incidence	= 0.00000	°
P6/P5	= 0.98000	
PWX	= 0	kW
P7/P6	= 0.96000	
P8/Pamb	= 1.03000	
WBld/W2	= 0.00500	
A8	= 0.01548	m²
TRQ	= 100.0	%
P2/P1	= 0.96700	
Loading	= 100.00	%
e444 th	= 0.82856	
WHcl/W2	= 0.05000	
PW_gen	= 102.0	kW
WLcl/W2	= 0.01000	
eta t-s	= 0.71424	
Ps8	= 101.325	kPa

Figure A.0.1: *Design Point Performance of Gas Turbine Model 1 - GasTurb*

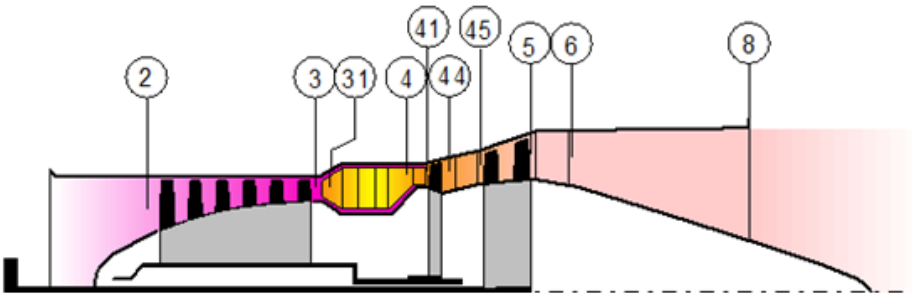

Turboshaft Alt= 0m ISA 60% Relative Humidity

Station	W kg/s	T K	P kPa	WRstd kg/s
amb		288.15	101.325	
1	0.833	288.15	101.325	
2	0.833	288.15	97.981	0.863
3	0.825	465.14	391.925	0.271
31	0.779	465.14	391.925	
4	0.795	1200.00	376.640	0.437
41	0.795	1200.00	376.640	0.437
43	0.795	1043.76	187.064	
44	0.836	1017.36	187.064	
45	0.836	1017.36	182.388	0.874
49	0.836	911.21	106.495	
5	0.845	906.55	106.495	1.428
6	0.845	906.55	104.365	
8	0.845	906.55	104.365	1.457
Bleed	0.004	465.14	391.925	

Efficiencies:	isentr	polytr	RNI	P/P
Compressor	0.7831	0.8200	0.967	4.000
Burner	0.9900			0.961
HP Turbine	0.8463	0.8350	0.698	2.013
LP Turbine	0.8440	0.8350	0.409	1.713
Generator	1.0000			

HP Spool mech Eff 0.9980 Nom Spd 44600 rpm
PT Spool mech Eff 0.9780 Nom Spd 35154 rpm

Ps0-P2= 3.344 Ps8-Ps0= 0.000

hum [%]	war0	FHV	Fuel
60.0	0.00659	42.744	Diesel

PWSD	=	102.0 kW
PSFC	=	0.5610 kg/(kw*h)
Heat Rate	=	23979.0 kJ/(kw*h)
V0	=	0.00 m/s
FN res	=	0.10 kN
WF	=	0.01589 kg/s
s NOx	=	0.07721
Therm Eff	=	0.15013
P45/P44	=	0.97500
Incidence	=	0.00000 °
P6/P5	=	0.98000
PWX	=	0 kW
P8/Pamb	=	1.03000
WBld/W2	=	0.00500
A8	=	0.01742 m²
TRQ	=	100.0 %
P2/P1	=	0.96700
Loading	=	100.00 %
e444 th	=	0.82882
WHcl/W2	=	0.05000
PW_gen	=	102.0 kW
WLcl/W2	=	0.01000
eta t-s	=	0.77723
Ps8	=	101.325 kPa

Iteration Variables:
Inlet Corr. Flow W2Rstd kg/s (0.5...1) = 0.862973

Iteration Targets:
Shaft Power Delivered = 102

Figure A.0.2: *Design Point Performance of Gas Turbine Model 2 - GasTurb*

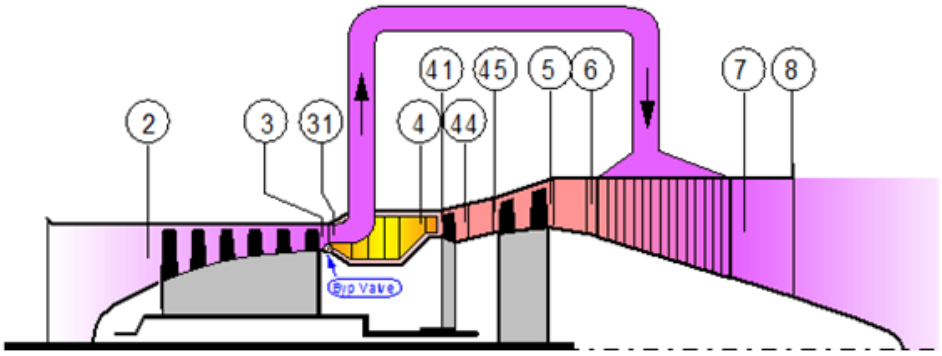

Turboshaft with Heat Exchanger Alt= 0m ISA 60% Relative Humidity

Station	W kg/s	T K	P kPa	WRstd kg/s
amb		288,15	101,325	
1	0,565	288,15	101,325	
2	0,565	288,15	97,981	0,586
3	0,559	450,33	391,925	0,181
31	0,528	450,33	391,925	0,171
35	0,528	957,63	384,087	
4	0,535	1350,00	369,107	0,318
41	0,535	1350,00	369,107	0,318
43	0,535	1207,05	220,540	
44	0,563	1171,92	220,540	
45	0,563	1171,92	215,026	0,536
49	0,563	1015,72	109,788	
5	0,568	1009,97	109,788	0,984
6	0,568	1009,97	107,593	
7	0,568	552,72	104,365	
8	0,568	552,72	104,365	0,766
Bleed	0,003	450,33	391,925	

Efficiencies:	isentr	polytr	RNI	P/P
Compressor	0,8552	0,8800	0,967	4,000
Burner	0,9900			0,961
HP Turbine	0,9230	0,9185	0,599	1,674
LP Turbine	0,8847	0,8760	0,410	1,959
Heat Exch	0,9000			
Generator	1,0000			

HP Spool mech Eff 0,9980 Nom Spd 61000 rpm
PT Spool mech Eff 0,9780 Nom Spd 41000 rpm

Ps0-P2= 3,344 Ps8-Ps0= 0,000

hum [%]	war0	FHV	Fuel
60,0	0,00659	42,744	Diesel

PWSD	=	102,0 kW
PSFC	=	0,2182 kg/(kW*h)
Heat Rate	=	9327,9 kJ/(kW*h)
V0	=	0,00 m/s
FN res	=	0,06 kN
P35/P3	=	0,98000
WF	=	0,00618 kg/s
s NOx	=	0,96485
Therm Eff	=	0,38594
P45/P44	=	0,97500
Incidence	=	0,00000 °
P6/P5	=	0,98000
PWX	=	0 kW
P7/P6	=	0,97000
P8/Pamb	=	1,03000
WBld/W2	=	0,00500
A8	=	0,00915 m²
TRQ	=	100,0 %
P2/P1	=	0,96700
Loading	=	100,00 %
e444 th	=	0,90552
WHcl/W2	=	0,05000
PW_gen	=	102,0 kW
WLcl/W2	=	0,01000
eta t-s	=	0,79791
Ps8	=	101,325 kPa

Iteration Variables:
Inlet Corr. Flow W2Rstd kg/s (0,5...1) = 0,585572

Iteration Targets:
Shaft Power Delivered kW = 102

Figure A.0.3: *Design Point Performance of Gas Turbine Model 3 - GasTurb*

	Parameter	Units
XN_LP_A	Low Pressure Spool Speed	rpm
Torque	Output Shaft Torque	Nm
SFC	Specific Fuel Consumption	kg/kWh
WF	Fuel Flow	kg/s
eta_ther	Thermal Efficiency	-
PWSD	Shaft Power Delivered	kW
XN_HP_A	High Pressure Spool Speed	rpm

XN_LP_A	Torque	SFC	WF	eta_ther	PWSD	XN_HP_A
35154	27.703	0.303	0.0085837	0.27796	101.98	44600
34630	27.953	0.30406	0.008562	0.27699	101.37	44600
34106	28.202	0.30523	0.0085402	0.27593	100.73	44600
33583	28.465	0.3063	0.0085172	0.27497	100.1	44600
33059	28.725	0.30749	0.0084941	0.2739	99.445	44600
32535	28.984	0.30881	0.008471	0.27273	98.751	44600
32011	29.241	0.31027	0.0084479	0.27145	98.021	44600
31487	29.513	0.31175	0.0084272	0.27016	97.315	44600
30964	29.743	0.31355	0.0083998	0.26861	96.44	44600
30440	29.957	0.31563	0.0083724	0.26684	95.493	44600
29916	30.153	0.3178	0.0083391	0.26502	94.463	44600
29392	30.349	0.32009	0.0083057	0.26312	93.414	44600
28868	30.582	0.32236	0.0082786	0.26127	92.452	44600
28345	30.832	0.32459	0.0082515	0.25947	91.516	44600
27821	31.134	0.32654	0.0082276	0.25792	90.706	44600
27297	31.47	0.32841	0.0082062	0.25646	89.957	44600
26773	31.852	0.33009	0.0081885	0.25515	89.304	44600
26249	32.251	0.3318	0.0081707	0.25384	88.652	44600
25726	32.691	0.33339	0.0081561	0.25262	88.07	44600
25202	33.135	0.33517	0.0081415	0.25128	87.447	44600
24678	33.546	0.33719	0.0081199	0.24978	86.692	44600
24154	33.954	0.33945	0.0080983	0.24812	85.885	44600
23631	34.339	0.34204	0.0080736	0.24624	84.976	44600
23107	34.738	0.34474	0.0080493	0.24431	84.056	44600
22583	35.161	0.34748	0.008026	0.24238	83.152	44600
22059	35.613	0.35024	0.0080038	0.24047	82.268	44600
21535	36.086	0.35305	0.0079808	0.23856	81.38	44600
21012	36.593	0.35583	0.0079582	0.2367	80.515	44600
20488	37.133	0.3586	0.0079357	0.23487	79.667	44600
19964	37.739	0.36116	0.0079152	0.2332	78.897	44600
19440	38.43	0.36346	0.0078985	0.23173	78.234	44600
18916	39.189	0.36563	0.0078844	0.23035	77.631	44600
18393	39.978	0.36794	0.0078699	0.22891	77.001	44600
17869	40.763	0.37063	0.0078528	0.22724	76.276	44600
17345	41.517	0.3739	0.0078322	0.22526	75.41	44600
16821	42.192	0.37811	0.0078061	0.22274	74.321	44600
16297	42.856	0.38284	0.0077781	0.21999	73.141	44600
15774	43.646	0.38723	0.0077547	0.2175	72.095	44600
15250	44.602	0.39091	0.0077343	0.21545	71.227	44600
14726	45.714	0.39399	0.0077151	0.21377	70.496	44600
14202	46.952	0.39693	0.0076993	0.21218	69.829	44600
13678	48.172	0.40067	0.0076797	0.21021	69.002	44600
13155	49.341	0.40535	0.0076531	0.20778	67.97	44600
12631	50.596	0.4104	0.0076291	0.20522	66.923	44600
12107	51.899	0.41606	0.0076047	0.20243	65.8	44600
11583	53.207	0.42254	0.0075751	0.19932	64.539	44600
11059	54.625	0.42938	0.0075455	0.19615	63.264	44600
10536	56.143	0.4369	0.0075173	0.19277	61.942	44600
10012	57.491	0.44669	0.0074791	0.18855	60.276	44600

Figure A.0.4: *Results from the Parametric Study performed with Gas Turbine Model 1 - GasTurb output file*

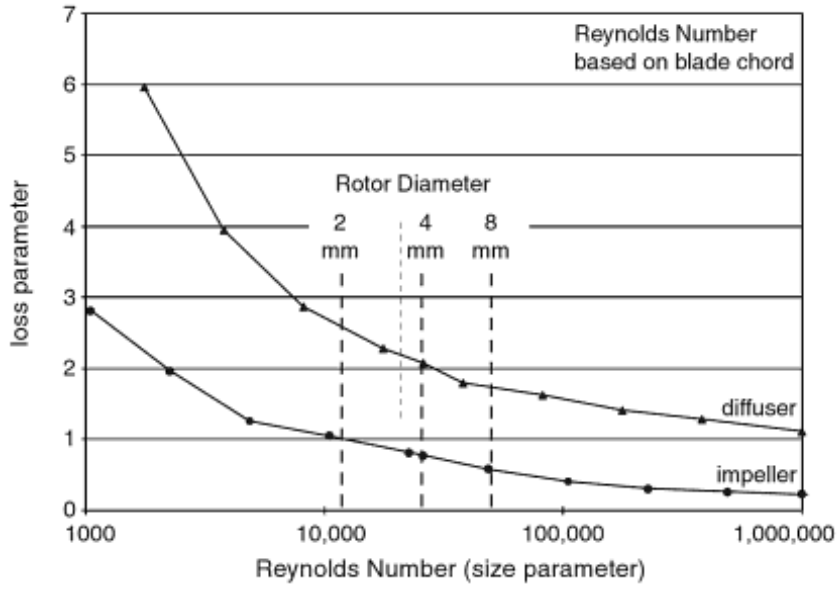

Figure A.0.5: *Compressor loss as a function of size. Loss parameter is a measure of the difference between the isentropic total pressure and the total pressure at the impeller exit [Lan09]*

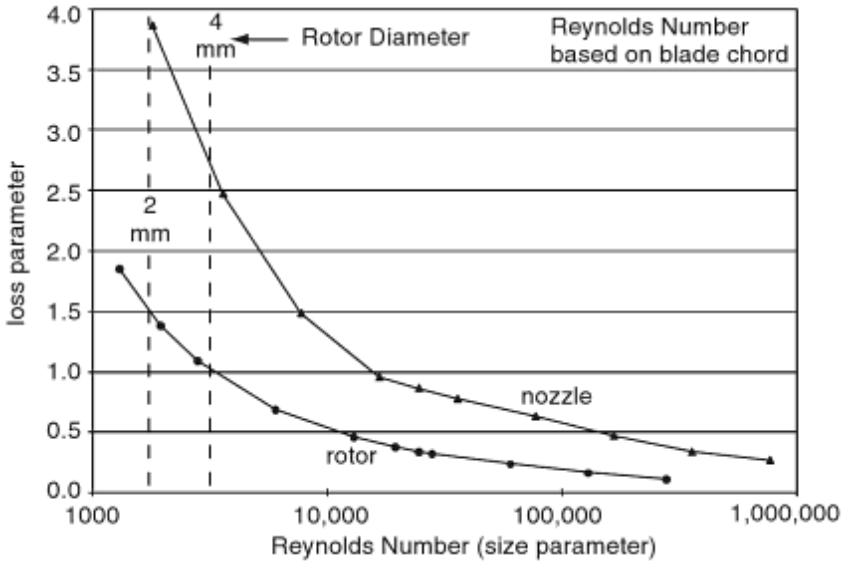

Figure A.0.6: *Turbine loss as a function of size [Lan09]*

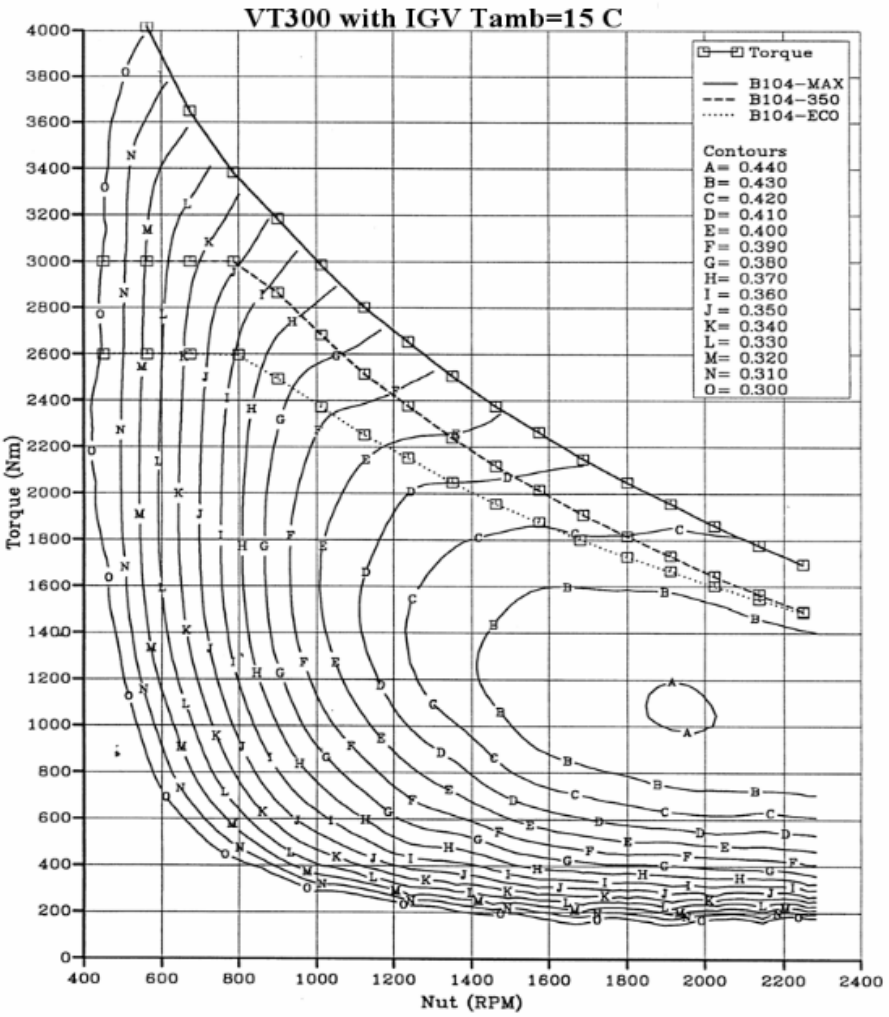

Figure A.0.7: *Efficiency Map of a Twin-Shaft Gas Turbine developed by Volvo [OS05]*

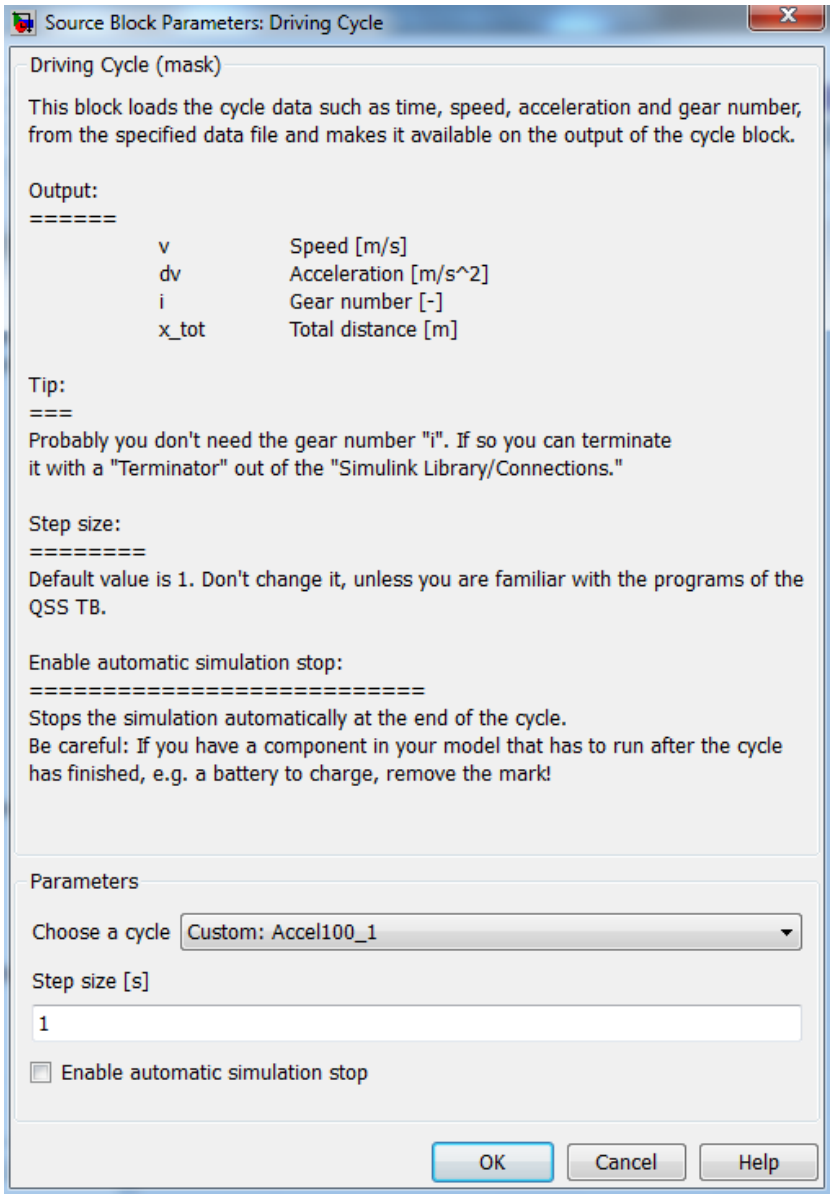

Figure A.0.8: *The user interface (mask) of the Driving Cycle block*

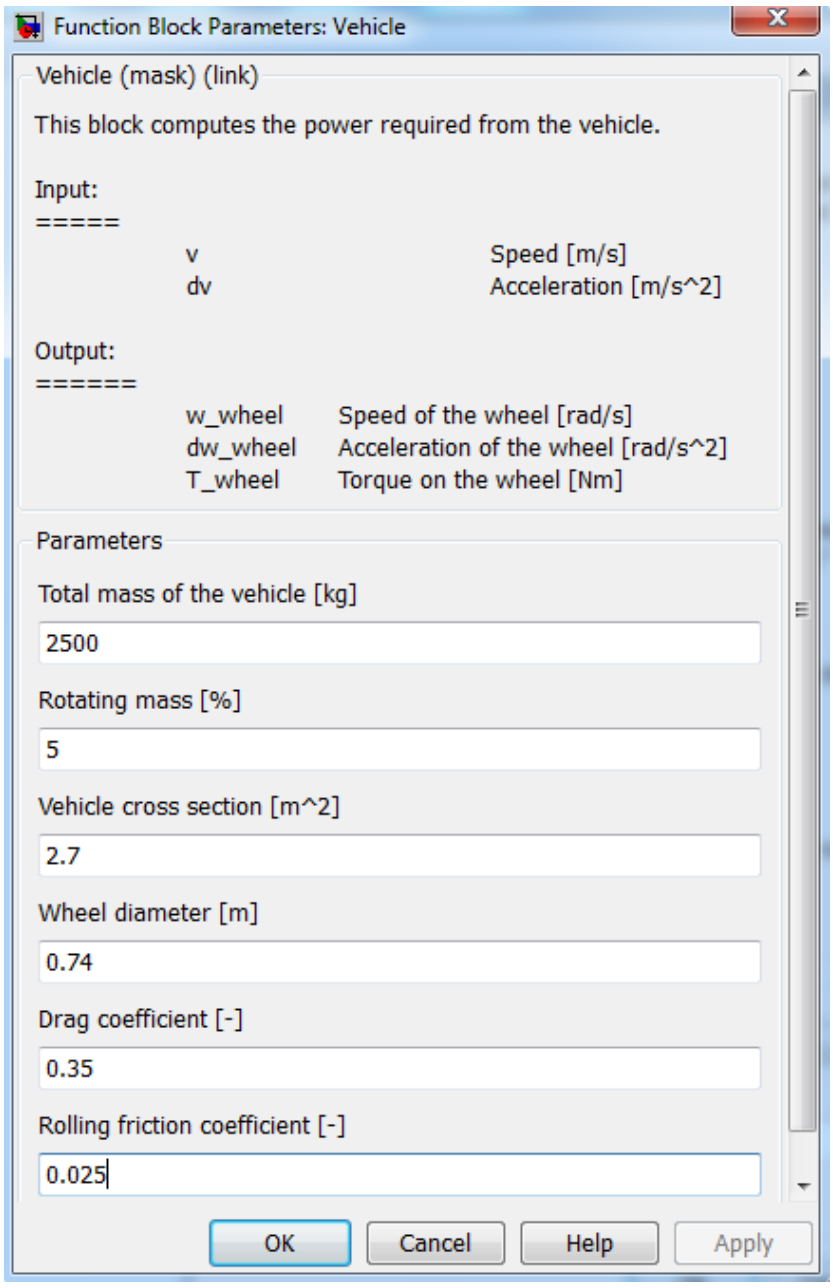

Figure A.0.9: *The user interface (mask) of the Vehicle block*

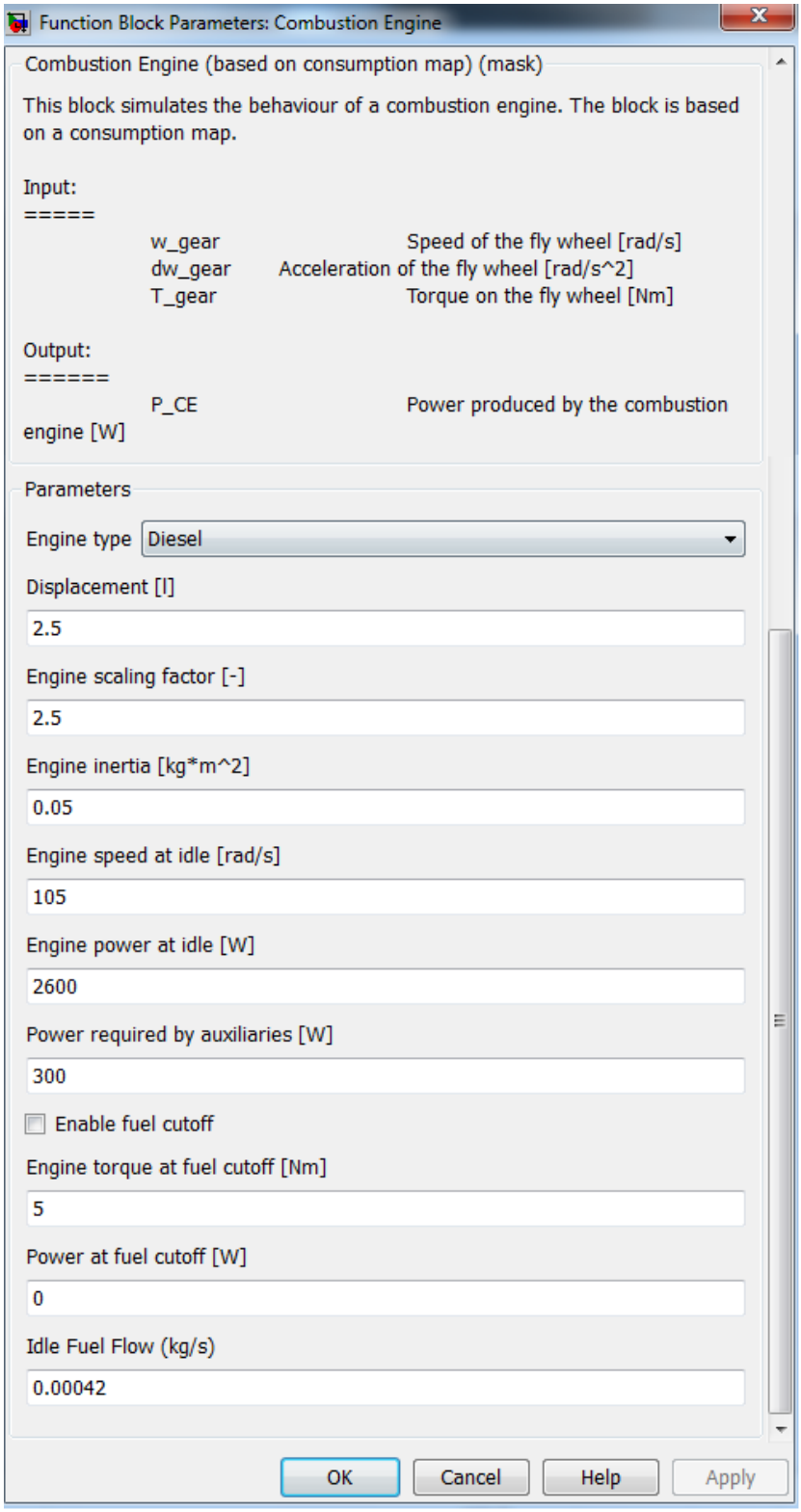

Figure A.0.10: *The user interface (mask) of the Combustion Engine block*

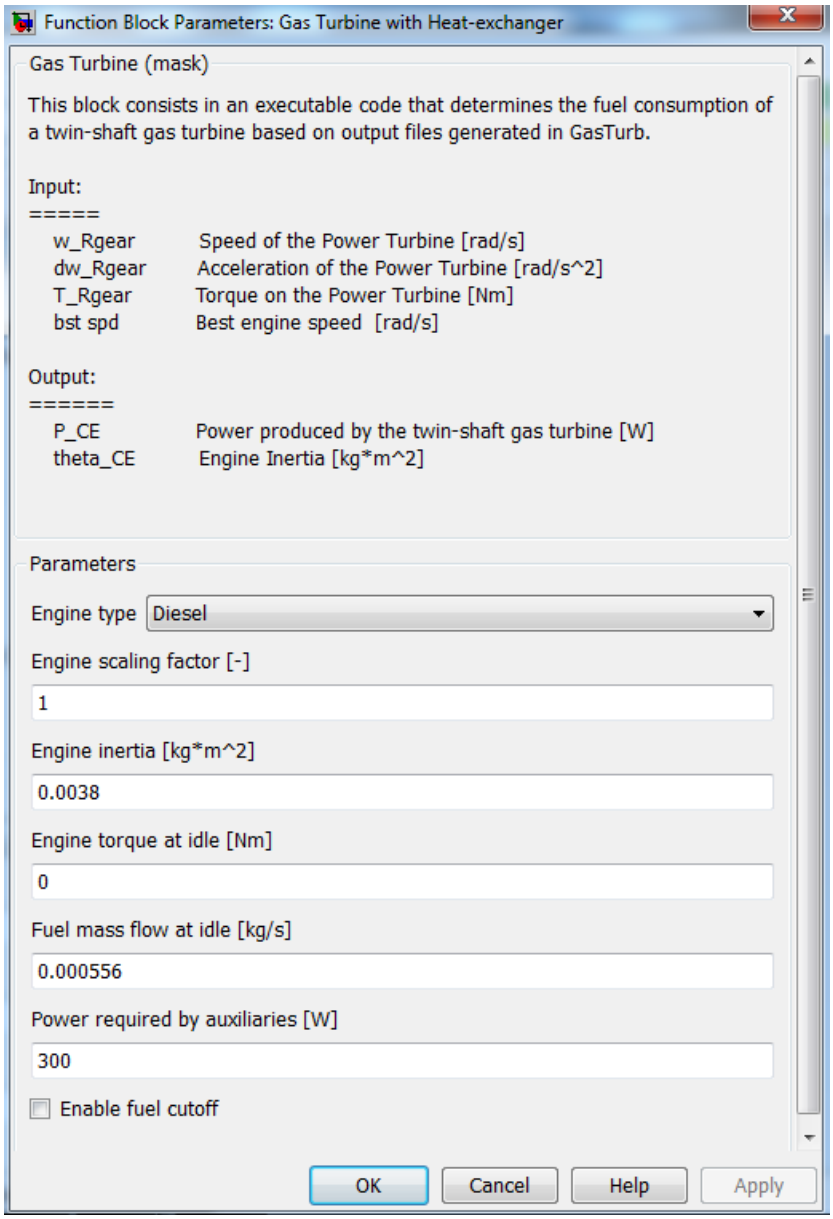

Figure A.0.11: *The user interface (mask) of the Gas Turbine block*

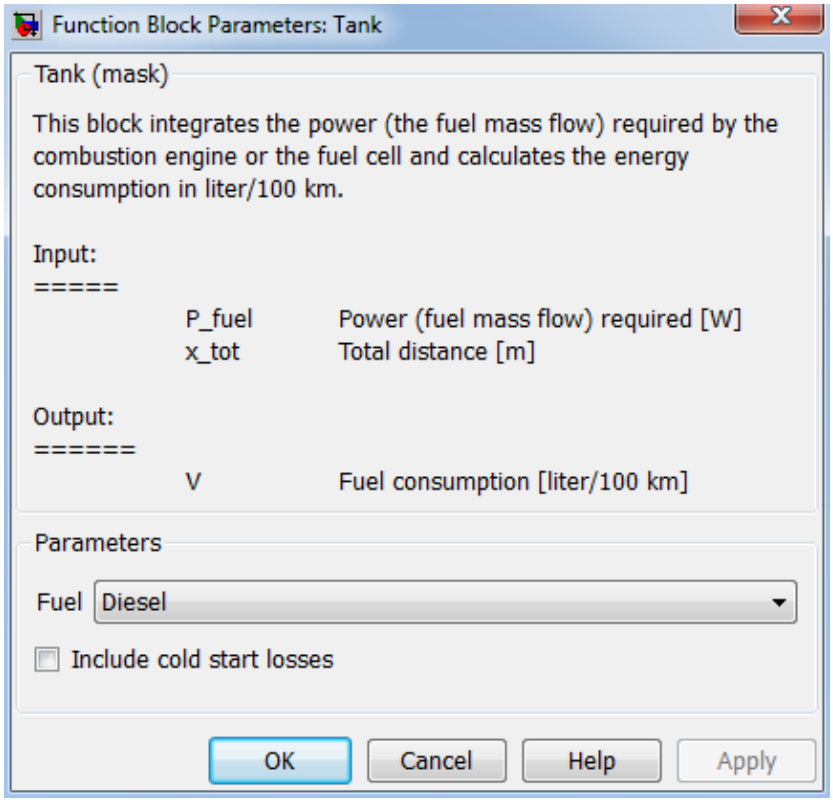

Figure A.0.12: *The user interface (mask) of the Energy Source block*

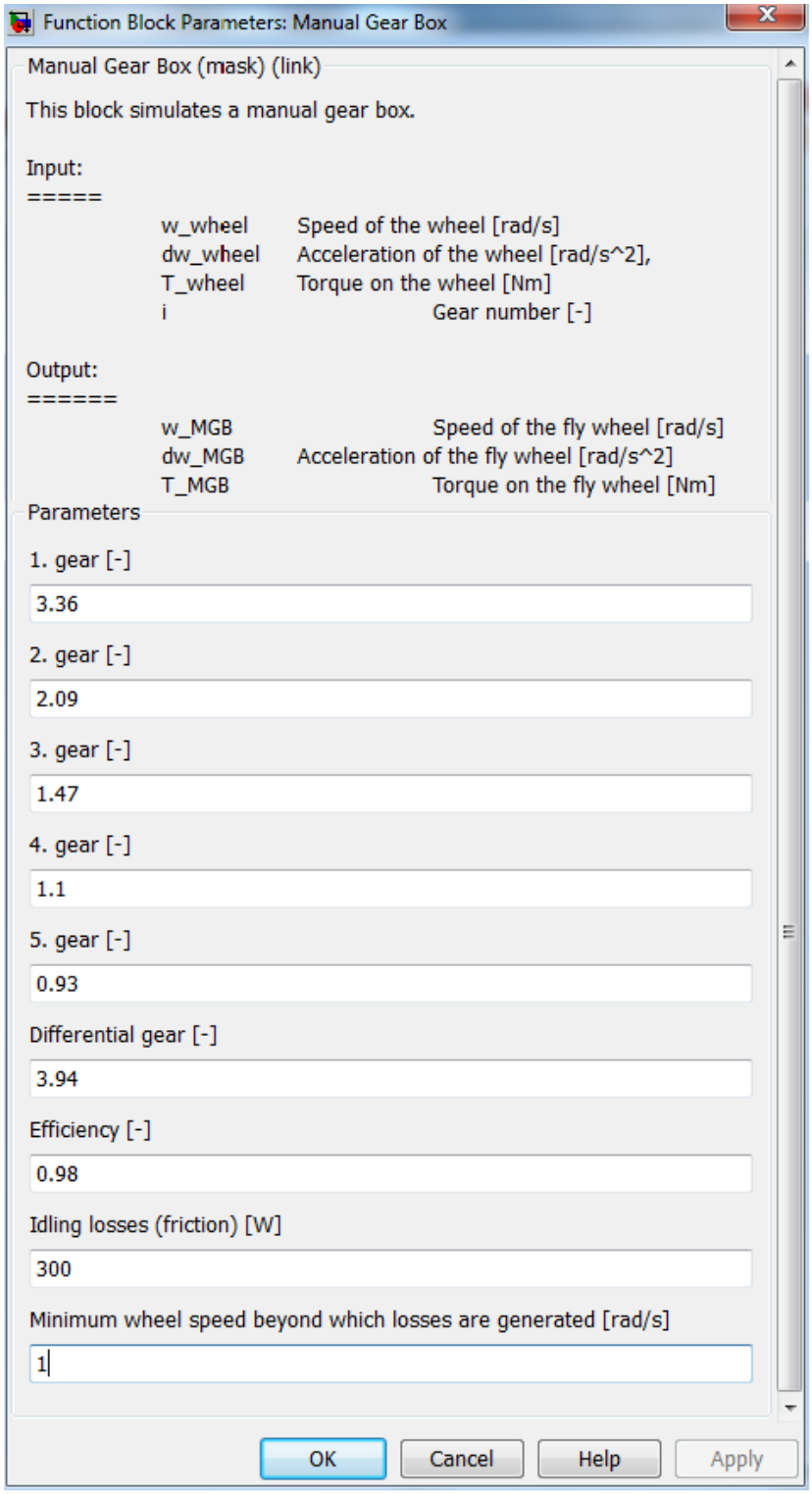

Figure A.0.13: *The user interface (mask) of the Manual Gearbox block*

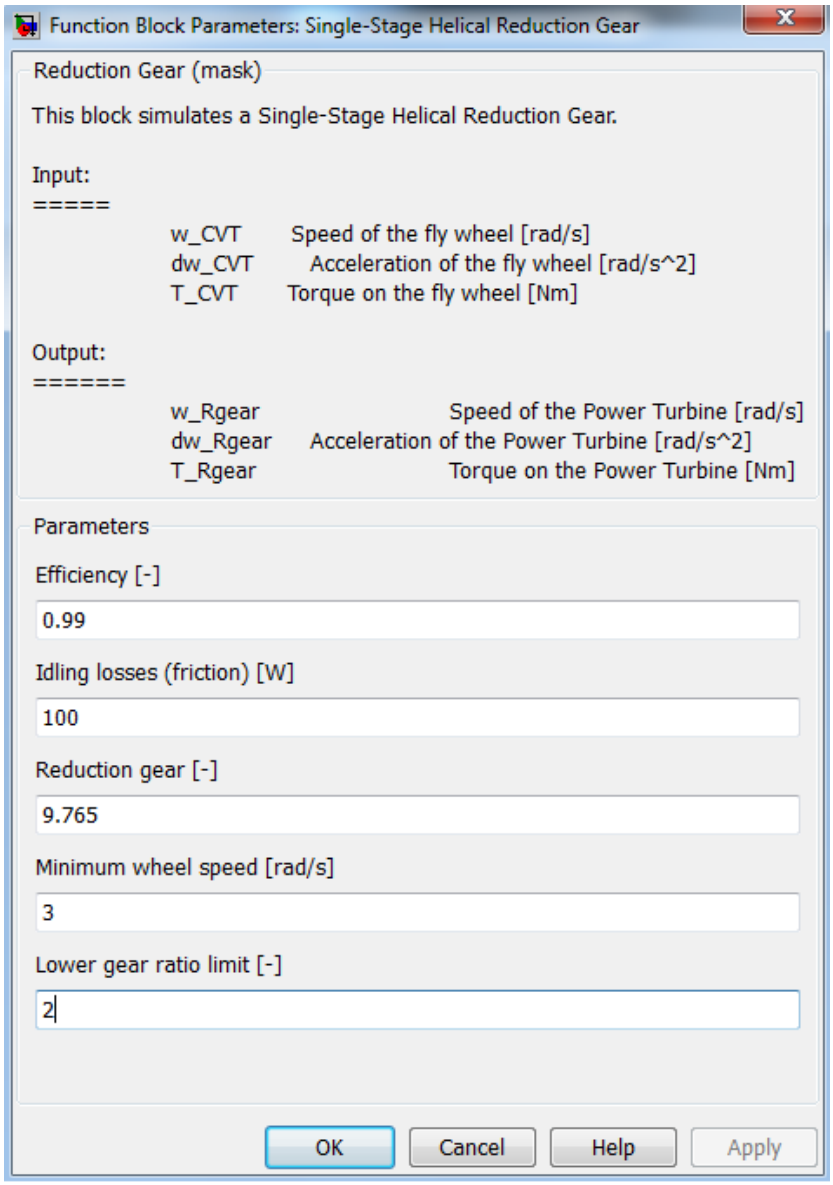

Figure A.0.14: *The user interface (mask) of the Reduction Gear block*

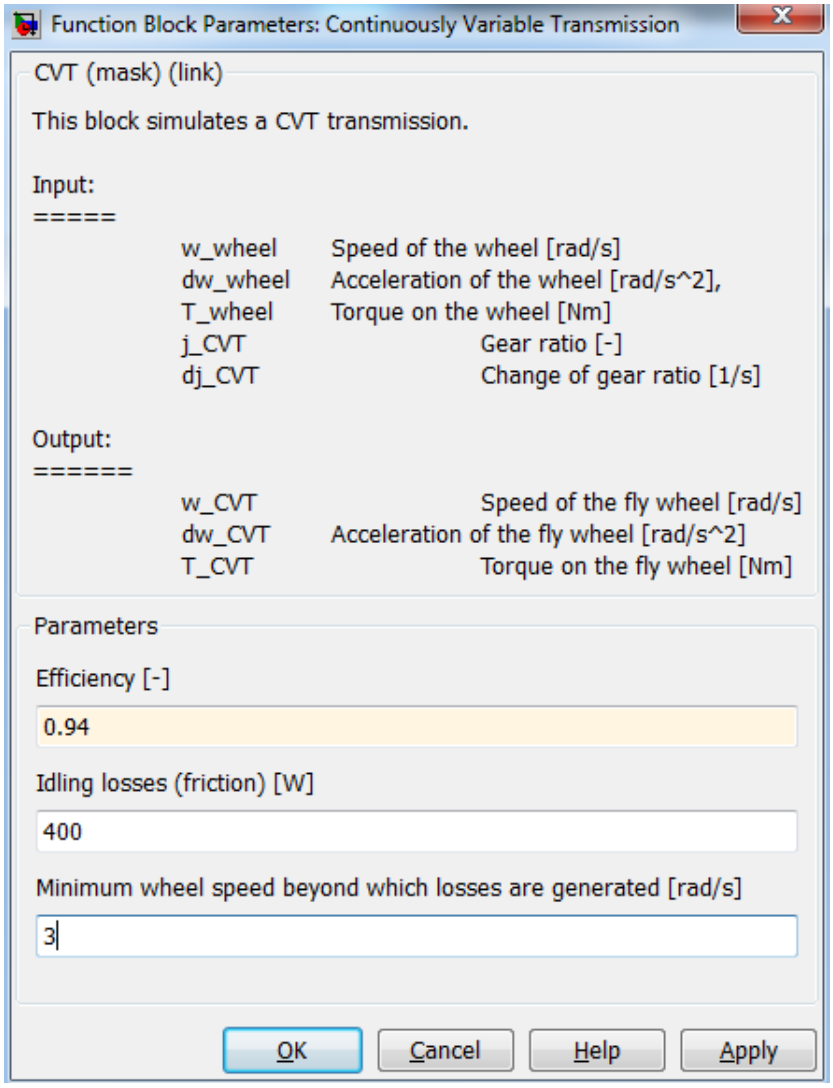

Figure A.0.15: *The user interface (mask) of the CVT block*

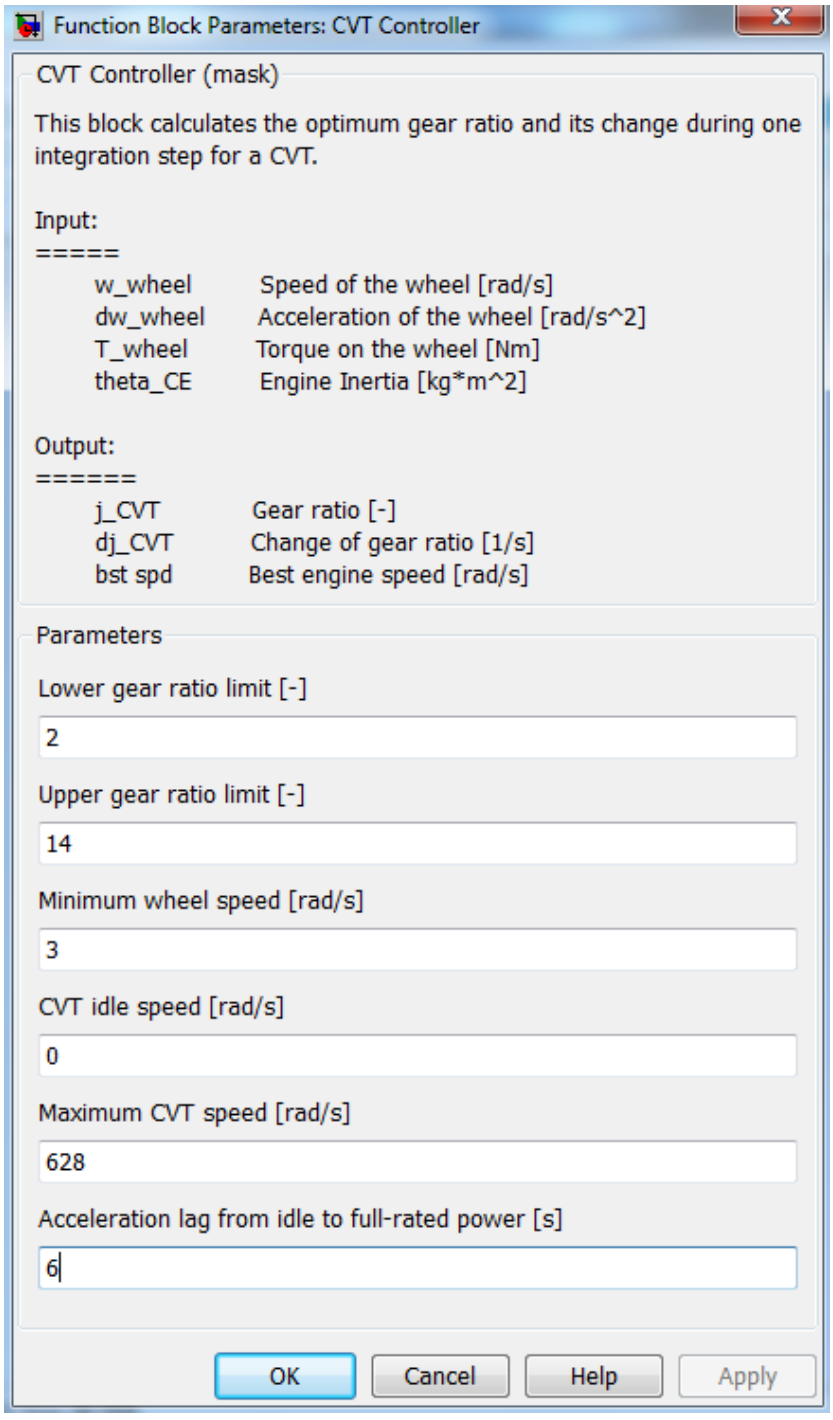

Figure A.0.16: *The user interface (mask) of the CVT Controller block*

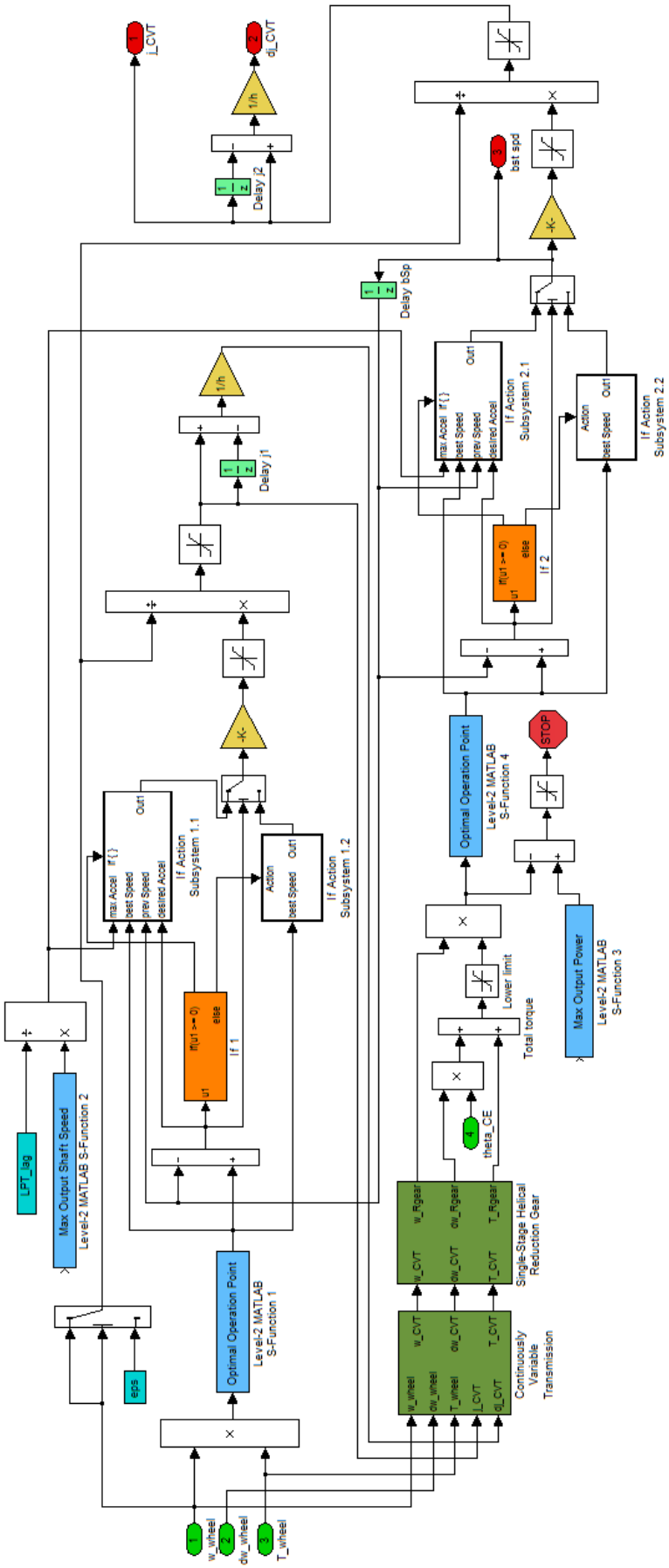

Figure A.0.17: *Top level of the CVT Controller block*